7 Hanford 300 Area

7.1 Introduction

This report is an exercise demonstrating the application of the Advanced Environmental Solutions, LLC (AES) Strategy to a highly transmissive, near surface aquifer in the Northwestern United States. This exercise is for testing the functionality for the Strategy only. Data utilized in this evaluation are based on readily available information. Most of this chapter is a recapitulation of Hanford data. An alternative to the current Conceptual Site Model of ground water flow is offered in section 7.3.

The Hanford Site borders the Columbia River and covers 1,517 square kilometers (586 square miles) just north of the city of Richland, Washington. In this case study, the AES Strategy provides a structured approach for studying the relationship between groundwater flow in the Hanford 300 Area, which is located in the southeast portion of the Hanford site, and the Columbia River. An accurate understanding of the 300 Area groundwater flow pattern will, in turn, aid in understanding the distribution and migration of contaminants, particularly hexavalent uranium, in the 300 Area. A map depicting the Hanford Site, including the 300 Area, is presented in Figure 7-1.

The ground water beneath the 300 Area has been contaminated by liquid effluent discharges from 3 main waste sites: the 300 area, 618-11 burial ground, and the 316-4 cribs/618-10 burial ground. These releases occurred from the late 1940s through the mid-1980s. Since the end of fuel fabrication activities, contaminated discharges have largely ceased, although discharges of uncontaminated effluent continued until 1994. Remedial actions have been completed that removed the structures and contaminated soil associated with most of these disposal sites. However, residual amounts of some contaminants remain in the underlying vadose zone, and their presence is indicated in ground water monitoring results.

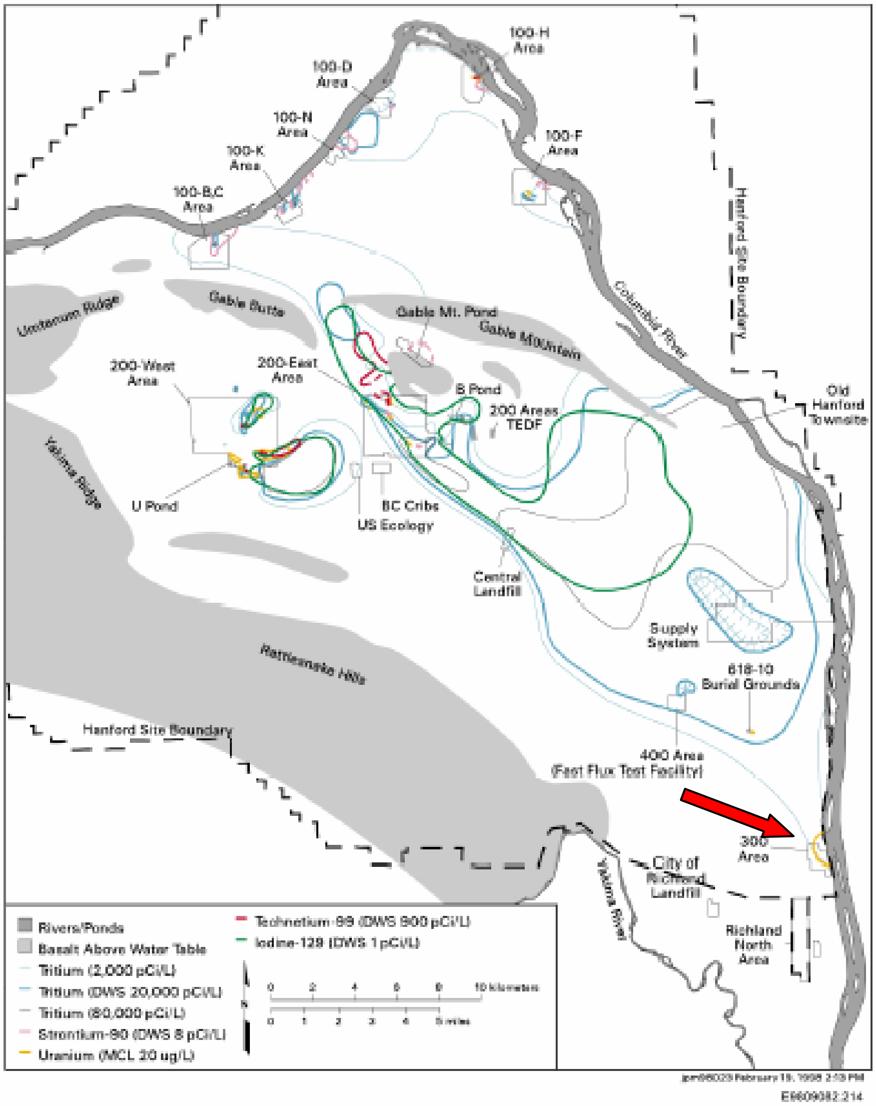

Figure 7-1. Hanford Site map including the 300 Area (DOE, 1999)

7.2 Compilation of Available Data

7.2.1 Geologic Setting

The Hanford Site lies within the Pasco Basin, a structural depression that has accumulated a relatively thick sequence of fluvial, lacustrine, and glaciofluvial sediments. Local geology as well as the regional geology play a strong role in contaminant transport.

7.2.2 Regional Geologic Information

Figure 7-2 and Figure 7-3 show the surface geology and major structural features of the area, respectively. The Pasco Basin initially developed on the underlying Columbia River Basalt Group, a sequence of continental flood basalts covering more than 160,000 km^2 (Vermeul et al., 2003).

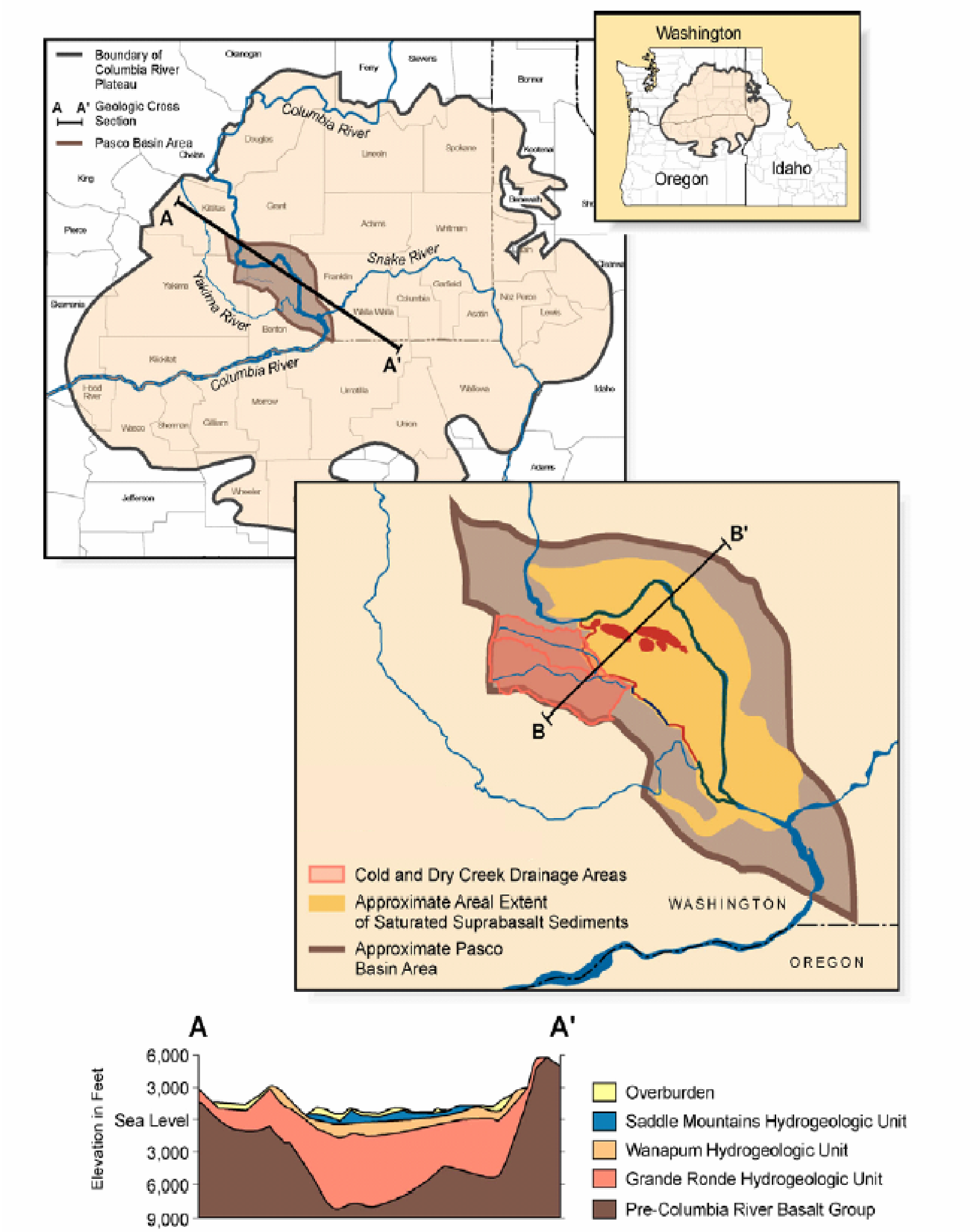

Figure 7-2. Hanford Site regional geologic setting (Vermeul et al., 2003)

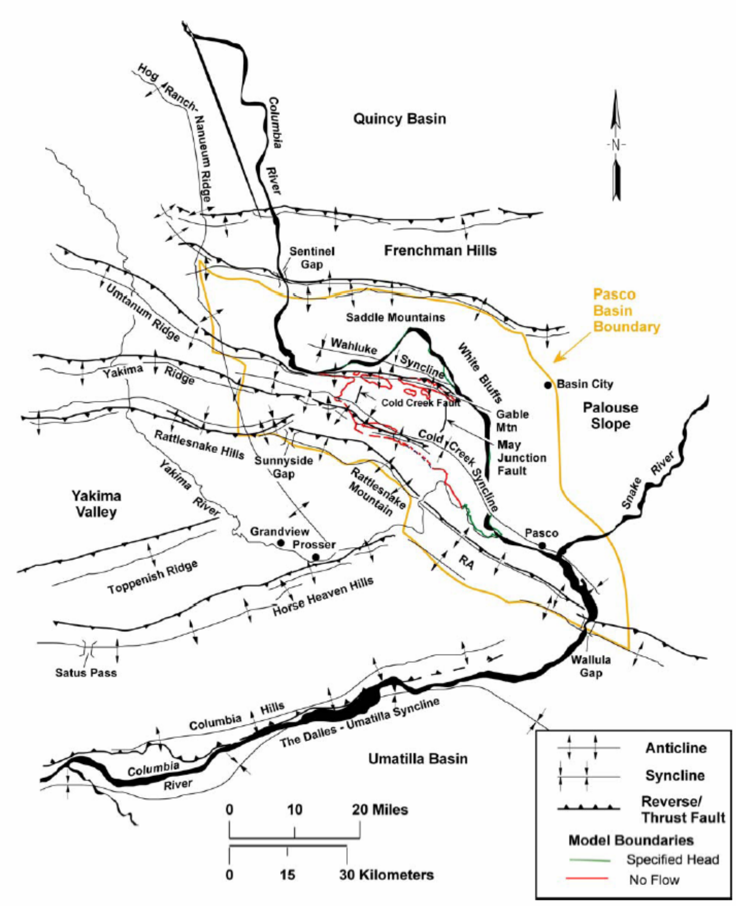

Figure 7-3. Structural geologic features of the Hanford Site within the Pasco Basin (Vermeul et al., 2003)

Overlying the basalt within the Pasco Basin are fluvial and lacustrine sediments of the Ringold Formation (Figure 7-4) (Lindsey et al., 1992). The ancestral Columbia River and its tributaries flowed into the Pasco Basin, depositing coarse-grained sediments in the migrating river channels and fine-grained sediments (silt and clay) primarily as overbank flood deposits. On at least two occasions, these river channels were blocked, forming lakes in the Pasco Basin and depositing extensive layers of fine-grained lacustrine sediments within the Ringold Formation.

7.2.3 Site-specific Geologic Information

The major geologic units in the Hanford Site area are the Miocene Columbia River Basalt Group (CRBG) and intercalated sedimentary rocks of the Ellensburg Formation. These are overlain by younger (Mio-Pliocene) sedimentary rocks of the Ringold Formation, the early "Palouse" soil/Plio- Pleistocene Unit, and the Pleistocene cataclysmic flood deposits of the Hanford Formation (Figure 7-4).

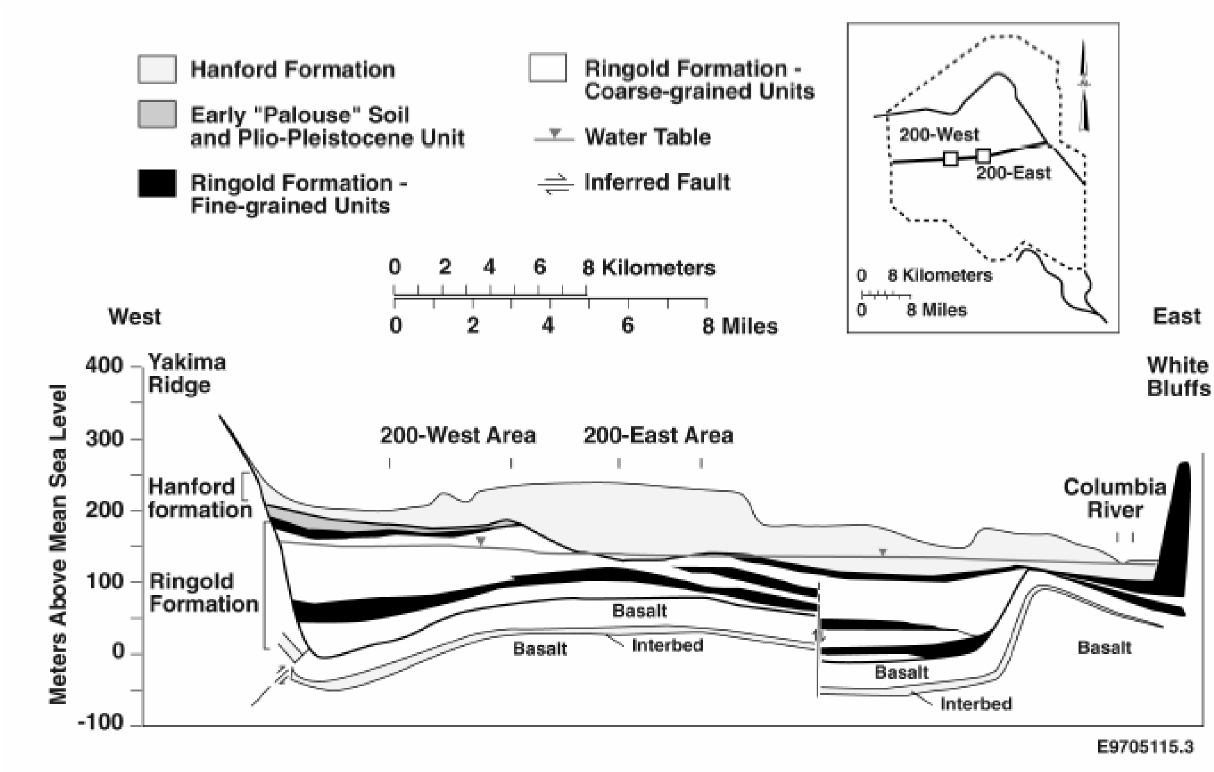

Figure 7-4. Major geological units at the Hanford Site (DOE, 1999)

The Plio-Pleistocene Unit is made up of sandy gravels that separate the Hanford Formation and the Ringold Formation in the east-central Cold Creek syncline and at the east end of the Gable Mountain anticline (east and south of the 200 East Area). These gravels are up to 25m (75 feet) thick. Along the western margin of the site, the "Palouse" soil separates the two formations. The Hanford Formation consists of pebble to boulder sized gravel, fine to coarse-grained sand, and silts of unconsolidated deposits from ice age flooding. The Hanford Formation generally lies above the water table throughout most of the Hanford Site, except in the 100 and 300 Areas (DOE, 1998).

7.2.4 Site-specific Hydrogeologic Information

Geologic descriptions are available from 67 boreholes in the 300 Area. All of these boreholes are deep enough to penetrate the contact between the Hanford and Ringold stratigraphic formations. EarthVision geologic modeling and visualization software was used to interpolate unit contacts between borehole locations and to create a three-dimensional model of the hydrogeologic framework. Figure 7-5 provides an index to the three cross sections shown in Figure 7-6, Figure 7-7, and Figure 7-8, which are drawn through the model to illustrate the framework (Peterson, 2005).

Highly transmissive Hanford formation gravels are found below the water table across portions of the 300 Area. The extent and thickness of saturated Hanford formation gravels vary as a consequence of changes in water-table elevation, which are caused by changes in the Columbia River stage. The saturated thickness of the Hanford formation in the 300 Area varies from 0 to 15 meters (0 to 49 feet). Aquifer pumping tests at five boreholes within the 300 Area reveal an average hydraulic conductivity of approximately

14,000 meters (45,932 feet) per day for saturated Hanford formation gravels. This indicates a highly transmissive hydrologic unit. The value is significantly higher than the average hydraulic conductivity for Hanford formation gravels elsewhere on the Hanford Site (i.e., approximately 2,000 meters (6,562 feet) per day (Peterson, 2005). Extrapolating from the known geology indicates that there is a high likelihood that zones of high permeability are present and are highly variable in their spatial distribution.

Ringold Formation gravels below the water-table range in thickness from 15 to 50 meters (49 to 164 feet). Aquifer pumping tests at seven boreholes in the 300 Area suggest an average hydraulic conductivity of approximately 125 meters (410 feet) per day, which is again higher than the average values for Ringold gravels elsewhere on the Hanford Site but considerably less transmissive than the overlying Hanford unit. Relatively higher conductivities may exist in the upper part of the Ringold Formation (i.e., Unit E gravel), where most pumping tests have been performed (Peterson, 2005).

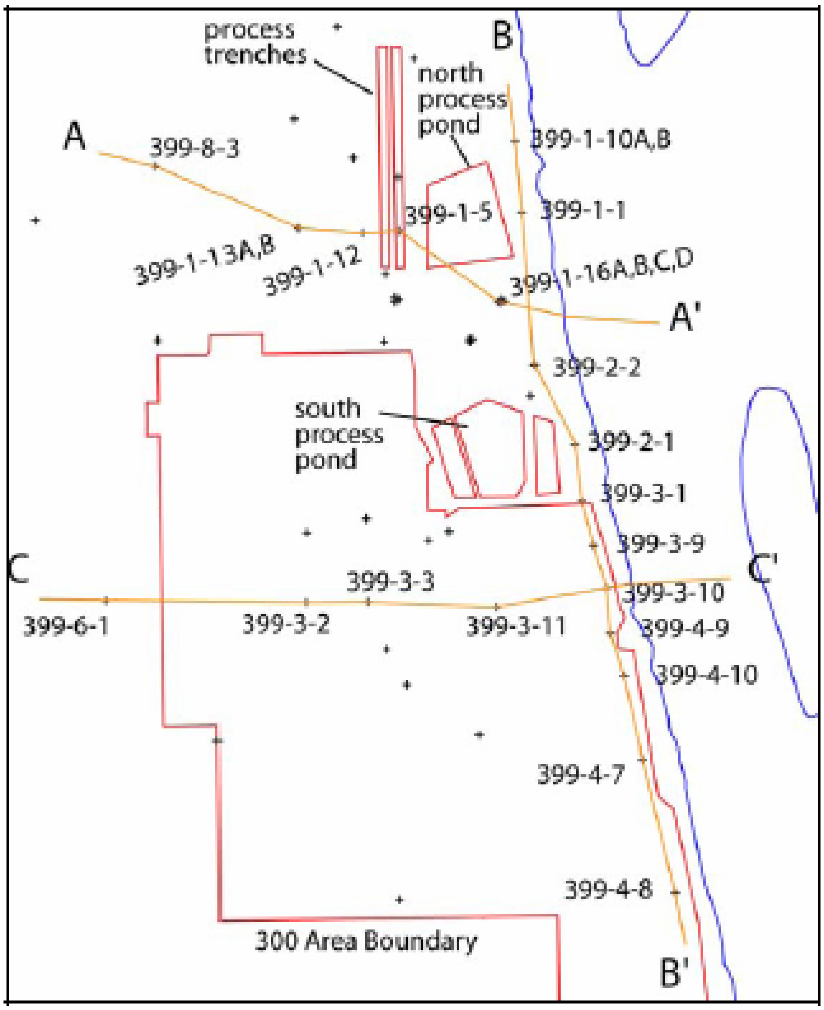

Figure 7-5. Index map to cross sections shown in Figures 6, 7, and 8 (Peterson, 2005)

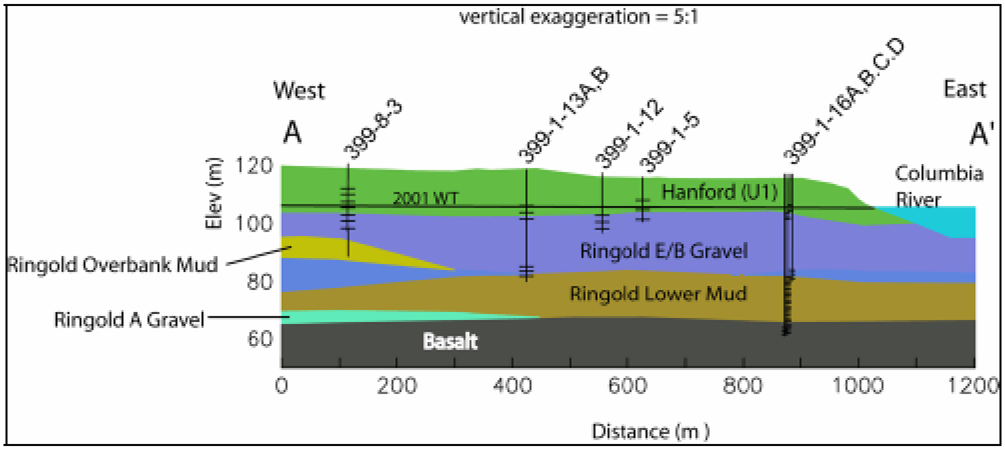

Figure 7-6. West to east cross section along flow path from 300 Area process trenches to the Columbia River (Peterson, 2005)

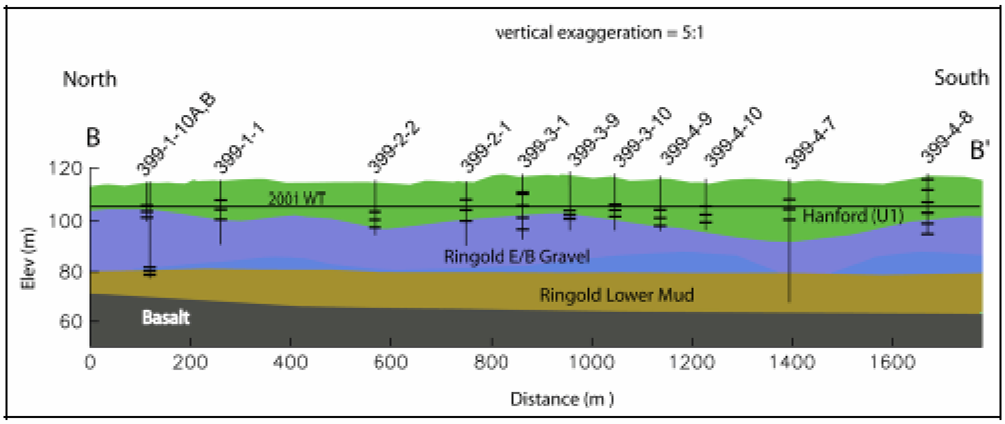

Figure 7-7. North to south cross section along shoreline wells (Peterson, 2005)

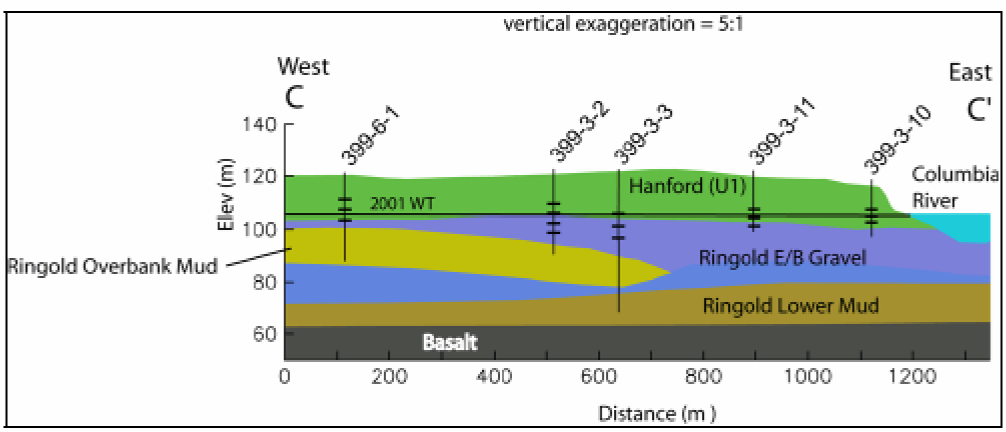

Figure 7-8. West to east cross section through central portion of 300 Area (Peterson, 2005)

7.2.5 Vadose Zone Data

The sediments beneath waste sites at Hanford are highly heterogeneous (for example, sediments include interbedded sand, silts, gravels, and boulders). Temporal and spatial variations in net water infiltration through current and past liquid discharges, water line leaks, and variable chemical interactions complicate description and understanding of contaminant transport, and lead to uncertainty in the evaluation of transport at contaminated sites. A number of knowledge gaps—including an insufficient understanding of source terms, geological and hydrologic properties, preferential flow, and chemical interactions–make current modeling of contaminant transport in the Hanford vadose zone unreliable.

Figure 7-9 presents three potential types of preferential flow models in the Hanford vadose zone: (1) fingering, (2) funnel flow, and (3) flow associated with clastic dikes or poorly sealed borehole annular space. Funnel flow can enhance lateral migration, and horizontal layering will tend to stabilize fingered flow, whereas cross-bedding concentrates and coalesces fingers. Flow through clastic dikes and poorly sealed well-annular spaces could exhibit a hysteretic Effect, which may appear during infiltration events (such as large rainfall events), and there may be flow impediments during drying (Faybishenko, 2000).

In the 300 Area, the vadose zone is relatively thin, ranging from about 1 to 30 m in thickness. It is generally composed of recent surficial deposits and portions of the Hanford formation and/or Ringold Unit E. Sediments from the upper strata of the Ringold Formation within the 300 Area is characterized by complex interstratified beds and lenses of sand and gravel. Ringold Formation deposits are generally more cemented and better sorted than those from the Hanford formation. Ringold strata typically contain a lower percentage of angular basaltic detritus than Hanford formation deposits. The Hanford formation is characterized by dark grayish-brown to dark olive-gray sandy gravel, typical of the gravel-dominated facies, with some silt and local sand stringers. The upper portion of the unit generally exhibits a pebble to boulder gravel, which becomes finer with depth, to a very fine-to-medium pebble gravel (DOE, 1998).

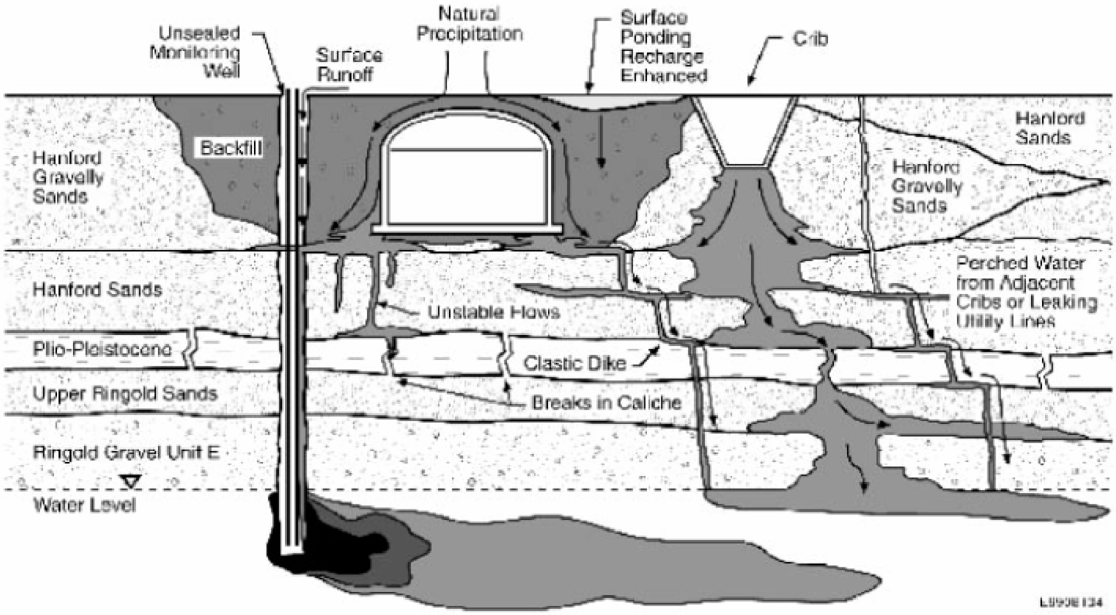

Figure 7-9. Conceptual model of fluid flow beneath single shell tanks at Hanford Site showing fingering, funnel flow, and flow associated with clastic dikes or poorly sealed borehole annular space (Faybishenko, 2000)

7.2.6 Hydrologic Data

Ground water flow beneath the 300 Area is generally directed toward the southeast. Ground water appears to converge beneath the 300 Area, with flow coming into the 300 Area from the northwest, west, and southwest. The uppermost aquifer (Hanford formation) is highly transmissive because of open framework gravelly sediment, thus leading to high flow velocities (i.e., meters per day). However, because the hydraulic gradient that drives the flow varies with Columbia River stage, actual movement paths of water can be variable when viewed on short time scales, such as days or weeks. When viewed over seasons and years, however, the net flow and movement of contaminant plumes follows the generally southeasterly course (Peterson, 2005).

It is not clear exactly what influence the Columbia River has on the overall ground water flow direction. Data indicates that the aquifer is in communication with the river and that the stage of the river does impact the lateral movement of water into and out of the aquifer. What is less clear is what influence the river has on the flow of ground water within the aquifer locally at the aquifer/ river interface. Improving our understanding of the relationship between the river and Area 300 groundwater through the implementation of the AES Strategy is the primary focus of this exercise.

7.2.7 Seasonal Variability in Water-Table Conditions

To better understand how the dynamic hydrologic system in the 300 Area influences the dispersal pattern of contaminant plumes, hourly hydraulic head data were analyzed to (a) determine the predominant ground water flow directions, and (b) assess variability in flow directions during the various seasons. The analysis used hourly measurements of hydraulic head made at 30 wells in the 300 Area during the period of March 1992 through February 1993, using pressure transducers. Water-table elevation contour maps were prepared for March, May, June, September, and December 1992 (Figure 7-10, Figure 7-11, Figure 7-12, Figure 7-13, and Figure 7-14, respectively). The contours were based on 22 wells deemed most representative of unconfined aquifer (i.e., water table) conditions. The values contoured were averages of all hourly measurements made during a particular month. The water-table maps for the various months reveal that the shape of the water table and, therefore, the inferred long-term ground water flow pattern, appears to show little variation from season to season. The overall elevation of the water table is higher during the seasonal high river discharge that occurs in May and June. The aquifer apparently equilibrates rapidly to changes in river stage, which is expected given the high transmissibility of the stratigraphic units (Peterson, 2005).

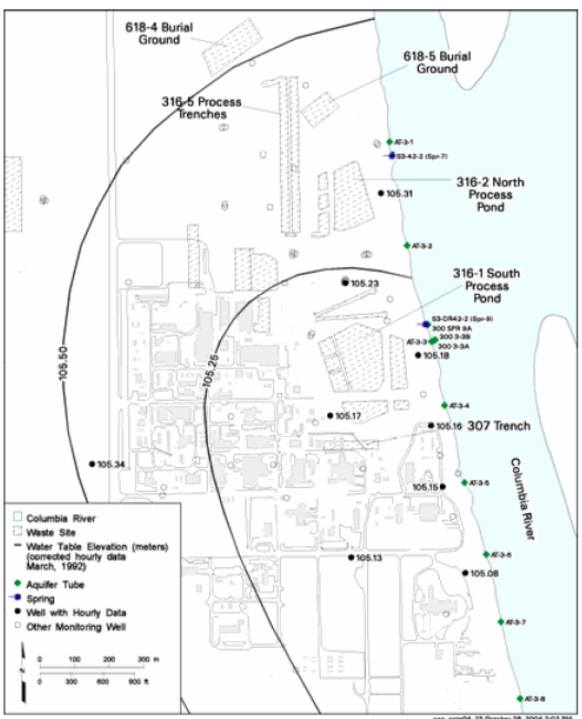

Figure 7-10. 300 Area water-table elevation, March 1992 (averaged hourly) (Peterson, 2005)

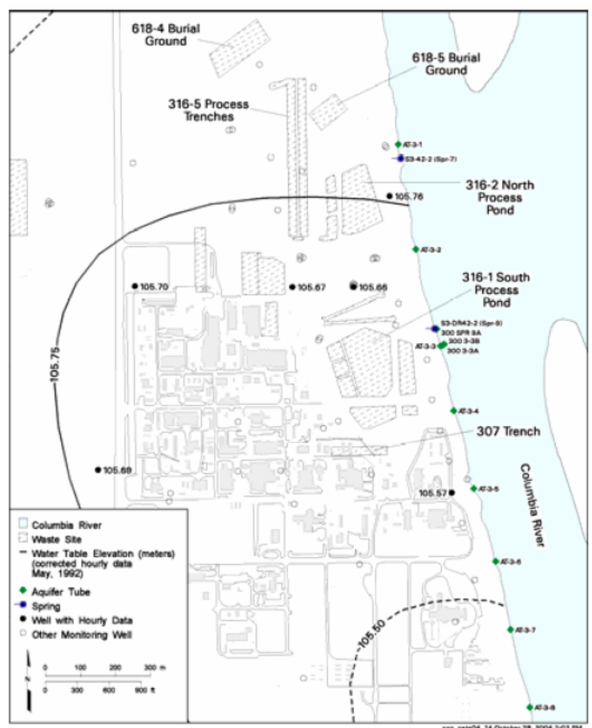

Figure 7-11. 300 Area water-table elevation, May 1992 (averaged hourly) (Peterson, 2005)

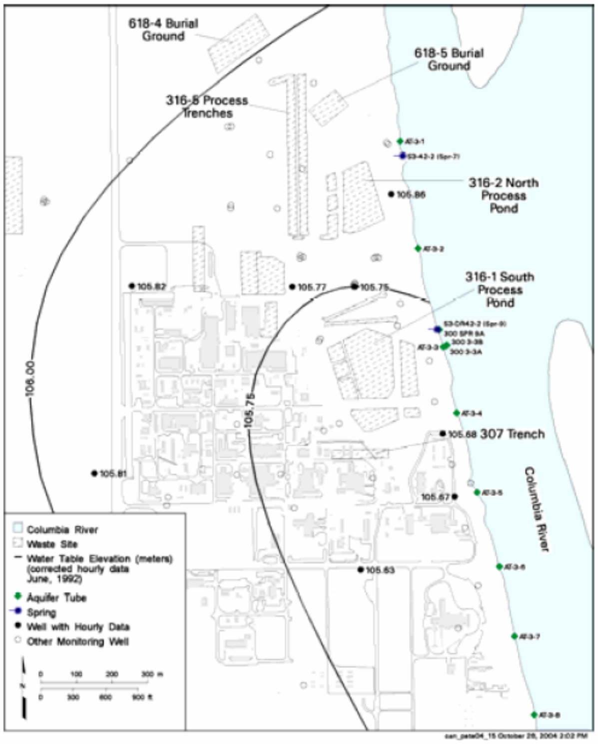

Figure 7-12. 300 Area water-table elevation, June 1992 (averaged hourly) (Peterson, 2005)

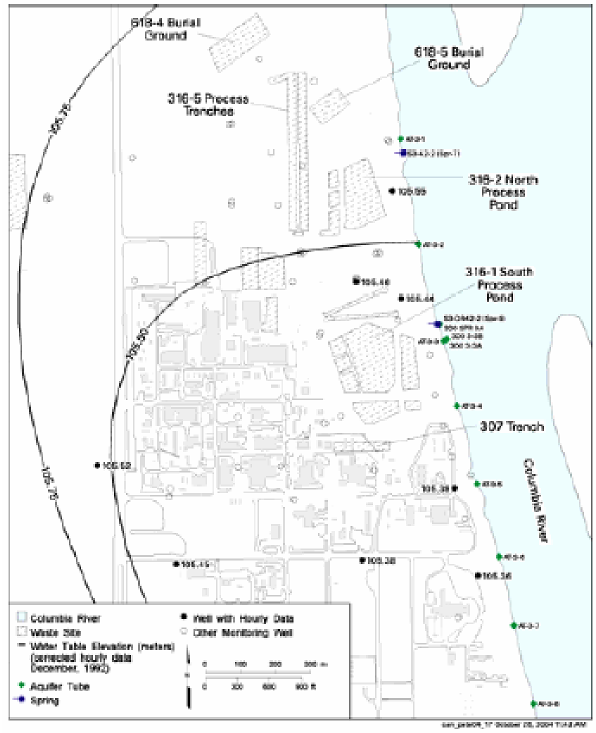

Figure 7-14. 300 Area water-table elevation, December 1992 (averaged hourly) (Peterson, 2005)

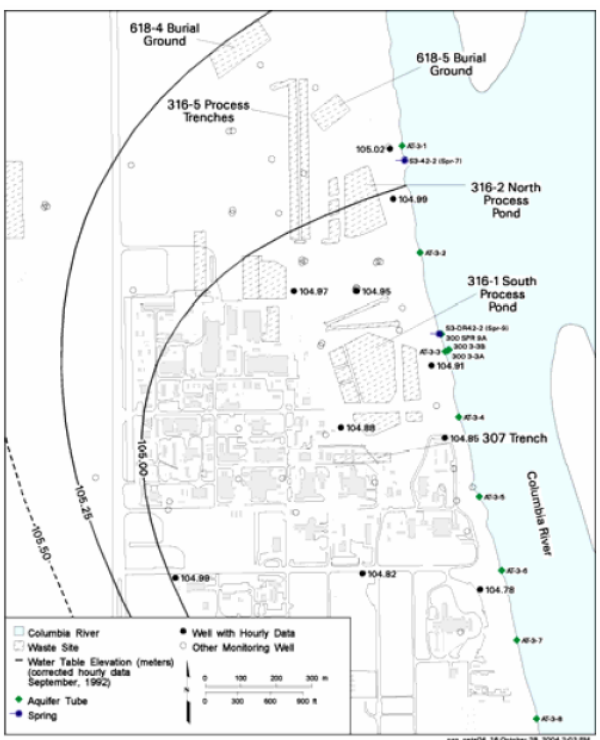

Figure 7-13. 300 Area water-table elevation, September 1992 (averaged hourly) (Peterson, 2005)

The fluctuating river stage causes corresponding fluctuations in water-table elevations. Typically, lines of equal topographic elevation result in flow in a parallel fashion from an unconfined aquifer into the adjacent stream. Water table contour shapes in the preceding Figure 7-10 through Figure 7-14 cannot be adequately explained by either topography or river infiltration into the aquifer. Contours at all seasons indicate that there could be an influence on the direction of ground water flow by the impinging river on the bank of the river. Consequently, dispersal of contaminants from a particular source may have a deflected path over the course of several years.

The water-table maps indicate that the ground water flow direction in the vicinity of the 300 Area process trenches, the last liquid waste disposal facility to receive uranium-bearing effluent, is generally to the south-southeast for all seasons (Peterson, 2005).

Periodic reversal of the hydraulic gradient (i.e., directed inland from the river) occurs near the river when the stage is high, but this change is not readily apparent in the monthly averaged data. Based on hydraulic gradients, Figure 7-10 through Figure 7-14 suggest that along the shoreline to the south of the process trenches, river water may be continually entering the aquifer, flowing south along the shore, and then discharging back to the river. The highly transmissive Hanford unit is thicker along this section of shoreline, which would possibly enhance this exchange (see cross section in Figure 7-7). The implication of having a fairly consistent long-term orientation of flow direction is that plume boundaries can be more accurately anticipated, especially when the source of the contaminant is also accurately known (Peterson, 2005). If however the flow direction is changing, then any conceptual site model and any monitoring program must take this into account.

Because of the highly transmissive character of much of the uppermost hydrologic unit beneath the 300 Area (Hanford formation), the water table elevation responds quickly to fluctuations in stage of the adjacent Columbia River. Consequently, the hydraulic gradient steepness and orientation may vary dramatically over the short time periods associated with daily river fluctuations. (Peterson, 2005).

7.2.8 300 Area Uranium Plume

The ground water beneath the 300 Area has been contaminated by liquid effluent discharges to a variety of disposal sites during a period of operations that extends from the late 1940s through the mid- 1980s. Since the end of fuel fabrication activities, contaminated discharges have largely ceased, although discharges of uncontaminated effluent continued until 1994. Remedial actions are underway and the structures and contaminated soil associated with most of these disposal sites have been removed. However, residual amounts of some contaminants remain in the underlying vadose zone, and their presence is indicated in ground water monitoring results (Peterson, 2005). Various ground water monitoring locations are provided in Figure 7-15.

The longevity of the 300 Area ground water uranium plume, despite attempted source term removal and copious water flow through the aquifer to the Columbia River, prompted an investigation into the processes controlling the release and transport of uranium at this site. The mildly alkaline pH and relatively high carbonate concentrations of the 300 Area porewaters are conditions that normally suppress hexavalent uranium

(U(VI)) adsorption on iron oxide-poor sediments as exist below the 300 Area; however, significant sorbed U(VI) concentrations (up to 250 mg kg^{-1} of uranium) are observed in the vadose zone. This sorbed U(VI) is believed to sustain the ground water plume through desorption as meteoric water infiltrates the vadose zone from above and as seasonal river stage fluctuations cycle ground water into the lower vadose zone from below. The lack of understanding of the distribution coefficient (Kd) for U(VI) makes modeling of the movement and mobility of uranium difficult.

The desorption or dissolution of uranium from capillary fringe sediments due to fluctuations in the water table controlled by changes in the adjacent river levels results in periodic pulsing of uranium into the ground water. This makes detailed characterization of the nature and extent of the contaminant plume within both the Vadose Zone and aquifer, along with compiling the detailed associated hydrogeologic and geologic conditions, paramount.

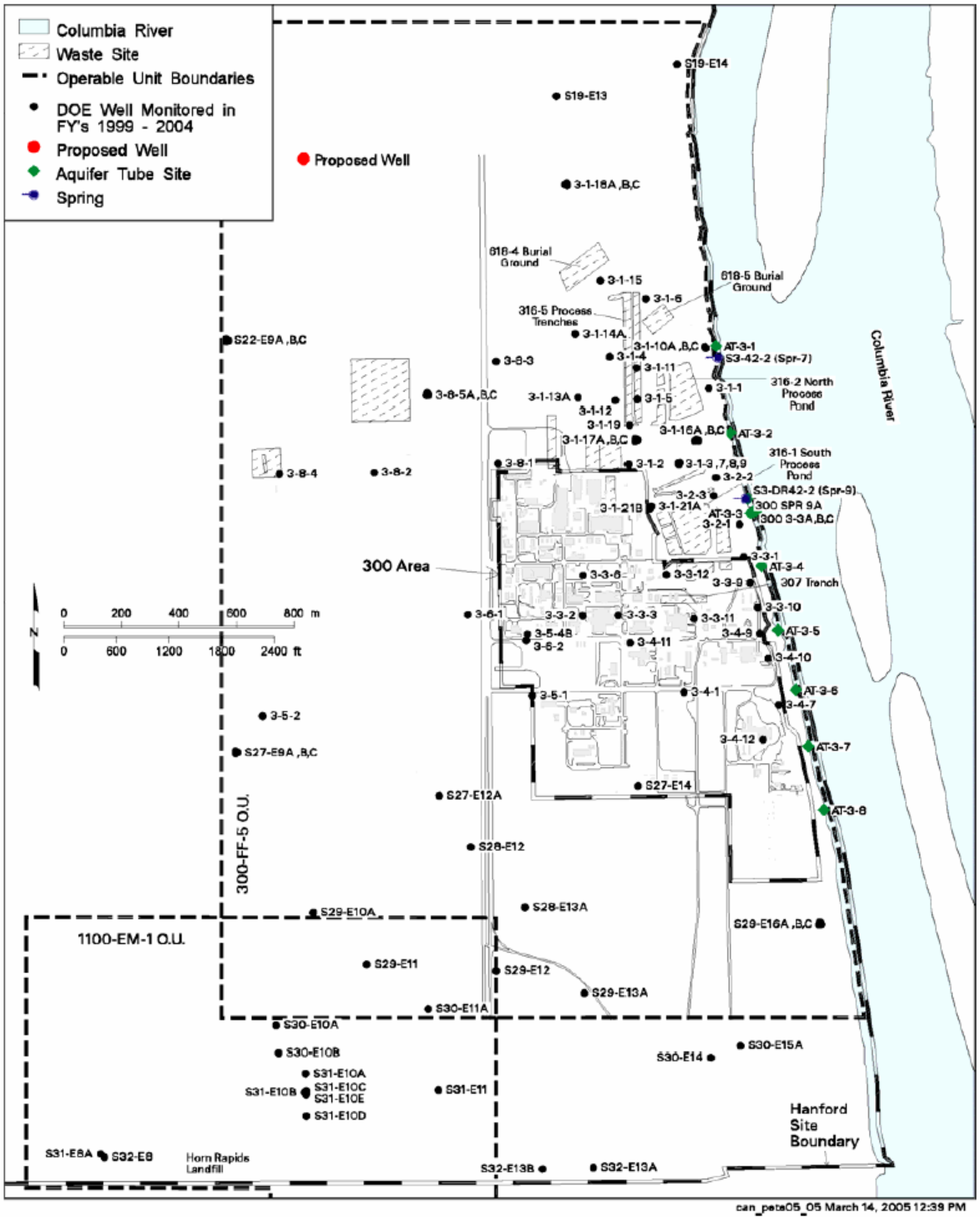

Figure 7-15. 300 Area ground water monitoring locations (Peterson, 2005)

7.2.9 Monitoring Considerations

Critical monitoring parameters to be considered in this type of environment include the collection frequency of water levels and ground-water samples. Annual monitoring of water-table levels would not likely show the short-term pulsing of the water table due to the changes in river levels. Fluctuations in the river stage not only occur seasonally, but hourly.

In addition, uranium concentrations in ground water from seeps collected at the edge of the Columbia River, near the point where ground water with the highest concentrations of uranium should discharge, were considerably lower than uranium concentrations collected from the river. This implies that there is a discharge of ground water through preferential pathways, potentially upwelling below the seep lines of the river or the uranium concentrations are coming from another source, possibly upstream. The concept of preferential pathways or the influence of river stage and pressure impact on the aquifer has not come into consideration in past ground-water models for the 300 Area. The geology consists of mostly river gravels of the Hanford Formation a highly variable formation with a likely potential for preferential pathways.

Development of semi-confined hydraulic heads due to infiltration of river water into the water table due to fluctuations in the river level could result in localized hydraulic pumping of ground water into the river. This condition may only exist for short periods of time during river level changes (Catalano et al., 2006).

Figure 7-16 provides a hydrogeologic conceptual model for movement of contaminants within the vadose zone and ground water below the 300 area in relation to changes in river stage (DOE, 2002).

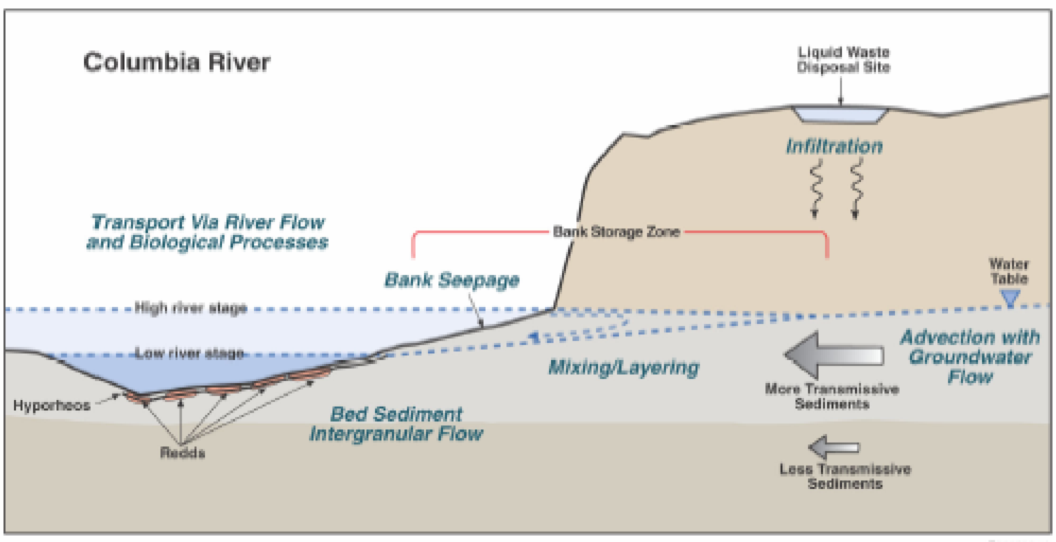

Figure 7-16. Hydrogeologic conceptual model of contaminant movement below the Hanford 300 Area (DOE, 2002)

7.3 Application of Ground Water Monitoring Performance Strategy

It is well documented that the 300-Area water table elevation changes in relation to the river stage. It is also well documented that a portion of a stream's flow may move through permeable materials adjacent to the stream. The USGS offers a stream transport simulator (OTIS) that includes inflow and storage in bank and bed materials. (Figure 7-17).

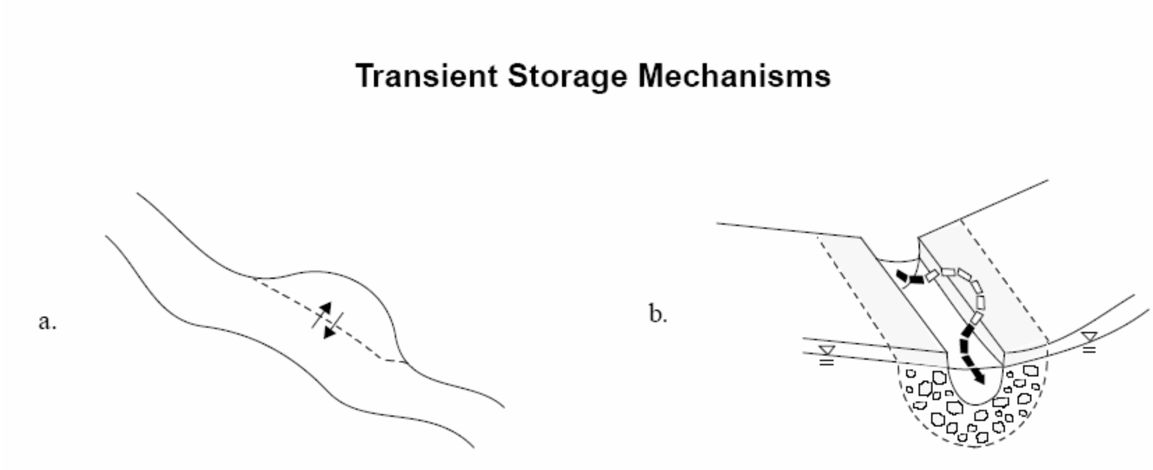

Figure 7-17. Transient storage mechanisms (Runkel, 1998)

Significant portions of the river flow may move through the coarse gravel of the streambed and, more importantly, the porous areas within the stream bank (Figure 7-17, Diagram B).

Modeling of river-ground-water interaction including surface water momentum is not generally done and requires computational hydrodynamic codes.

In the case of the Hanford 300 Area, transient migration of water into the bank of the outside bend of the adjacent Columbia River may have resulted in the downstream migration of contamination within Water Table Aquifer. As proposed in Figure 7-18, flow in the Columbia River adjacent to the 300 Area impacts the western bank (cutbank) just north of the 300 Area (north of the 618-5 Burial Ground Facility).

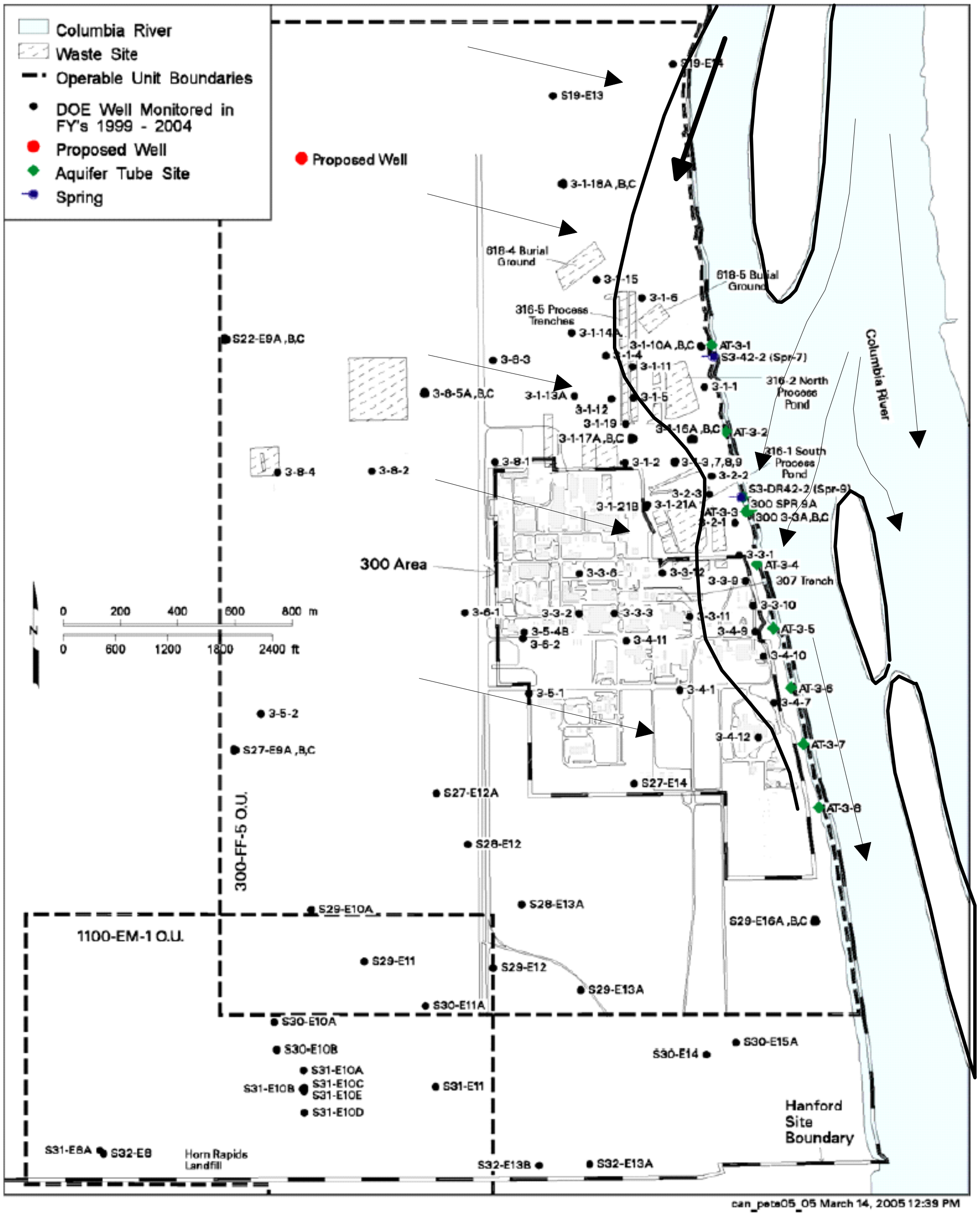

Figure 7-18. Alternative conceptual model of Hanford 300 Area showing potential infiltration and downstream flushing of formation

The arrows pointing from left to right across Figure 7-18 represent the movement of ground water towards the Columbia River. The bold arrow at the top of Figure 7-18 suggests the dominant intrusion and lateral movement of surface water from the Columbia River into the water table aquifer. The other arrows in the Columbia River follow general surface water flow. The curved line presents the conceptualized extent of surface water intrusion into the water table aquifer.

It is well documented that the water table in the 300 Area rises and falls with the changes in the river stage. The outside of bends in the river may also be impacted as well by water forced into the formation. The impact of the river on the water table may not be limited just to a simple lateral moving in and out of the formation. The water being forced into the formation can produce a "flushing effect" resulting in a downstream component of flow within the formation. Based on the geometry of the river, this flushing effect would be expected in the 300 Area in two locations: one at the upstream point where the river turns southeasterly and impacts the west river bank and adjacent to the 307 Trench, where river flow around the island adjacent to the 618-5 Burial Ground would impact the west river bank.

Figure 7-19 shows the actual extent of forced water intrusion and its effect on nitrate concentrations in ground water from 2002 (represented by the curved colored (teal) line). The shape of the contact between higher and lower nitrate concentrations mimics the shape of the water forced into the formation by the river, as proposed in Figure 7-18.

Downstream movement of water within the formation would also result in the downstream migration of contaminants as indicated for uranium in Figure 7-20 below.

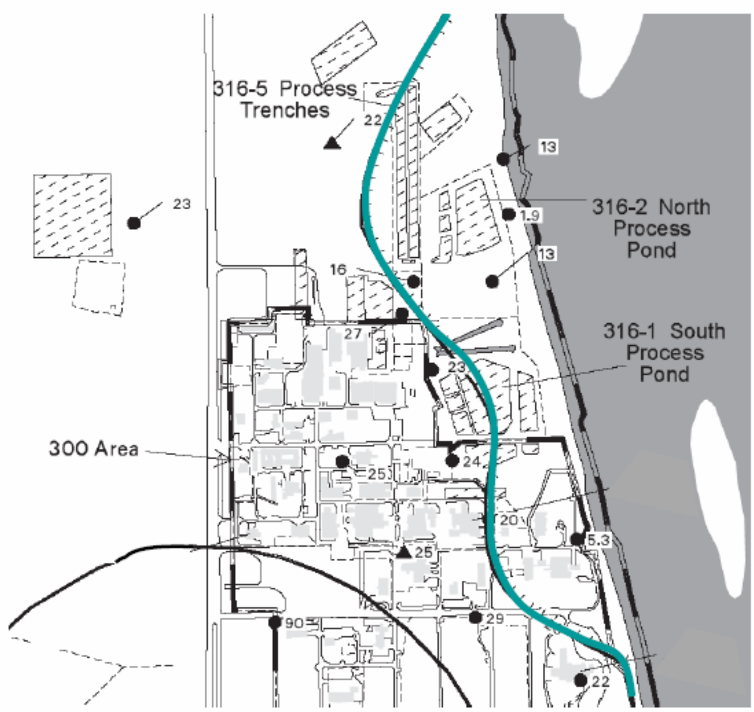

Figure 7-19. Extent of river water intrusion as estimated from nitrate concentrations in 2002(Yabusaki et al, 2004)

Shaded 300 Area Uranium, August 1997

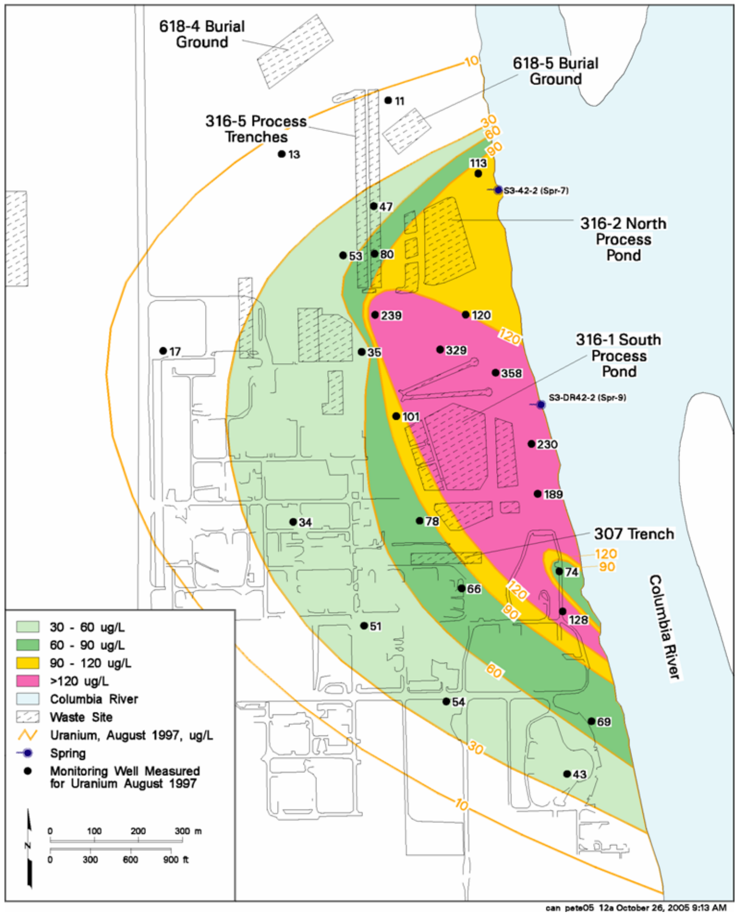

Figure 7-20. 300 Area Ground-Water Uranium Concentrations, August 1997

7.3.1 Performance Indicators and FEPs

Performance indicators and features, events, or processes (FEPs) for the Hanford 300 Area uranium plume include, but are not limited to:

The primary system performance indicators in our analysis of the Hanford 300 area are the shapes of the published uranium and nitrate contaminant plumes.

River stage is incorporated in all recent Hanford flow and transport modeling, but so far as we can determine, hydrodynamic effects of flow impinging on the cutbank of the Columbia River have not been incorporated in the CSM.

Re-analysis of existing monitoring data from wells in and near the 300 Area may provide insight into the distribution of river water components that could be related to hydrodynamic effects.

Additionally pressure measurements along the river bank might be possible.

7.4 Monitoring Strategy Application Conclusions

By applying the Strategy, we were able to perform a thorough compilation of the available geologic and hydrogeologic data for the Hanford 300 Area and gain a better understanding of the interaction of the Columbia River System with ground water.

Transient migration of water into the bank of the adjacent Columbia River at the 300 Area may produce a component of movement that can produce a “flushing effect” resulting in the downstream migration of contamination within the formation containing the Water Table Aquifer.

Thus, we have proposed an alternative to the 300 Area conceptual model that may improve the explanation of contaminant flow and transport at the Hanford 300 Area. Performance Indicators suggesting this revision to the conceptual model included the shape of the uranium plume and the position of the 300 Area on the cut bank of the Columbia River.

Hydrodynamic modeling should be evaluated as a means of evaluating the potential for a bidirectional component of contaminant movement in the water table.

Water-table monitoring collection frequencies could be adjusted to show the short-term pulsing of the water table due to the changes in river levels. Fluctuations in the river stage not only occur seasonally, but hourly. In addition, detailed changes in the river stage need to be documented. By evaluating these fluctuations in the water table in relation to the changes in river stage, conclusions can be drawn on the effects of transient migration of river water within the formation and subsequent movement of uranium.

In addition, the concept of preferential pathways could be further explored.

7.5 Hanford References

Catalano, J. G., et al. "Changes in Uranium Speciation through a Depth Sequence of Contaminate Hanford Sediments." *Environmental Science and Technology Magazine*. 2006.

Department of Energy (DOE). DOE/RL-98-48, Rev. 0, Volume II. "Ground water/Vadose Zone Integration Project Background Information and State of Knowledge." U.S. Department of Energy: Richland, Washington. 1998.

DOE. DOE/EIS-0222-F. "Hanford Comprehensive Land-Use Plan Environmental Impact Statements." U.S. Department of Energy: Richland, Washington.1999.

DOE. DOE/RL-2002-11, Rev. 0. "300-FF-5 Operable Unit Sampling and Analysis Plan." Prepared by CH2M HILL Hanford, Inc. for the U.S. Department of Energy: Richland, Washington. 2002.

DOE. Site Transition Plan for the Rocky Flats Environmental Technology Site, Office of Legacy Management and Office of Environmental Management, DOE-LM&EM/GJ-662-2005, March 2005.

Faybishenko, B. "Vadose Zone Characterization and Monitoring" in: Looney, B and Falta, R, *Vadose Zone Science and Technology Solutions*, Vol. 1.pp. 133-509. 2000.

Lindsey, K. A., et al. WHC-SD-EN-TI-012, Rev. 0 "Geology Setting of the 200 East Area: An Update." Westinghouse Hanford Company: Richland, Washington.1992.

Peterson RE (ed.). PNNL-15127. "Contaminants of Potential Concern in the 300-FF-5 Operable Unit:" Expanded Annual Ground water Report for Fiscal Year 2004. Pacific Northwest National Laboratory: Richland, Washington. 2005.

Runkel, R.L. "One-Dimensional Transport with Inflow and Storage (OTIS): A Solute Transoprt Model for Streams and Rivers." U.S Geological Survey, Water-Resources Investigations Report 98-4018. 1998.

Vermeul, V.R., et al. PNNL-14398. "Transient Inverse Calibration of the Site-Wide Groundwater Flow Model (ACM-2)." FY 2003 Progress Report. September 2003.

Yabusaki, S., et al. Powerpoint Presentation: "Objectives and Tentative Scientific Approach for Uranium Reactive transport Modeling in the 300 Area." PNNL. May 10-11, 2004.

8 Analysis of Characterization and Monitoring Data

8.1 Introduction

Accurate analysis of site characterization and monitoring data is a crucial, and often challenging, part of development of a sound ground-water monitoring strategy. This Chapter overviews data analysis methods that may aid development and implementation of the Integrated Ground-Water Monitoring Strategy, and offers suggestions for avoiding common pitfalls related to review of environmental data. While this is not a comprehensive discussion of all the issues, it focuses on lessons learned through review of site data from around the DOD, DOE, and NRC complex.

Development of an optimized ground-water monitoring strategy requires an adequate understanding of flow, transport, and risk. In some cases, careful review of existing data yields sufficient information to understand flow and transport, and thereby to choose a confirmation monitoring scheme. In other cases, additional characterization may be necessary to reduce model uncertainty in order to optimize the monitoring approach. In either case, the concepts in this chapter are intended to help you maximize the value of the data available to you. Topics covered include:

- Data types
- Basic statistical analysis
- Methods for identifying data errors and outliers
- Quality control charts and the T-Test
- Mann-Kendall Test – lessons learned
- Rainfall data – methods of analysis and sources of uncertainty
- Finding correlation between monitoring well data
- Water level measurements
- Unmixing of multimodal data
- Cluster Analysis
- Factor Analysis
- Methods for analyzing mapped data, and
- Quality assurance

In addition to these topics, we would like to emphasize the value of 3D conceptual modeling of spatial data in understanding flow and transport. In Chapters 1-7 numerous modeling examples are provided, along with modeling software recommendations. In our experience, this sort of visualization can tremendously aid in understanding a subsurface system.

8.1.1 Data Types – Characterization versus Monitoring

Generally speaking, characterization and monitoring entail different sorts of measurement activities. Specifically, characterization includes measurement of intrinsic properties of a site. Also, characterization measurements at a given point may be made only once, although some site characteristics like rainfall, response of wells to rainfall, response of wells to tides, or establishing a water quality baseline could require extensive periods of observation. Characterization and monitoring data will have geographic and time coordinates (x, y, z, t) and may vary across the site in 4-dimensional space.

Monitoring is often measurement of something that is expected to change, with the change meaning something in terms of risk-related processes such as plume movement. Monitoring data are acquired to evaluate progress of some ongoing process, or to alert the site operator to an off-normal situation. Monitoring data are generally acquired at a fixed point in space, so vary only in time. These would include results from sampling from a device such as a lysimeter or a well that has been placed in one point. Results may derive from field measurements (e.g., pH, alkalinity, conductivity, turbidity radon …) or may derive from measurements on a sample sent to a laboratory (e.g., anion content, organic content, cation content, radionuclide content…). Establishing baseline values for measurements to be made at a monitoring point, (x, y, z, t) is part of characterization, and detecting changes in the baseline are part of monitoring effort.

Much of the uncertainty in estimating risk from subsurface contamination can be traced to uncertainty in site characterization and monitoring design. For example, it does not matter if a ground-water sample is analyzed to femto-Curie levels of Sr-90 if the sampling point is not chosen appropriately. Similarly, it does not matter if a flow and transport model is built and forced to calibrate if features in the site geology that control flow are not characterized adequately.

In addition, selection of appropriate chemical methods is important. It does no good to monitor for a given constituent of concern if the method detection limit is not below regulatory requirements or other action levels (Example: method detection limit is 10 mg/L and the MCL is 1 mg/L). Ideally methods should be chosen to provide quantitative data for all analytes at their ambient levels, with very few “below detection” results. Missing values, or truncated data sets, limit one’s ability to glean understanding of the system being tested.

An Integrated Ground-Water Monitoring Strategy does not include site characterization and pre-operational monitoring, but must include review and evaluation of characterization data and existing monitoring data in order to select critical monitoring points within the system. If characterization is adequate, and if the characterization has been used correctly in flow, transport, and risk models, then the task of confirmation monitoring design is simplified.

If characterization is not adequate, then selection of monitoring points is more difficult. The site manager must decide whether the risk associated with the remaining uncertainties is acceptable or not, and take appropriate action. This action could mean re-running a Performance Assessment (PA) model, and could also include filling gaps in characterization if the PA indicates unacceptable risk. Reducing model uncertainty by installing monitoring systems could be called characterization.

8.1.2 Data Evaluation versus Statistical Analysis

The distinction between data analysis and statistical hypothesis testing is important. Many of the data analysis techniques violate assumptions made in formal statistics, but produce useful results; likewise, many formal statistical tests may provide useful insight even when the data tested (e.g., log-normal data) violate the test assumptions.

Data evaluation is the process of looking for associations, trends, patterns, or outliers in the data. The purpose is to alert an investigator to something in the data structure that may have implications about a process or anything that might have meaning to the investigator. Multivariate data analysis has recently been popularized as “data mining.”

Statistical analysis of data is the process of testing a data point against some hypothesis about the data. Classically this comes from quality control in a production operation or manufacturing setting. Section 8.1.3, below contains a more detailed discussion on quality control analysis using the T-Test.

Below are several recommended sources for additional reading about data evaluation and statistical analysis:

Velleman, Paul F., article in The American Statistician (1993) 47:1, 65-72 (and its discussion in various internet sources) presents an enlightening discussion of this topic.

EPA (2003, 2004), in their *Guidance for Monitoring at Hazardous Waste Sites*, discusses some of the objectives of data analysis and statistical testing. Their discussion is from a different viewpoint than that presented here, but the common feature is that the purpose of the data analysis is to provide a person or team with a basis for making a decision either about the monitoring system or about what the data are telling in terms of risk so that a decision can be made.

NIST (2004) has an online statistical handbook that goes into depth on data analysis. They list the objectives of data analysis:

1. Maximize insight into a data set;
2. Uncover underlying structure;
3. Extract important variables;
4. Detect outliers and anomalies; and
5. Test underlying assumptions.

They also point out that there is no prescription for data analysis. The operator must understand the philosophy of data analysis and apply this to the problem at hand.

8.2 Univariate data

Univariate means basically that we consider one variable at a time. In nature we often find that the population from which we draw samples is formed from the mixing of several sources. For example, copper in soil samples may be ascribed to underlying bedrock, or two types of bedrock and to atmospheric deposition from a smelter. Even contaminants, such as TCE, in a given water sample may be present from leaking tanks at multiple upgradient areas.

Sometimes it is obvious that there are multiple sources for a given analyte, and we can estimate how to partition the data so as to better understand the sources. Sometimes the underlying chemical or geochemical processes leading to the observed values produce a time-varying distribution – for example, a spill or burial may dissipate with time. This might result in monitoring observations that fit an exponential function.

Univariate populations may fit the familiar so-called normal or Gaussian distribution. Sometimes taking the logs of the data may produce an apparent fit to the normal curve. A number of distribution types have been recognized by statisticians, and statistical tests have been developed for each. Most familiar statistical terms such as the Pearson product-moment correlation coefficient assume a Gaussian distribution and lose meaning for strongly skewed data sets.

Statistical tests that do not depend on the population or sample distribution have been developed. Generally these are based on ranking the numbers and using ranks rather than values. (c.f. Kendall, 1975; Siegel, 1956) This chapter only provides a glimpse at some practical issues so that the data problem holder will seek expert help for data analysis.

8.2.1 Basic Statistical Analysis

Basic univariate analysis includes the computation of the mean (Equation 1), standard deviation (Equation 2), variance (square of the standard deviation), coefficient of variation (standard deviation divided by the mean), and identification and possible rejection of extreme observations (discussed in Section 8.2.2 below).

Equation 1. Mean

$$m = \frac{1}{N}\sum_{i=1}^{N} H_i$$

Equation 2. Standard deviation

$$\sigma = \sqrt{\frac{\sum_{i=1}^{N}(H_i - m)^2}{N-1}}$$

In the above equations, *m* is the sample mean of the observations, *N* is the number of observations, *H* is the observed values, σ is the standard deviation of the observations.

For time-series data sets, trend analysis with the Mann-Kendall test provides us more information about the temporal variation of the water heads and concentrations. The Mann-Kendall test is discussed in detail in Section 8.2.4 below.

8.2.2 Identification of Outlier Points

An important part of data analysis is identification and assessment of potentially erroneous data points. A measurement may be read, recorded, or transcribed wrongly, or a mistake may be made in the way in which a treatment was applied for this measurement. A major error greatly distorts the mean, the standard deviation, the variance, and the coefficient of variation, and affects conclusions about the trends and correlations. The principal safeguards are vigilance in carrying out the operating instructions in the measuring and recording process, and eye inspection of the observation data.

If a figure in the data to be analyzed looks suspicious, an inquiry about this observation sometimes shows that there was a gross error. If no explanation of an extreme observation is discovered, we may consider rejecting it. The discussion of rules for the rejection of observations began well over a century ago in astronomy and geodesy. Most rules have been based on something like a test of significance (Snedecor and Cochran, 1976). The investigator computes the probability that a residual as large as the suspect would occur by chance if there is no gross error. If this probability is sufficiently small, the suspect is rejected. Anscombe and Tukey (1963) present a rule that rejects an observation whose residual has the value of d if $|d| > Cs$, where C is a constant to be determined with the following equation which is obtained from Snedecor and Cochran (1976), and s is the standard deviation of the observations calculated from Equation 2.

Equation 3. Anscombe and Tukey significance test

$$C = K\left(1 - \frac{K^2 - 2}{4(N-1)}\right)\sqrt{\frac{N-1}{N}}$$

$$K = 1.4 + 0.85z$$

In Equation 3, N is the number of the observations, z is corresponding to the one-tailed probability value of $\frac{N-1}{N}P$ in the normal distribution, where P is the small premium which is involved in a rejection rule, say 2.5% or 5%.

After rejecting the outlier points, we carry out the statistical analysis with the treated data sets. The results are compared with those obtained with the original observation data sets.

8.2.3 Quality Control Charts: the T-Test

A classic example of statistical analysis is 'Student's T-Test'. This test is often used to analyze monitoring well results and other types of univariate analysis. Originally, William Sealy Gossett developed this test to detect off-normal conditions in the production of Guinness beer. In this case, a new measurement (e.g., sugar content, specific gravity…) can be compared with historical data representing "normal" conditions. The result is a confirmation or rejection of a hypothesis that the new measurement is drawn from the normal population. Because any introductory statistics text will include the T-test, we will not discuss it further here.

The results of a T-test can be expressed graphically in the form of a "control chart" for process monitoring on which the target value is plotted as a horizontal line against time with parallel lines at the uppermost and lowermost "normal" bounds (at some confidence level for acceptance of the "is normal" hypothesis) (Figure 8-1).

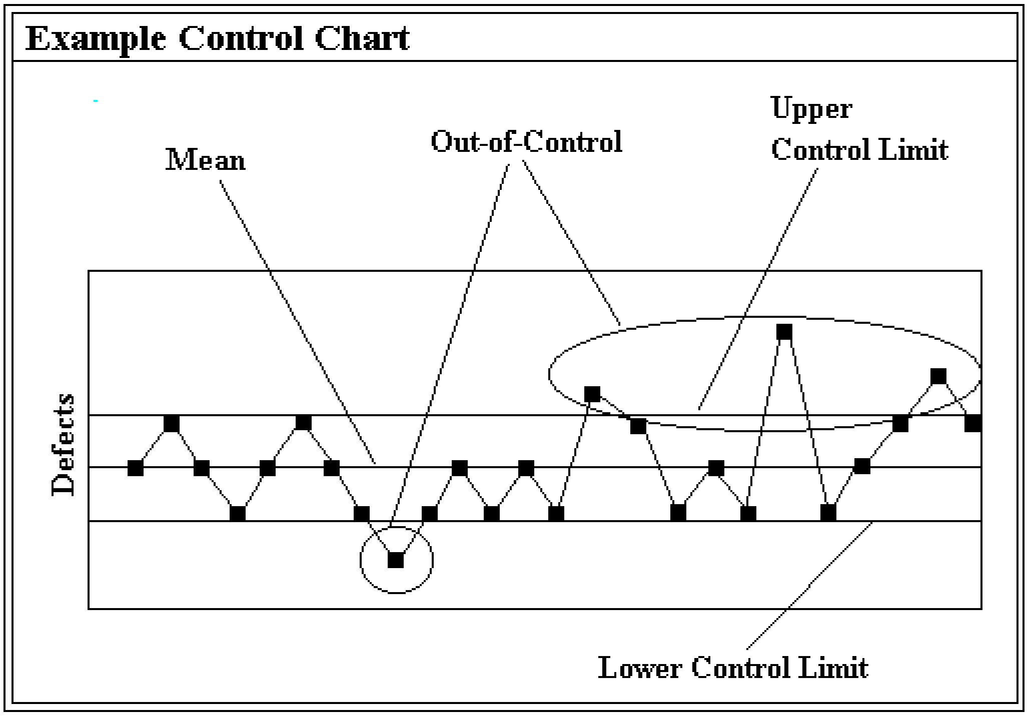

Figure 8-1. Example control chart

A version of this method is typically used in ground-water monitoring programs to spot anomalous results as they are returned from the lab. Characterization, or pre-operation monitoring is used to establish an expected range for some variable – say pH, or water level. This expected range is used to bound 'normal' values for the variable – and periodic measurements are compared to the normal value, commonly by displaying them on a chart. Visual inspection of the chart or a computerized notice alerts the operator to an off-normal condition. The operator then decides on an action. In the case of a plant producing thousands of items per hour, this may mean an immediate adjustment of operating conditions. In the case of a ground-water monitoring result, the action might include a recheck of the analysis, and following that, possible re-sampling of the field site. All off-normal results should be referred to technical experts for evaluations – the job of inspecting control charts is often assigned to technicians who may not have the perspective to fully evaluate the potential meaning of an off-normal observation..

If the off-normal condition is confirmed, then its meaning must be determined so that any possible risk implications can be judged. This may mean re-running a computer simulation, it may mean revising a conceptual model. It could indicate a release of contamination, or the impending approach of an unknown plume. It could point to an analytical or sampling problem. It may trigger a regulatory reporting requirement. Interpretation is the responsibility of the individual investigator in the context of extensive site-specific knowledge.

Time-trends are also revealed with the control chart method. Changes in variance or upward or downward trends in the mean will be revealed in such a chart. This is especially important in judging behavior of a contaminant plume, or for tracking progress of a remediation process.

The methods of univariate data analysis and statistics have been developed mainly since the 18th century: Gauss, Bayes onward. The reader is referred to basic statistics texts for information. My favorite is: Peatman, John G., (1936, '41, '47) "Descriptive and Sampling Statistics."

Guidance

When preparing a control chart:

- Plot all measurements against time.
- Watch for changes in variance.
- Watch for data outside the expected range.

8.2.4 Applying the Mann-Kendall Test

To evaluate the presence of trends in the time-series observations at individual monitoring wells in this report, we applied the Mann-Kendall test, which is commonly reliable in the interpretation of environmental data (Helsel and Hirsch, 2002; Soderberg et al., 2005). This test is often applied on data sets from monitoring wells to assess the stability of a contaminant plume and it is an important tool in the decision making process that relates to ground-water monitoring network design.

The Mann-Kendall test is non-parametric and therefore does not assume an underlying distribution in the data sets. It can address missing data values and be modified to account for seasonality or predictable fluctuations (Soderberg et al., 2005). In the Mann-Kendall test, a statistical parameter *S* is valuated with Equation 4 by comparing each data point to the data points that occur after it in the time series (Gilbert, 1987).

Equation 4. Mann-Kendall test

$$S = \sum_{i=1}^{N-1} \sum_{j=i+1}^{N} \operatorname{sgn}(H_j - H_i), \qquad \operatorname{sgn}(H_j - H_i) = \begin{cases} 1, & \text{If } H_j - H_i > 0 \\ 0, & \text{If } H_j - H_i = 0 \\ -1, & \text{If } H_j - H_i < 0 \end{cases}$$

In Equation 4 above, *H* indicates observed values, and the sign of *S* indicates the direction of the trend (i.e. positive *S* indicates an upward trend, negative indicates a down trend and 0 value indicates flat or no trend). *S* and *N* are then used to read a p-value from a statistic table (Gilbert, 1987), and the p-value is a measure of the significance of the trend. When $N < 10$, a two-tailed test is used to test for both upward and downward trends in a single alternative hypothesis.

For large data set ($N > 10$), *S* can be modified to be approximated by a normal distribution. Another statistical parameter, *Z,* is calculated by Equation 5:

Equation 5. Z calculation

$$
Z = \begin{cases} (S-1)/\sigma_s & \text{If S} > 0 \\ 0 & \text{If S} = 0 \\ (S+1)/\sigma_s & \text{If S} < 0 \end{cases}
$$

$$
\sigma_s = \sqrt{\frac{N(N-1)(2N+5) - \sum_{i=1}^{N} T_i i(i-1)(2i+5)}{18}}
$$

In the above equation, *T* is the number of tied values. With a calculated Z value we can compute a p-value from the normal distribution to evaluate the significance of the trend found from *S* value.

The example in Figure 8-2 below illustrates how simple the Mann-Kendall test really is. The next few figures illustrate that use of this simple test may, in some cases, actually obscure information that should be gleaned from the data. We provide this as an example to make the reader more aware of possible sources for misinterpretation when applying this test.

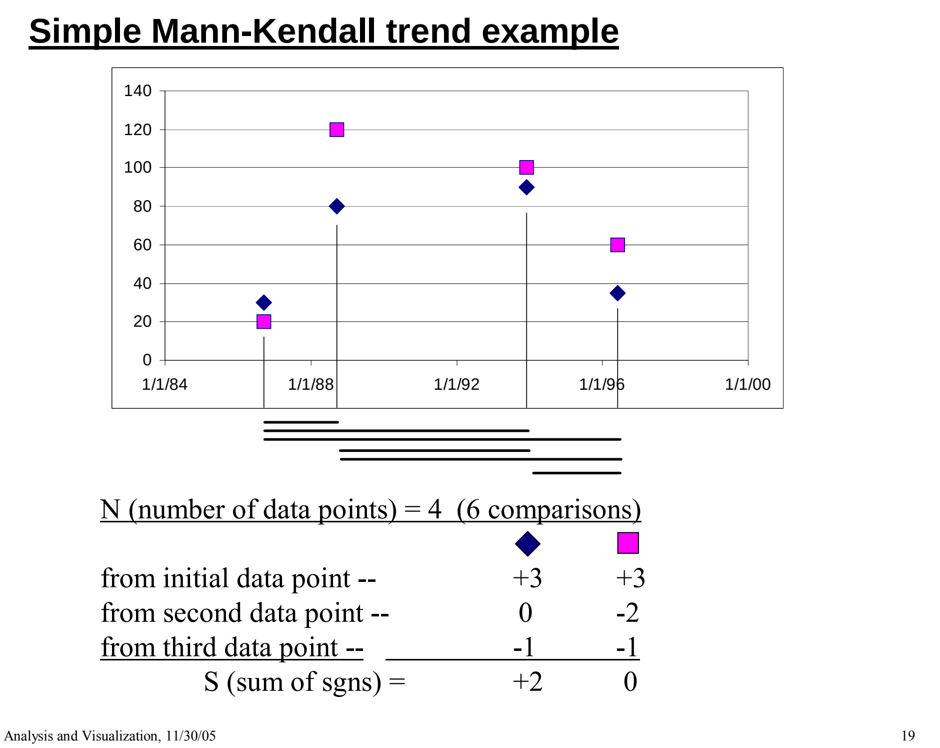

Figure 8-2. Mann-Kendall Example

Figure 8-3, labeled "Seasonal Kendall Slope Estimator," shows PCE concentrations over several years at a monitoring well. For each sampling point a determination is made as to whether the subsequent sampling events result in a higher of lower concentration. The plotted data in Figure 8-3 yield a -18 value – or a strong downward trend.

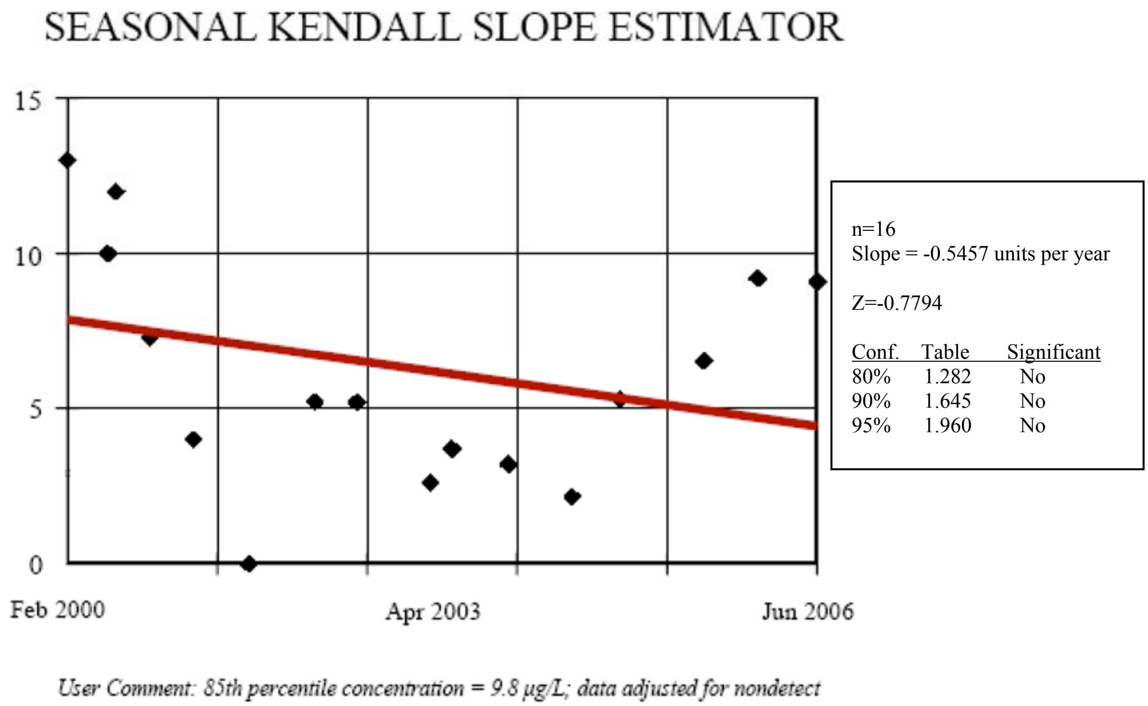

Figure 8-3. Published figure indicating declining PCE concentrations in ug/L (DOE, 2006)

A simple linear regression evaluation of the data provided in Figure 8-3 is represented in Figure 8-4. This simple regression evaluation also shows an overall reduction in PCE concentrations over time. However, a closer examination of the data reveals a steep downward trend over six sampling events, followed by an upsurge and gradual decline over the next six sampling events, and finally an increasing concentration trend for five sampling events.

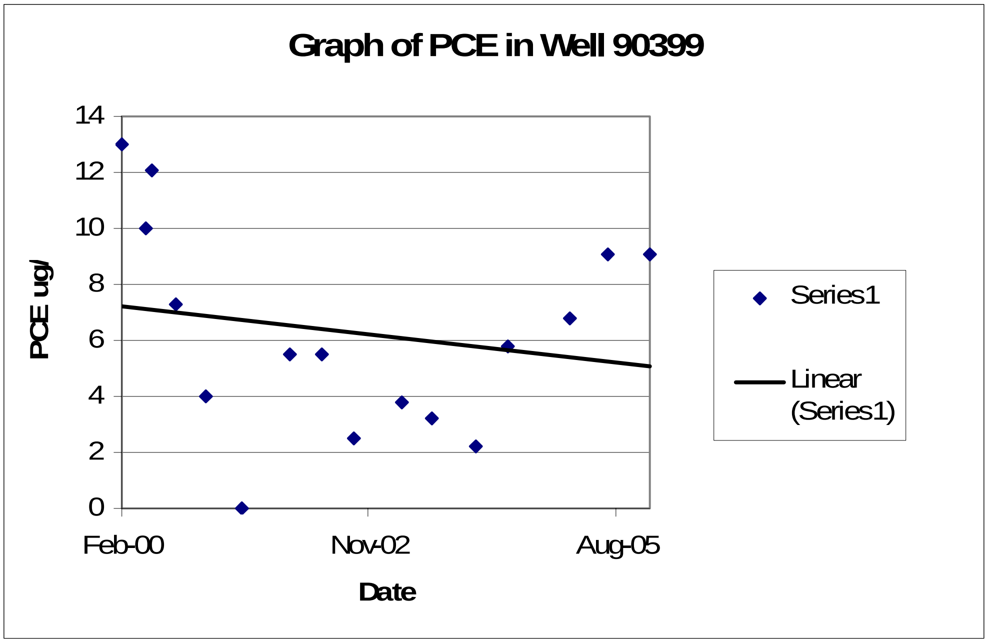

Figure 8-4. Linear regression fit to PCE data from MS-EXCEL

Figure 8-5 shows the data broken into three groups with trend lines for each. It is possible that the three slopes represent some hydrogeological phenomenon such as contaminant release from a pool or from the vadose zone as a function of infiltration or water level. We discuss a similar example at Rocky Flats elsewhere in this document. The line equations are of the form y=mx+b, where m is the slope and b the intercept. Excel uses Julian dates which are around 30,000, but displays dates as days, months, and years, thus the slope is a very small number even though the line plots as a steep line.

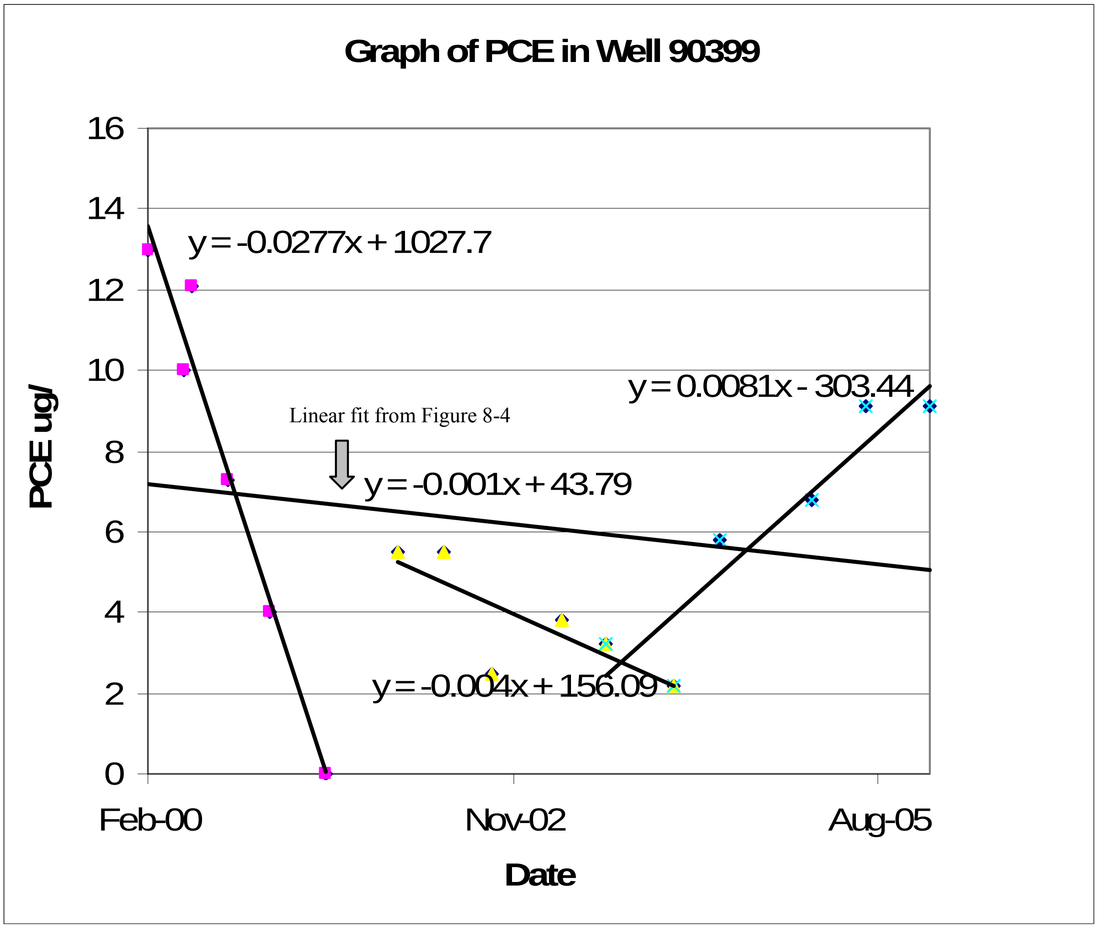

Figure 8-5. Parsing time series data into three groups.

The simple determination that there is an overall downward concentration with time at this observation point is correct. Unfortunately, presenting only this conclusion may obscure the fact that the ground water / contaminant system is displaying complex behavior that might indicate future non-compliant excursions of contaminant concentrations.

An example based on monitoring of VOCs at the DOE Rocky Flats Site is discussed in Chapter 5 above. In the example monitored results decline and remain low for long periods of time until an unusual weather event seems to flush contaminant from a bedrock pool into the water table flow system. This example provides insight into the issue of when to stop monitoring. Weather, including decade-long precipitation cycles may control apparent trends in contaminant amounts.

8.3 Rainfall Data – Sources of Uncertainty for Infiltration

Infiltration rates and permeability are two key variables controlling the accuracy of ground-water flow and transport models. Infiltration comes from rainfall and from engineered features such as leaking water systems and disposal or retention ponds. This section provides background for understanding uncertainty in infiltration. It specifically illustrates the importance of exploring all possible water sources when developing a conceptual model, and the importance of verifying that rain station data matches observed site conditions.

8.3.1 Consider All Water Infiltration Sources

Often the amount of leakage from water supply systems is poorly known. It can be estimated by shutting off the water supply to and from storage tanks and measuring loss over a period of time. A forty year old water system at the Savannah River Site in a non-industrial area – i.e. where drinking, sanitary supply, and fire suppression were the only water lines in about a five-acre area – was shown to leak almost 100 gpm, which would have gone undetected had the supply well not been turned off in support of aquifer performance testing (ref. personal knowledge). That was about one gallon per square foot per day. Because the leakage was underground in a grassy or paved area, most of this water moves downward as infiltration. By way of contrast, infiltration from rainfall was on the order 15" of rain per year or one cubic foot per square foot per year. That was 7.5/365 gallons per square foot per year or 0.02 gallons per square foot per day. Thus infiltration from leaking water lines was much greater than natural infiltration in this area. This case illustrates the importance of identifying all known water sources, natural and man-made, that could influence a system, and assessing the impact that these sources could have on the water table and infiltration.

8.3.2 Ensure Rain Station Data Match Facility-Specific Gauging

Infiltration is often estimated from rain gauging stations and estimates of the balance between evaporation, runoff, and infiltration. In the next few paragraphs, tables and figures will illustrate that facility-specific gauging should be done if local rainfall is to be known with any precision.

The Savannah River Site has a number of weather and rain gauging stations. We are grateful to the DOE Savannah River Operations Office for access to daily rainfall data.

The raw data from the five rain gauging stations presented in Figure 8-6 include 8000 records taken over 22 years. Visual presentation of data points in scatter plots by month reveals that while winter rainfall patterns are relatively uniform over a large area, summer rainfall varies significantly even at short distances. Figure 8-7 compares rainfall data from the mid-1980's through 2002 at Stations F and H, which are located just two miles apart. In this graph, Station F data is on the Y axis and Station H is on the X axis. Perfectly correlated data would group along a single line. As we can see from the data in July, rainfall measurements are quite scattered indicating that rainfall at one station is not indicative of the same intensity of rainfall at the other due in part to frequent isolated thundershowers. January data is more tightly grouped and is representative of data seen in the winter months due in part to the passage of large weather systems.

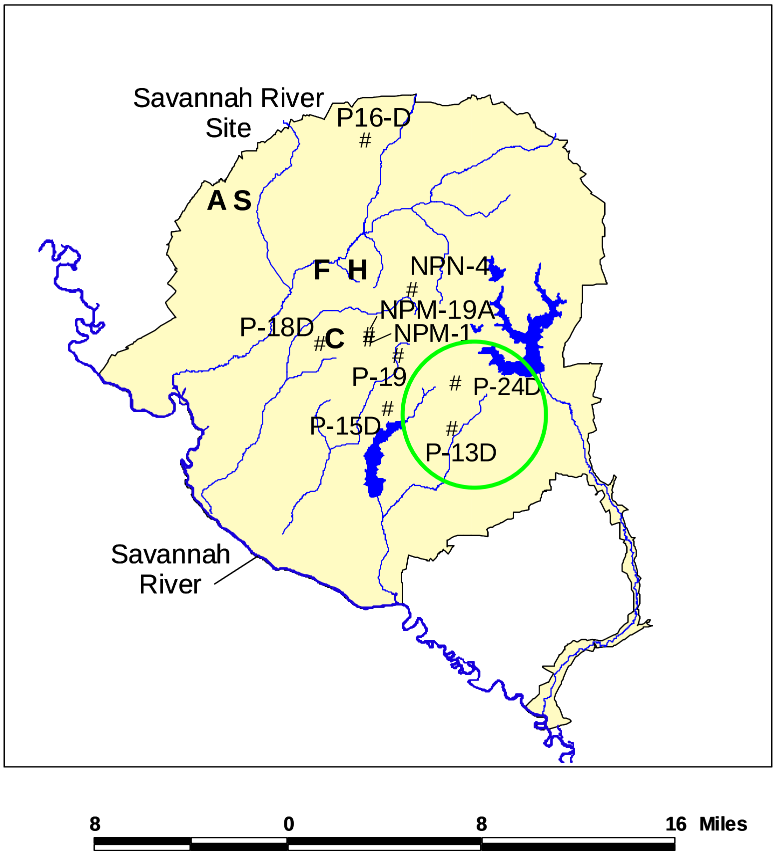

Figure 8-6. SRS rain gauging station and well locations. Rain stations are located under respective station identifier A, C, F, H, and S. Well locations are denoted by black dots. Adapted from Jones, 1990.

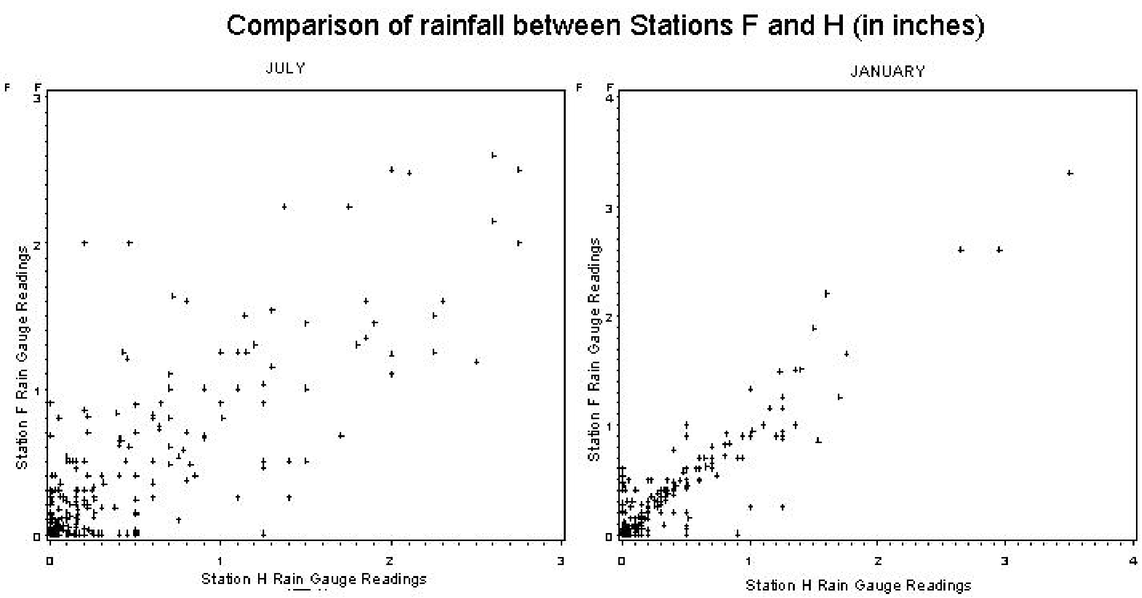

Figure 8-7. Rain data for Stations F and H, which are only two miles apart, show that particularly in summer, rainfall patterns are highly variable, even over short distances.

Figure 8-8 compares 17 years of rainfall data at Stations C and S. The Figure illustrates that at a distance of seven miles, rainfall readings vary significantly. In July, for example, it is not uncommon to see a variation of more than an inch between stations.

In Figure 8-9, data from all five stations was used to show the correlation as a function of distance. As shown in the Figure, summertime rainfall patterns are significant, and vary much more than winter rainfall. Another possible factor is the azimuthal relation between gauging stations. Winter or summer, most weather systems move from west to east in this area. Station H is almost due east of station F, whereas station S is almost due north of station C.

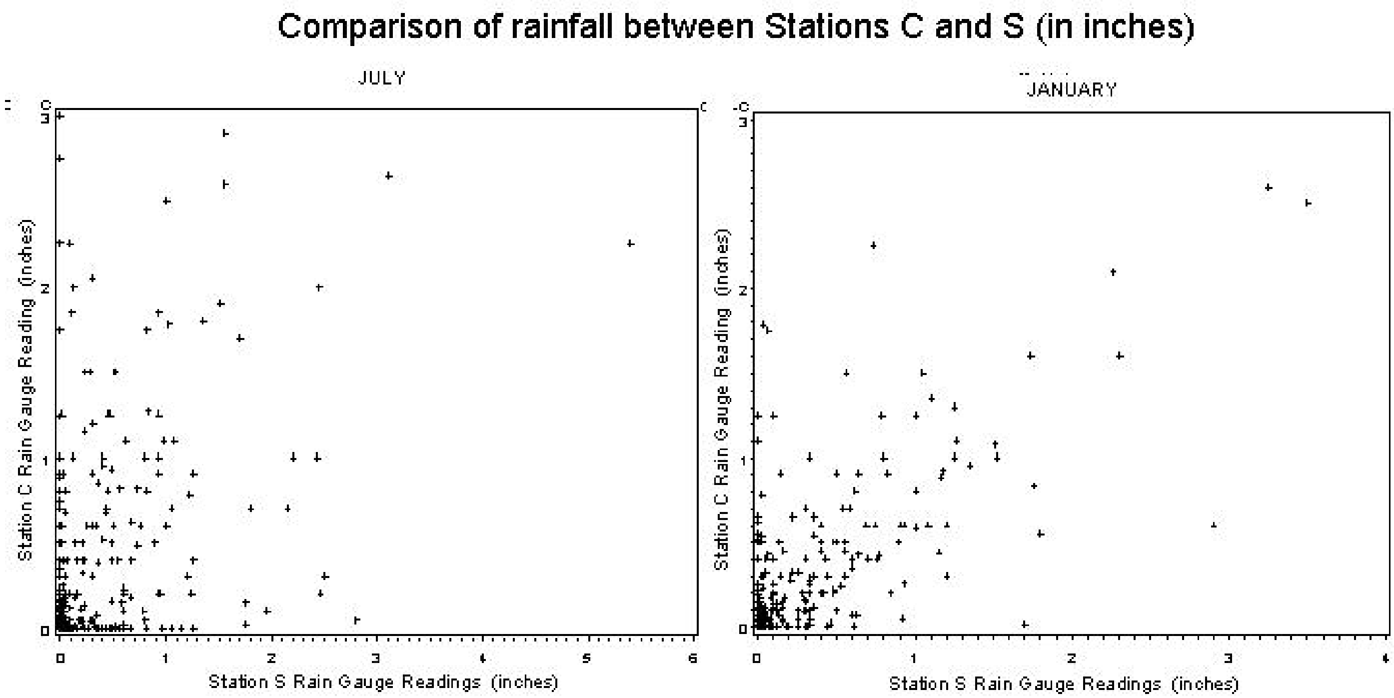

Figure 8-8. Rain Gauges C and S are about 7 miles apart and show significant variation in observed rainfall.

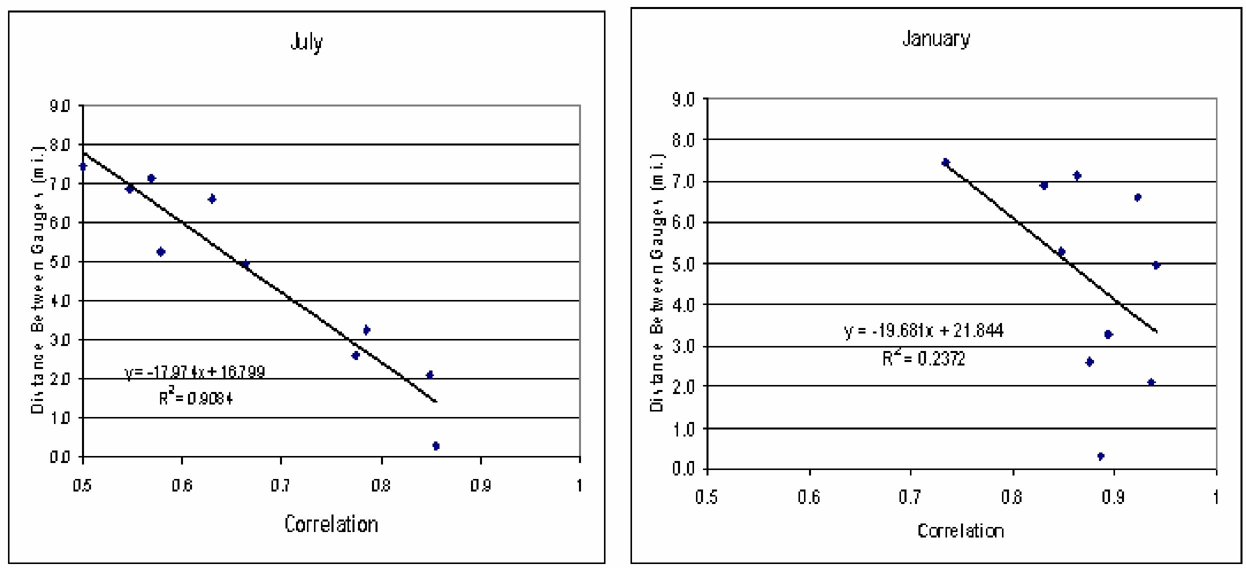

Figure 8-9. Correlation of rainfall as a function of distance in July and January.

This case illustrates the need to ensure that rain measurements used in conceptual modeling match actual observations. A surprisingly short distance can make a large difference in the amount of rainfall received. Further, the correlation between rainfall and distance to the station can vary significantly by season. Site managers should be aware of this phenomenon if observed data do not closely match modeled contaminant movement.

8.4 Correlations between different wells

To interpret the relationship between data in different monitoring wells, we can compute the correlation coefficients among them. Understanding the correlation between wells can help us to analyze the hydrogeologic conditions and build the conceptual site models. For example, the correlations between two wells which are located in two aquifers separated by a confining layer, may give us information about the continuation of the confining layer and the hydraulic connections of the two aquifers. The correlation coefficient (ρ_{ij}) is computed by Equation 6 below.

Equation 6. Correlation coefficient

$$\rho_{ij} = \frac{C_{ij}}{\sigma_i \sigma_j} = \frac{E(H_i H_j) - m_i m_j}{\sigma_i \sigma_j}$$

where C_{ij} is the covariance. H indicates the observed value, E is the expected frequency, and m is the mean. Considering the significance of the correlation, we define:

If $\rho_{ij} > 0.9$, H_i and H_j are positively correlated;
If $\rho_{ij} < -0.9$, H_i and H_j are negatively correlated;
If $-0.1 < \rho_{ij} < 0.1$, H_i and H_j are not correlated, or independent.

A real data set from Savannah River Site, South Carolina, is used to test the statistical methodology introduced above. In this data set, there are water head observations from

137 monitoring wells, in which each well includes about 16 time-series water head observations. The computer code developed here is used to compute the mean, variance, standard deviation, coefficient of variation, and the Mann-Kendall trend parameter for each well. To evaluate the significance of the trends, we also compute the p-value for each trend analysis. Finally, the correlation coefficients between different monitoring wells are calculated to help us to evaluate the conceptual site models for ground-water flow and transport modeling. The results of the first 10 wells of this data set are listed in Table 8-1. Fortran 90 code for the computations is included as Appendix B to this chapter.

Figure 8-10 presents selected water head curves to demonstrate the results from statistic analysis. Wells P-15D and P-18D, P-15D and P-19TD, P-15D and P-25TA, and P-19TD and P-25TA are positively correlated, P-15D and P-22D are negatively correlated, and P-22D has a downward trend but all others have an upward trend. An outlier point was removed from P-18D, P-19TD and P-25TA.

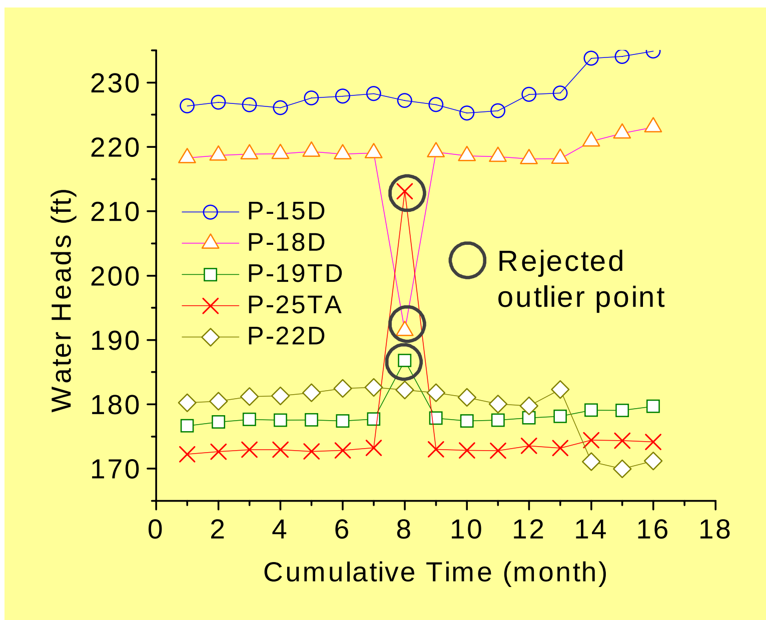

Figure 8-10. Rejection of outliers

The three outlier points shown in Figure 8-10 are on the same date at widely-spaced wells. On this same date, other wells do not show unusual water levels. It is very likely that a sampling error was made, and that no-one checked the data before they became part of the permanent database.

Laboratory analytical data for this database are always compared to trends from the previous three results, and a deviation calculated. When the deviation is greater than a certain portion of the average deviation of previous measurements or exceeds a regulatory limit, the new point is flagged for human review. This simple QA check can and should be implemented as data from field measurements are entered into any database.

QA is discussed further below.

Table 8-1 . Statistical analysis of water head observations from Savannah River Site

Original Statistic Analysis of the Observations

WellNam	AqNam	ObNm	MinVal	MaxVal	MeanV	Varian	Stand	CoefV	Mann	ModM	Trend	p-val
P-15D	WT	16	225.27	234.90	228.34	8.83	2.97	0.013	58.	2.57	Uptrend	0.005
P-16D	WT	16	210.41	216.96	214.20	3.41	1.85	0.009	-39.	-1.72	Downtren	0.044
P-16TC	uprK	16	220.15	221.50	220.74	0.11	0.33	0.002	11.	0.45	Uptrend	0.320
P-17D	WT	16	275.47	285.06	276.98	5.30	2.30	0.008	-24.	-1.04	Downtren	0.153
P-18D	WT	16	191.44	223.06	217.63	47.61	6.90	0.032	27.	1.17	Uptrend	0.122
P-19TD	TD	16	176.65	186.80	178.46	5.20	2.28	0.013	73.	3.27	Uptrend	0.001
P-19TC	uprK	16	176.72	179.59	177.99	0.45	0.67	0.004	80.	3.56	Uptrend	0.000
P-22D	WT	16	169.98	182.62	179.35	17.77	4.22	0.024	-31.	-1.37	Downtren	0.085
P-24TA	TA	16	180.85	184.34	183.11	0.69	0.83	0.005	0.	0.00	Flat	0.500
P-25TA	TA	16	172.25	213.12	175.69	93.77	9.68	0.055	63.	2.80	Uptrend	0.003

Modified Statistic Analysis of the Observations (After rejecting the outlier points)

WellNam	AqNam	ObNm	MinVal	MaxVal	MeanV	Varian	Stand	CoefV	Mann	ModM	Trend	p-val
P-15D	WT	16	225.27	234.90	228.34	8.83	2.97	0.013	58.	2.57	Uptrend	0.005
P-16D	WT	16	210.41	216.96	214.20	3.41	1.85	0.009	-39.	-1.72	Downtren	0.044
P-16TC	uprK	16	220.15	221.50	220.74	0.11	0.33	0.002	11.	0.45	Uptrend	0.320
P-17D	WT	15	275.47	279.31	276.44	1.01	1.00	0.004	-19.	-0.89	Downtren	0.189
P-18D	WT	15	218.12	223.06	219.37	2.02	1.42	0.006	26.	1.24	Uptrend	0.108
P-19TD	TD	15	176.65	179.69	177.90	0.59	0.77	0.004	74.	3.65	Uptrend	0.000
P-19TC	uprK	16	176.72	179.59	177.99	0.45	0.67	0.004	80.	3.56	Uptrend	0.000
P-22D	WT	16	169.98	182.62	179.35	17.77	4.22	0.024	-31.	-1.37	Downtren	0.085
P-24TA	TA	16	180.85	184.34	183.11	0.69	0.83	0.005	0.	0.00	Flat	0.500
P-25TA	TA	15	172.25	174.45	173.19	0.40	0.63	0.004	64.	3.13	Uptrend	0.001

Following Wells are Highly Positively Correlated: R > 0.95

P-17D	WT	and	P-18D	WT	0.95
P-19TD	TD	and	P-19TC	uprK	1.00

Following Wells are Positively Correlated: 0.9 < R < 0.95

P-15D	WT	and	P-18D	WT	0.90
P-15D	WT	and	P-19TD	TD	0.92
P-15D	WT	and	P-25TA	TA	0.91
P-19TD	TD	and	P-25TA	TA	0.94
P-19TC	uprK	and	P-25TA	TA	0.93

Following Wells are not Correlated: -0.1 < R < 0.1

P-16D	WT	and	P-16TC	uprK	0.02
P-16D	WT	and	P-17D	WT	0.07

Following Wells are Negatively Correlated: R < -0.9

P-15D	WT	and	P-22D	WT	-0.90

All Correlation Coefficients of Water Head Between Wells

		P-15D WT	P-16D WT	P-16TC uprK	P-17D WT	P-18D WT	P-19TD TD	P-19TC uprK	P-22D WT	P-24TA TA	P-25TA TA
P-15D	WT	1.000	-0.106	0.747	0.858	0.901	0.918	0.892	-0.902	-0.498	0.907
P-16D	WT	-0.106	1.000	0.017	0.073	-0.157	-0.200	-0.122	0.125	0.103	-0.324
P-16TC	uprK	0.747	0.017	1.000	0.833	0.839	0.713	0.710	-0.601	-0.357	0.590
P-17D	WT	0.858	0.073	0.833	1.000	0.953	0.781	0.751	-0.868	-0.697	0.671
P-18D	WT	0.901	-0.157	0.839	0.953	1.000	0.874	0.850	-0.887	-0.656	0.788
P-19TD	TD	0.918	-0.200	0.713	0.781	0.874	1.000	0.997	-0.842	-0.432	0.941
P-19TC	uprK	0.892	-0.122	0.710	0.751	0.850	0.997	1.000	-0.805	-0.396	0.932
P-22D	WT	-0.902	0.125	-0.601	-0.868	-0.887	-0.842	-0.805	1.000	0.574	-0.857
P-24TA	TA	-0.498	0.103	-0.357	-0.697	-0.656	-0.432	-0.396	0.574	1.000	-0.320
P-25TA	TA	0.907	-0.324	0.590	0.671	0.788	0.941	0.932	-0.857	-0.320	1.000

8.5 Water Level Measurements

Water level measurements are relied upon to estimate flow direction in aquifers. There is extensive literature on water level diurnal changes and response to rainfall. Typically, water levels are measured during quarterly sampling events. For special studies, an attempt may be made to measure all wells in a study area (e.g., model area) in a very short time span. In the Charleston Naval Weapons Station case described in Chapter 2, water levels change enough to suggest very different flow directions at different times.

Figure 8-11 illustrates the variation of water level between sampling events as captured by a continuous recorder (see line starting at March 31, 2003). Note that a change of over ten feet was missed by the periodic sampling.

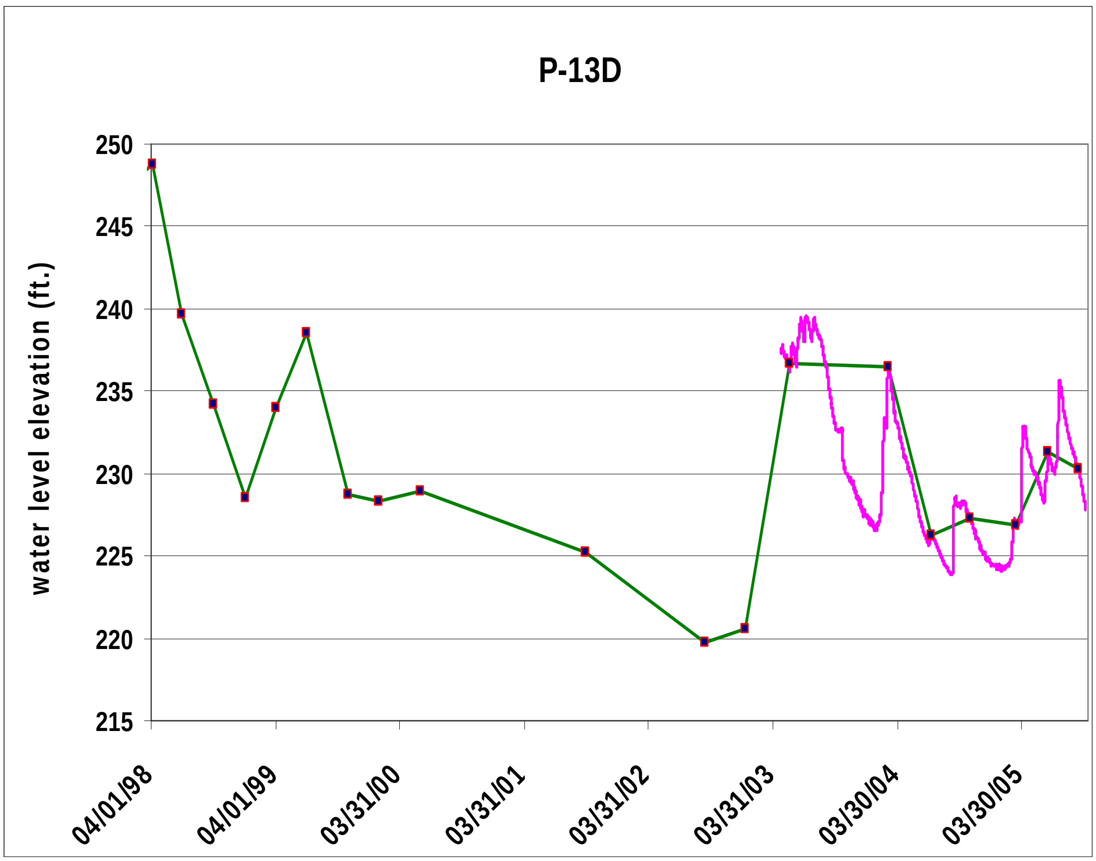

Figure 8-11 Periodic and continuous water level measurements compared for SRS well P-13D. Courtesy Bill Jones, SRNL.

8.6 Unmixing of Multimodal Data

Concentration data from different contaminant sources (or permeability measurements from different types of sediment facies) may present bi-modal or multimodal distribution. This section will introduce an inverse method to identify the individual modes or sources with statistical approaches.

Previous studies assume that if the measurements from an individual source have a log-normal distribution (Sinclair, 1981; Gilbert, 1987), then, the density function of the whole data set can be represented by the linear combination of a number of separate log-normal probability density functions (Heslop et al., 2002); that is, a distribution curve is composed of a finite number of log-normal populations. Under this assumption, a mixture of *N* separate populations can be represented at a given field by the frequency function *f*(*x*),

Equation 7

$$f(x) = \sum_{i=1}^{N} p_i \eta_i (m_i, \sigma_i)$$

$$\eta_i(m_i, \sigma_i) = \frac{1}{\sigma_i \sqrt{2\pi}} \exp^{-\frac{(x-m_i)^2}{2\sigma_i^2}}$$

$$\sum_{i=1}^{N} p_i = 1$$

where $\eta_i(m_i, \sigma_i)$ corresponds to a log-normal probability density function with mean m_i, standard deviation σ_i and non-negative mixing proportion p_i.

Sampled frequency values are therefore a discrete realization of the continuous frequency function and as such should be considered as an incomplete data set. Fitting is normally performed on the mixture frequency distribution to identify the number of modes or sources and to estimate the unknown parameters including mean, standard deviation, and proportion of each mode. For two or three mode problems, an Excel macro can be used to estimate these parameters by trial and error method. Figure 8-12 presents an example for identifying the distributions of two contaminant sources.

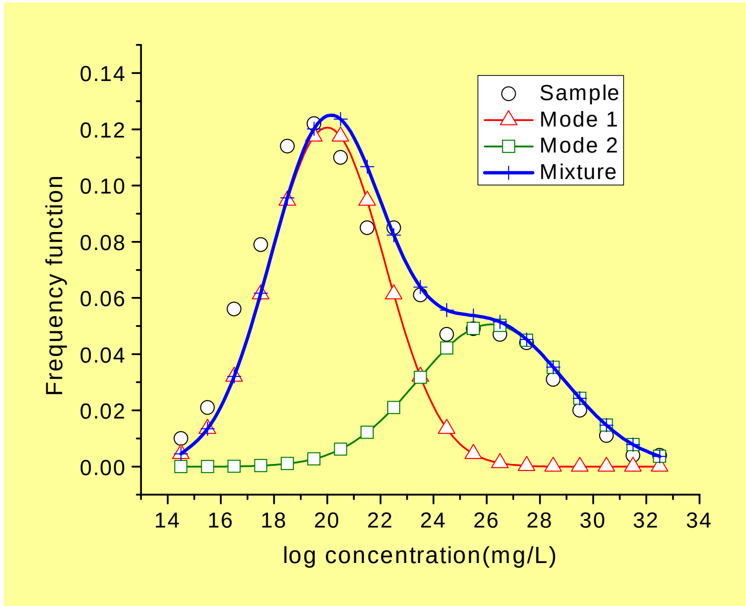

Figure 8-12. Unmixing bimodal data

The two identified modes in Figure 8-12 represent the distribution of two contaminant sources. The first has a mean log concentration of 19.96 mg/L, standard deviation of 2.15, proportion of 0.65, and the second has a mean log concentration of 26.16 mg/L, standard deviation of 2.76 and proportion of 0.35.

For the more complex problem with more than three modes or sources, the expectation-maximization (EM) algorithm (Dempster et al., 1977, and Heslop et al., 2002) can be used for the inverse analysis. This algorithm uses the maximum likelihood estimation (MLE) to maximize the probability that the sample data fit well to the computed frequency function. A brief explanation of this equation is below, but the reader is referred to the sourced text for a more detailed description on the EM algorithm.

Using a two-step procedure (expectation and maximization), the EM algorithm iteratively determines the MLE of the parameters that describe the mixture distribution of a given incomplete data set. Before EM iteration can begin, it is necessary to provide an initial estimation of the parameters. Expectation (E-step) is performed first, and involves the determination of the complete data log-likelihood constrained by the observed (incomplete) data and the previously made estimation of the parameters. MLE (the M-step) is then performed for the estimated complete data log-likelihood (obtained during the E-step). From this maximization procedure, new estimates of parameters are determined. The E- and M-steps are repeated, with the new parameter-values produced during each M-step being utilized in the complete data likelihood determination in the subsequent E-step. By the stepwise improvement of the parameter vector the log-likelihood of the observed data is increased until a predefined convergence criterion is reached. More information on the algorithm and its application to finite mixture models can be found in Dempster et al. (1977); Jones & McLachlan (1990); McLachlan & Peel (2000) and Heslop et al. (2002).

Determining the number of modes (or components) contributing to the mixture distribution is not trivial, because the goodness of fit of a finite mixture model will always improve as the number of components in the mixture is increased. To assess the number of individual components that should be included in a model, we adopted the technique of Kruiver et al. (2001), which is based on a comparison of the residuals (calculated between the measured and modeled curves) for fits involving different numbers of components. The technique compares the variances and means of the residual arrays for two competing models. If the inclusion of an additional component does not significantly reduce the variance and mean of the residual array (assessed using an F-test and Student's t-test, respectively) then the more complex (higher-component) model is unnecessary on a statistical basis. The use of the fitting procedure based on the EM algorithm provides an effective method for determining the contributions and characteristics of individual source populations.

The statistics of a concentration data set from a synthetic site with three possible contaminant sources are shown in Figure 8-13 and Figure 8-14. The identified distributions of three sources and the estimated parameters are listed in Table 8-2.

Table 8-2. The identified distributions of three sources and the estimated parameters

Source	Mean log concentration (mg/L)	Standard deviation	Proportion
Mode 1	1.58	0.126	0.54
Mode 2	2.08	0.122	0.32
Mode 3	2.55	0.100	0.14

Figure 8-13 presents the statistics of contaminant concentration data and the corresponding cumulative probability distribution whereas, Figure 8-14, presents this distribution for each of the three contaminant sources.

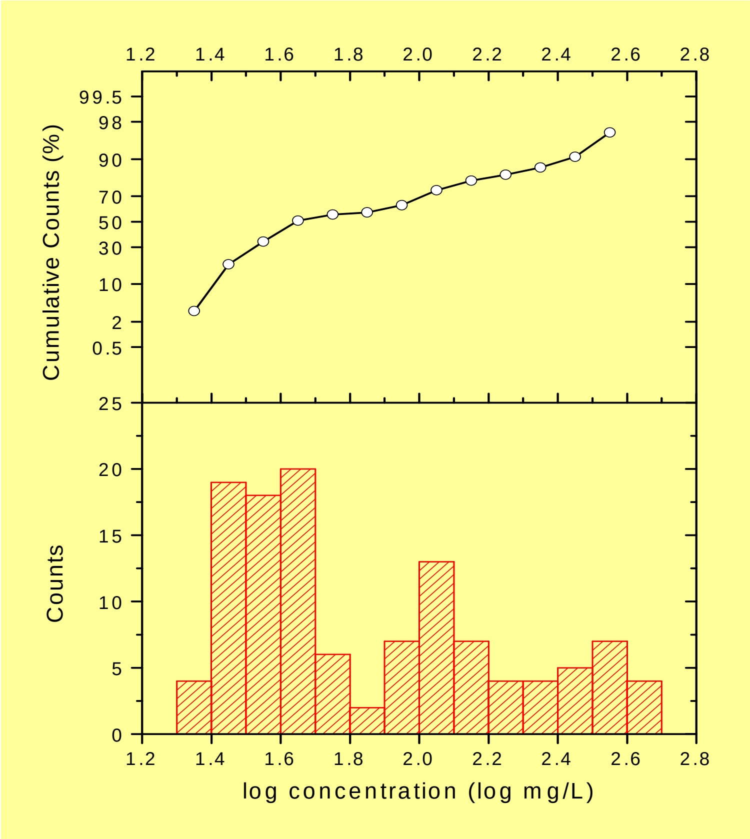

Figure 8-13. Probability plot

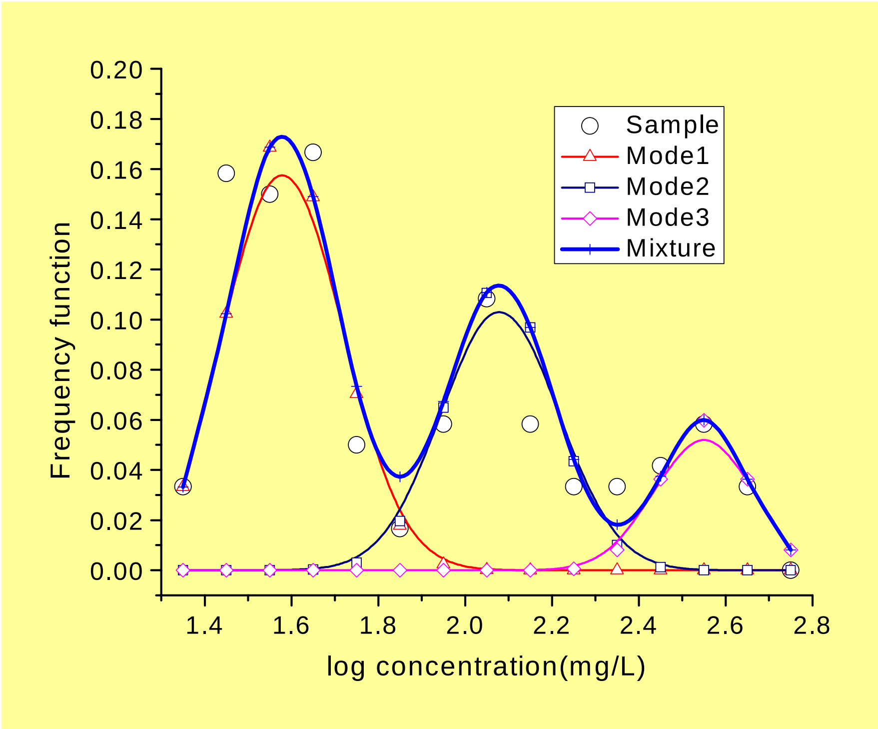

Figure 8-14. Tri-modal distribution

Dissecting plots of mixed population data has been used in exploration geochemistry for many years to distinguish mineralized from barren areas. The reader is referred to online sources starting with authors Sinclair, Miesch, and McCammon and the program Probplot, An Interactive Computer Program to Fix Mixtures of Normal (or Log Normal) Distributions with Maximum Likelihood Optimization Procedures**,** distributed by the Association of Applied Geochemists (www.appliedgeochemists.org).

8.7 Multivariate Analysis Methods: Cluster and Factor Analysis

Multivariate data analysis includes studies of cluster analysis, a method to show the closeness of relationships between samples or variables in n-space (where n is the number of variables), and correlations and structure of correlation matrices (factor analysis). (Samples in n-variable space (R-mode) or variables in n-sample space (Q-mode).)

Cluster analysis is a powerful method to examine data in part because its results can be presented in a simple graph. Analytical results containing a dozen variables can be flattened for quick review onto a plane.

Results are often displayed as a tree that reduces n-dimensional data to a 2-dimensional display. These methods were developed largely in the 20^{th} century – the term factor analysis first appearing in 1931 and cluster analysis in 1939. Their use requires many computations – for example cluster analysis requires the computation of n! distances between samples in n-space several times. Advent of the high-speed digital computer has made the methods commonplace.

These methods are not really statistical tests – they are data analysis and presentation procedures, and they may be applied without concern for many of the assumptions underlying many statistical tests. (See NIST, 2004 and Tukey, 1977 for discussions of exploratory data analysis.) Readily available statistical packages such as SPSS and SAS are capable of performing all of these analyses. More recently, there are some shareware programs or add-ons for programs such as MS-EXCEL that will perform most of the needed multivariate data analyses. Some of these add-ons can be currently found at: http://statpages.org/javasta2.html#Excel.

8.7.1 Case Study: Multivariate Data Analysis at Mill Tailing Site

Let us go through a test case using ground-water monitoring data from a uranium mill tailings disposal site. The data were obtained from reports available in the NRC electronic reading room system. We will use factor analysis to look for structure in the data, and cluster analysis to examine a hypothesis about the possibility that the sampled wells draw from two different bodies of subsurface water.

Figure 8-15 is a cross-section of the mill tailings site looking northeast. A steep change in the elevation of a clay layer dividing an upper from a lower water-bearing zone led us to propose an alternative conceptual model in which a fault cuts the layer, as shown in Figure 8-15.

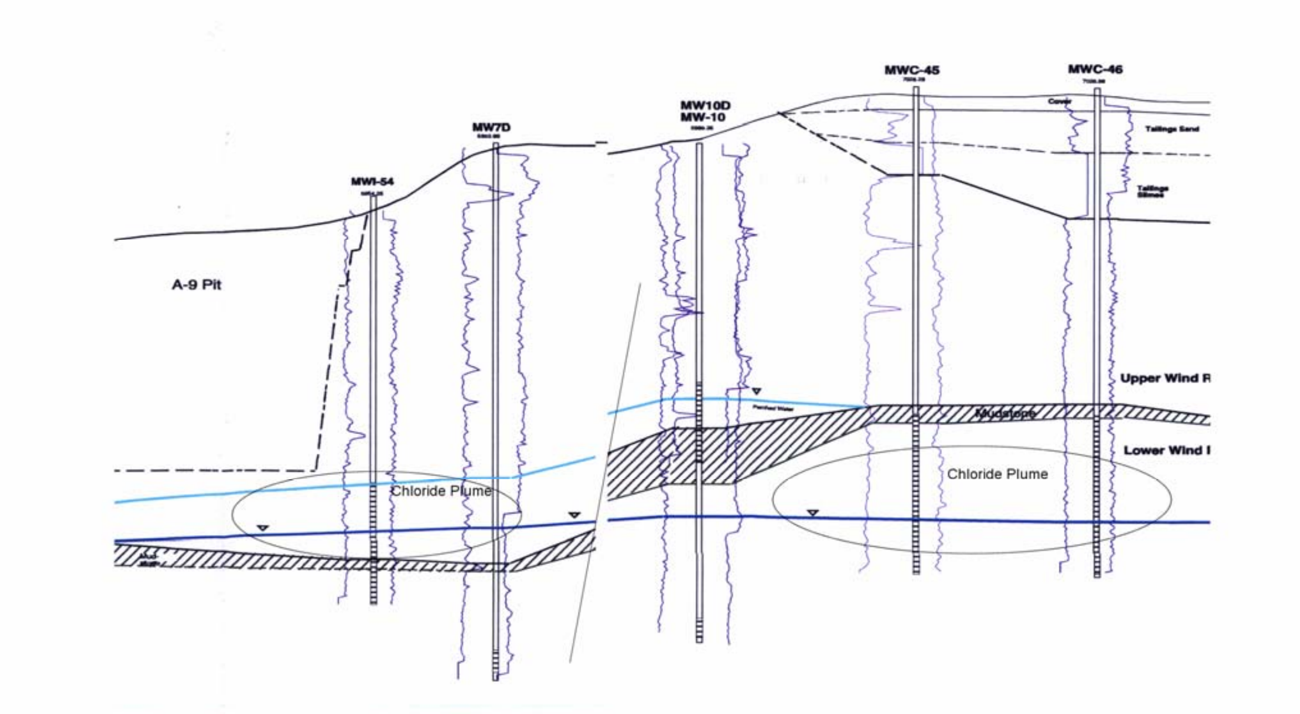

Figure 8-15. Cross section showing concept of merged water bodies. Our study examines whether this water is separated into two isolated chambers.

Chloride plumes exist at the site above the clay on the left of this figure, and below the clay on the right of the figure. This supported the conceptual site model in which there was no permeability barrier, and that the mapped plumes were really one. The water samples are designated as belonging to a West or Southwest "flow regime" in the site data report, which treats these regimes as separate water bodies.

Cluster analysis using SPSS on the data shown in Appendix 8-A support the hypothesis that the West and Southwest regime samples have different chemistry, and so the water can be presumed to represent two zones. This supports the site data report's position that the permeability barrier (clay layer) may be continuous, rather than faulted. Thus the proposed alternative CSM hypothesis is rejected. The Sections below explain in detail the methodology used to perform this multivariate analysis, and the rest of the results from this particular case study.

8.7.1.1 Multivariate Analysis – Step by Step Guidance

Step 1. Obtain the data electronically.

In this case we downloaded pdf copies of tables and re-typed them into an EXCEL spreadsheet.

Step 2. Data conditioning.

This could include standardizing data to z-scores or ranks, or converting data to logs or roots in order to limit the range of magnitudes. It also includes deciding what to do with truncated or censored data sets. It our case we eliminated about 15 of the samples because they were not analyzed for a number of constituents. We eliminated one analyte (Beryllium) because it was not detected in any samples, and we converted a lot of the non-detects for Arsenic into half the value reported as the detection limit. We also simplified the variable names to save space.

We will not write step-by-step instructions for data conditioning because it should only be conducted by someone familiar with the process.

Step 3. Develop hypotheses to be evaluated, or questions to be answered.

In this case, questions to address included:

- Do the data readily reveal any underlying controlling processes; and
- Can we use water chemistry to substantiate or refute the hypothesis that that the wells represented two "flow regimes" – perhaps different aquifers?
- Are there any outlier samples? (The operator must decide what these mean once they are identified.)

Step 4. Decide what analysis to apply.

- Factor analysis looks at correlations among all the variables. This method is typically ideal for discovering close associations or lack of associations between variables.
- Cluster analysis can quickly reveal outliers and can show whether samples fall into natural groupings in variable space.

Step 5. Use available software for the analysis.

We used SAS and SPSS. Results are discussed below.

8.7.1.2 Cluster Analysis Results

SPSS was used to divide the 137 observations (from Appendix 8-A) into ten groups based on their proximity in variable space. The data were then examined using cluster analysis to help identify outlying data points and look for data trends, and factor analysis to identify correlations in the data. (Similar results were obtained with SAS, but are not presented here.)

Figure 8-16 presents some of the cluster results discussed above in a "family tree" format called a dendrogram. It is clear that Observations 5 from well LA2, 64 from A8, 69 from DOMW1, and 115 from MW30 are outliers because these observations fell into clusters unique for their wells (see data table in Appendix 8-A). They are marked by decreased water quality that does not follow a trend across time, as the subsequent observations at the wells contain normal data for the wells.

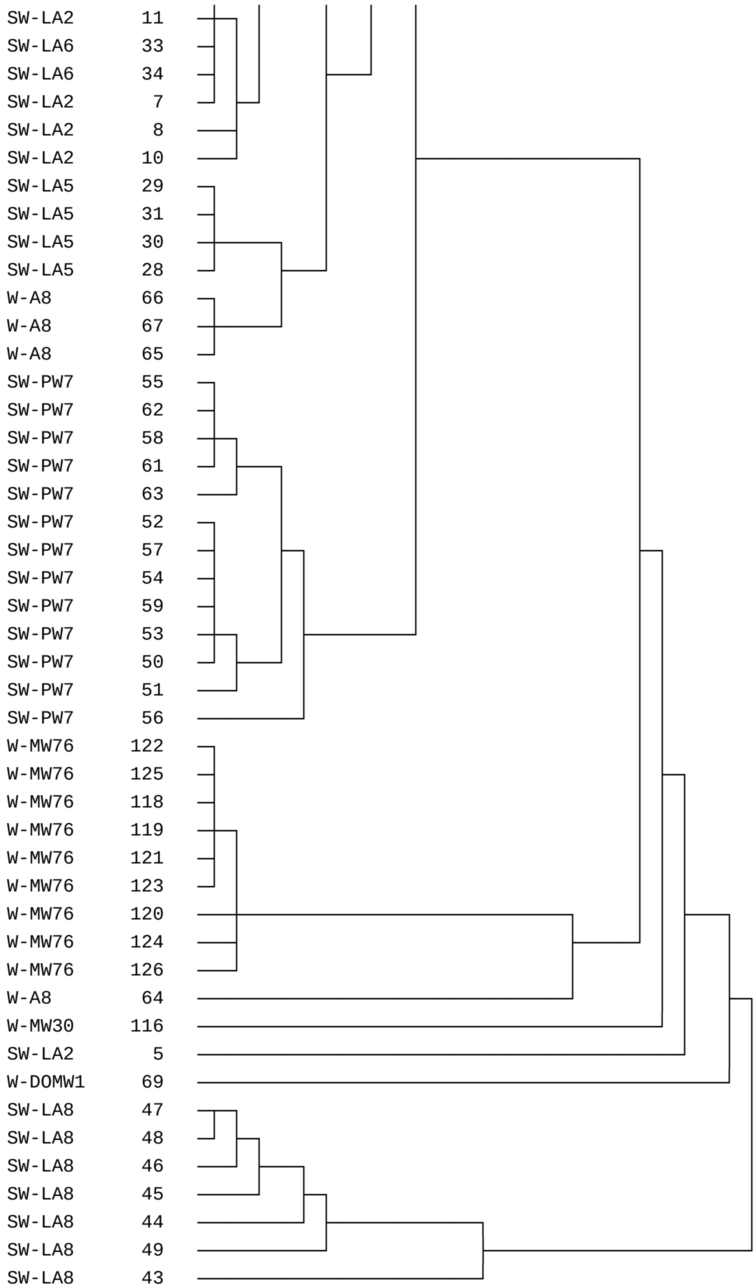

Figure 8-16. Dendrogram (partial) of the clusters for the water analyses presented in Appendix 8-A. The left-most column is the well name and the right column indicates the observation number.

Once the outliers have been identified through cluster analysis, the data can be evaluated to determine what causes these samples to stand out. Before rejecting or removing these outliers, it is critical to evaluate results of other constituents from the same well during the same sampling period or from other wells in the same sampling period to determine if the results represent potential sampling errors or real pulses of contaminants.

Examination of Figure 8-16 reveals the following:

- Out of 4 observations from well A8, 3 fell in Cluster 1. Observation 64 stands out as an outlier (single-member cluster 7). Examination of the data table reveals this sample has higher gross-alpha and radium than other samples from that well.
- Out of 15 observations from well MW30 all fell in Cluster 1, with the exception of observation 115, which fell in Cluster 9. A very high sulfate analysis was reported for this sample. This could represent a bad analysis, or the passage of a plume not otherwise observed in the semi-annual sampling.
- 14 of 15 Samples (observations) from well LA2 fell in cluster 3. Observation 5 again represents a single-member cluster (number 2) and reference to the data table reveals a Th230 analysis that is out of line with the entire data table, suggesting a typographical error in recording data.
- 6 of 7 observations from well DOMW1 clustered together. Observation 69 is identified as an outlier, and is high in sulfate, chloride and total dissolved solids relative to other samples from this well.
- Not all wells sampled have odd observations, for example all 9 observations from well MW76 fell in Cluster 10,

Water chemistry data further supports dividing the wells into two major groups. The majority of the wells screened in the Southwest flow regime falling into Clusters 1 and 3 and the majority of wells screened in the West flow regime falling only into Cluster 1 thus, supporting the hypothesis that the West and Southwest flow regimes are separated into two isolated water bodies.

Please note that there is abundant material on cluster analysis and cluster dendrograms on the Internet. These materials should be consulted for further general information.

8.7.1.3 Factor Analysis Results

Next, a factor analysis was performed on the data in Appendix 8-A to determine relationships between samples or variables in n-space. Factors are not presented here, but results of correlation coefficients are presented in Table 8-3**.**

Table 8-3. Correlations between monitoring data variables

	as	Cl	galpha	pb210	ra	Ra226	ra228	so4	tds	u	th230
as	1.00000	-0.24668	0.22502	0.03648	0.06288	0.07260	-0.00517	0.12385	0.10167	0.11758	0.01139
cl	-0.24668	1.00000	0.27811	-0.07228	0.14136	0.05518	0.42869	0.41603	0.41539	0.29323	0.16194
galpha	0.22502	0.27811	1.00000	0.18202	0.06628	0.05021	0.10118	0.49497	0.60718	0.96203	0.24884
pb210	0.03648	-0.07228	0.18202	1.00000	0.49116	0.53849	0.04436	0.15358	0.09250	0.16585	0.07580
ra	0.06288	0.14136	0.06628	0.49116	1.00000	0.98053	0.57561	0.57808	0.54190	0.00793	-0.01624
ra226	0.07260	0.05518	0.05021	0.53849	0.98053	1.00000	0.40389	0.49020	0.44462	-0.00777	-0.05480
ra228	-0.00517	0.42869	0.10118	0.04436	0.57561	0.40389	1.00000	0.65338	0.67449	0.07046	0.15290
so4	0.12385	0.41603	0.49497	0.15358	0.57808	0.49020	0.65338	1.00000	0.92958	0.45045	0.12761
tds	0.10167	0.41539	0.60718	0.09250	0.54190	0.44462	0.67449	0.92958	1.00000	0.57897	0.17896
u	0.11758	0.29323	0.96203	0.16585	0.00793	-0.00777	0.07046	0.45045	0.57897	1.00000	0.29619
th230	0.01139	0.16194	0.24884	0.07580	-0.01624	-0.05480	0.15290	0.12761	0.17896	0.29619	1.00000

Correlations obtained in the factor analysis indicate:

- Gross alpha correlates with uranium (R=.96)
- Radium is highly correlated with Radium 226 (R=.98), but only moderately correlated with Radium 228 (R=.57) and lead 210 (R=.49)
- Radium correlates with Sulfate (R=.58) and total dissolved solids (R=.54).
- Radium does not correlate with Uranium (R=.008)
- Uranium correlates with sulfate (R=.45) and total dissolved solids (R=.58).

A possible interpretation is that Ra comes from the mill tailings in which it has been separated from U and that much of the observed U is natural.

8.8 Analysis of Mapped (Spatial) Data

This Section discusses data analysis of spatial data. Specifically, if focuses on a discussion of the following three topic areas:

- Testing for outliers in mapped data;
- Determining the distribution of uncertainty – the completeness transform;
- Incongruity;

Information learned in these three areas often provides useful insight about site performance, or rather, help locate areas of uncertainty at the site. The areas of uncertainty then become candidate areas for validation monitoring points.

For characterization data, spatial statistical analysis methods developed within the mining industry for mine planning are often useful for determining whether a site has been adequately characterized. We did not include geostatistics in this analysis.

Parameters being measured may fall into a number of classes that may vary across the site in different patterns. If we were developing a gold mine, we might only test core samples for gold. More generalized site characterization will include measurements for many things, but the general approach is similar for each.

8.8.1 Outliers in Mapped Data

Generally, mapped data are presented in the form of contoured maps. Such maps may be produced with computers, but for data analysis it is best to hand contour the data. In the process of hand contouring, any points that cause problems in the drawing of smooth contours will become apparent. With computer contouring the operator has less opportunity to interact with the data, and thus less opportunity to spot outliers, but these may still produce contoured "bulls eyes." Any bulls-eyes in contoured data, or deviations from smooth contours in a variable, such as water levels (piezometric surfaces) should be visited to determine whether the data point is valid and whether it represents an opportunity to re-evaluate the conceptual model.

Characterization and monitoring data should be evaluated for outliers and trends that might suggest alternative conceptual models. Examples might include water levels that deviate from smoothed contour piezometric maps or trend surfaces.

Guidance includes:

- Hand contour spatial data to gain insight
- Computer contouring is highly dependent on data point spacing and is accurate only for regularly spaced data
- Question any closed contours (bulls eyes) in a piezometric or concentration map in the context of the site model.

8.8.2 Uncertainty in Mapped Data

Geostatistical methods were developed to quantify uncertainty in geologic measurements so that decisions about whether to proceed with mining in an area, or to determine whether additional drilling was needed to fill in data gaps before a risk-informed decision could be made. This is a very active field of research today, especially as applied to petroleum reservoirs. (Yarus and Chambers, 1994).

This section presents case studies drawn from real data that illustrate site-specific conceptual model revisions required by anomalous data. In two cases the non-fitting data were first discarded, and only after subsequent analysis, were identified as clues leading to revision of the conceptual site model.

For the purpose of preparing a map, a geologic variable such as a stratigraphic top, water level, or other parameters, can only be known with certainty at the control points. While there may be errors in measuring variables at control points, these are distinct from errors in estimating values between control points.

The interrelationships between spatial autocorrelation of the surface, the spacing between control points, and the likely error of interpolated points are formalized in regionalized variable theory, a branch of statistics devised initially for the analysis of mining problems (Matheron, 1965). Under this statistical theory, geologic variables are considered to be composed of two components:

1) a gentle regional trend or *drift*; and
2) autocorrelated residuals or deviations from the drift.

Once the drift has been removed (by subtracting a series of trend surfaces or moving averages) the degree of similarity between points is given by the semivariance. This is the variance of the differences between all possible pairs of points on the map that are the same distance apart, and is closely related to the autocorrelation. A plot of semivariance vs distance is called a semivariogram, and rises from zero at zero distance to a maximum value equal to the total variance around the drift. The distance at which the semivariance becomes a maximum is called the "range," and is also the distance at which the autocorrelation of the mapped surface will drop to zero. The value at which the autocorrelation reaches maximum on the semivariogram is called the "sill". The autocorrelation (y axis) of a semivariogram plot may not always start at zero. This is due to the "nugget effect", which represents inherent variability plus sampling variability at zero distance for the database.

Once the form of the semivariogram has been determined, it may be used in a surface estimation procedure called universal kriging (Matheron, 1965). Provided the drift has been properly removed, this procedure provides a contoured surface with the smallest errors possible with any estimation procedure. Kriging also yields an estimate, in the form of a map, of the possible errors at all estimated points. This is a map of the +or– bounds on the mapped surface at every point within the map area. Areas of high estimation error then become the subject of additional characterization input. Estimation error could refer to a contoured map of pressure heads, to a contoured map of contaminant concentrations, or to patterns on a geologic map.

A recent paper by Cumbest and others (Personal communication, 2004 – it remains unpublished in 2007) gives a refined technique to apply geostatistical methodology to evaluate the thoroughness of a geotechnical investigation relative to investigation design goals. The technique basically uses the spatial distribution of the model error to map the probabilities that the model estimation values are in exceedance of specified design values. This is accomplished by calculating the probability of exceedance using the probability density function ($\eta_i(m_i,\sigma_i)$) (Equation 7) for the standard normal variable. The standard normal variable in this case is defined as the difference between the estimated value and the specified design value. The resulting probabilities are then converted to thoroughness by using the complement to the binominal entropy function. In essence, in locations where the estimated model values are known to be in exceedance of the specified design value (i.e. probabilities very near 1 or very near 0) result in thoroughness of very near 100 percent. At locations where the model error is large relative to the difference between the estimated and design values the probabilities of exceedance are not well known (i.e. very near 0.5) are associated with a thoroughness very near zero. Other locations exhibit a continuum of thoroughness values depending on their assigned probabilities.

Guidance

- Areas of poor characterization coverage are areas where monitoring points are needed.
- Kriged estimates of errors (see discussion in Section 8.8.2), or the geotechnical thoroughness transform may be useful.

8.8.3 Incongruity between Mapped Variables

The investigator should visually compare all sets of mapped variables for a site. One obvious test of a computer flow model, for example, is to see if model flow directions are consistent with apparent plume movement from monitoring data. In Figure 8-17, below, water table gradients from a site flow model indicate a dominantly westward flow direction, but plumes suggest a northwestward flow direction, which is more consistent with regional geology.

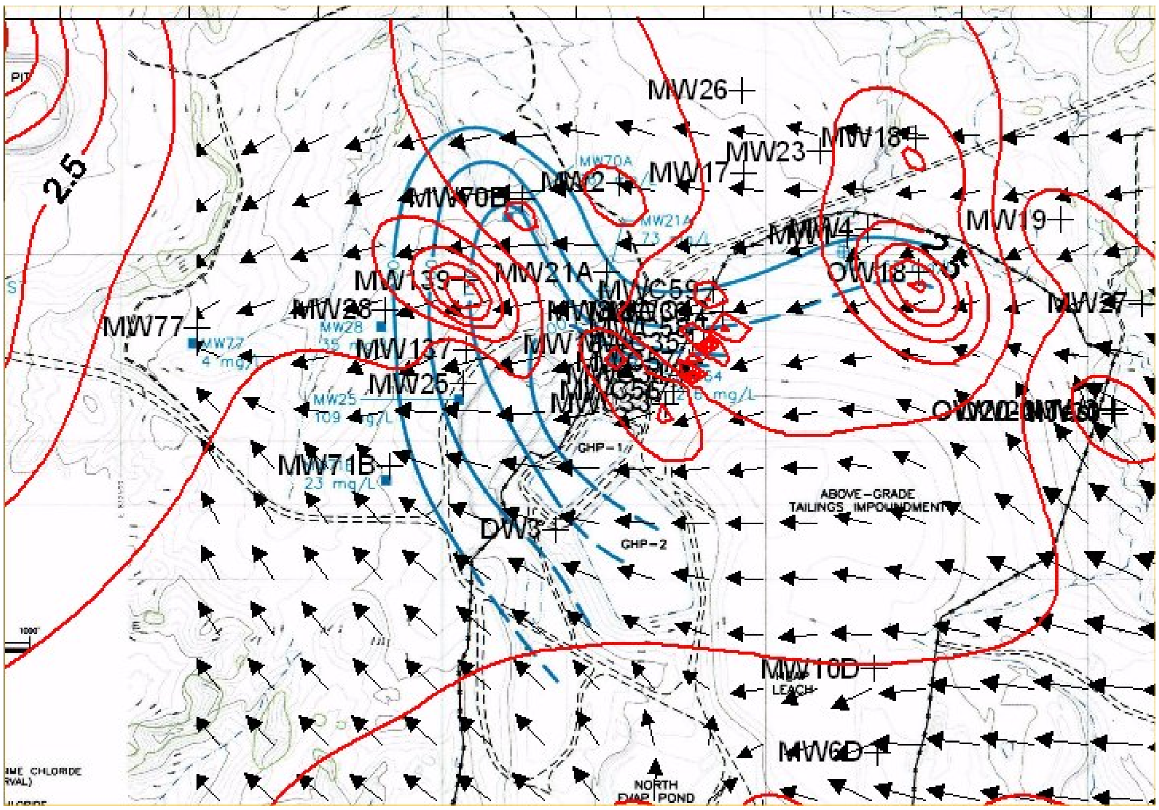

Figure 8-17. Map of chloride plume (blue) superimposed on a vector potentiometric data (arrows), and contoured hydraulic conductivity data (red).

Figure 8-17 shows that the direction of plume flow is in good agreement with the zone of high hydraulic conductivity. This indicates that the hydraulic conductivity has a greater influence on plume migration direction than does the potentiometric surface.

Figure 8-18. Typical alluvial fan

Published reports for the site in Figure 8-17 suggest that the environment of deposition was a series of alluvial fans. As shown in the photograph in Figure 8-18, alluvial fans are deposited by radial streams exiting from mountains onto a plain or valley. With the abrupt drop in stream gradient, sediments are deposited, the channel is choked and flow escapes to form another channel, resulting over time in a fan-shaped deposit. Before this channel switching occurs flooding may transport fine-grained sediment outside the channels, while coarser sediment remains in the channel bottom. From time to time lakes and swamps may fill the valley, resulting in deposition of fine grained and organic-rich sediments. The channel deposits will tend to be more permeable than the overbank sediments, and thus offer preferential flow directions to underground water.

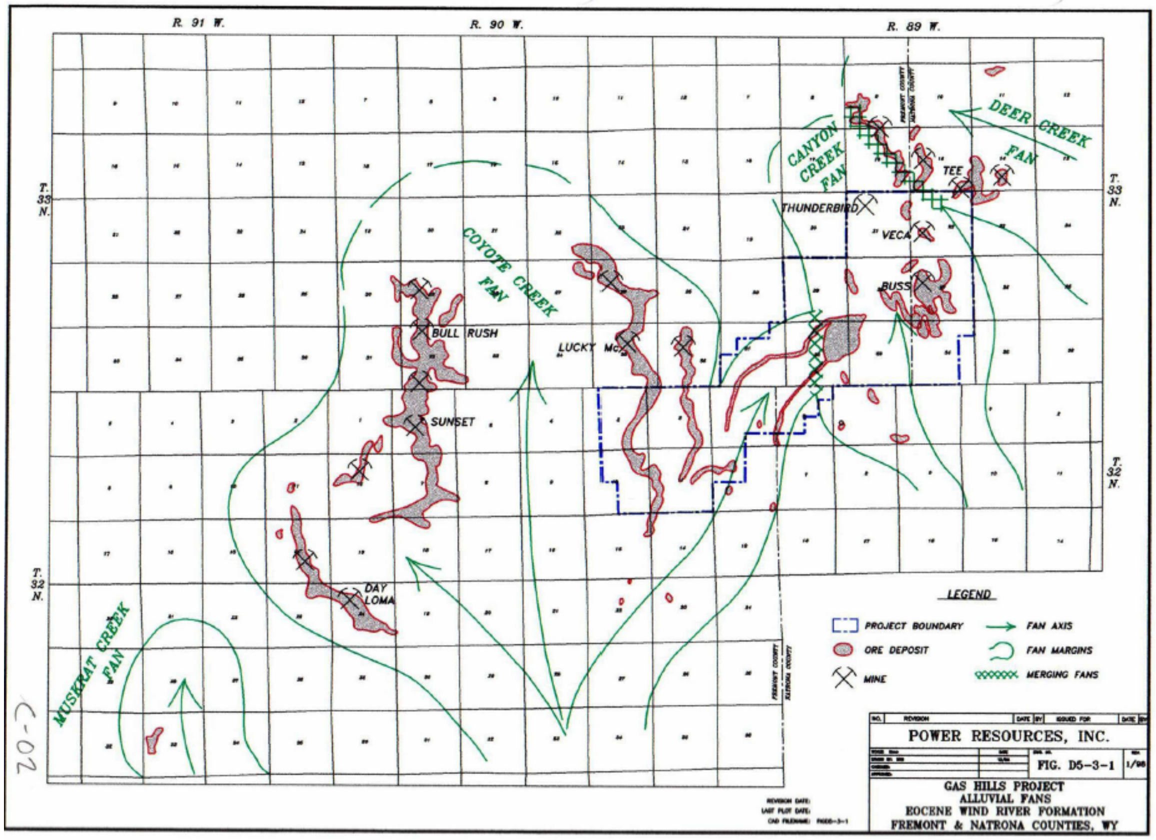

Figure 8-19. Diagram of alluvial fans in Wyoming

The site presented in Figure 8-17 is near the area of Figure 8-19 and has a similar geologic setting. Any high permeability zones at the site should follow trends suggested by the arrows on this figure. Permeability data for the site are presented in Table 8-4. Two companies performed aquifer testing on six wells, but used different aquifer thicknesses in computing hydraulic conductivity, K, from transmissivity results. We suspect that one company (referred to in this report as Company A) may have used screen lengths, while the other company (referred to in this report as Company B) used an estimate of total aquifer thickness of 240. We have used the screen length from Company B's results to compute a column of K adjusted for screen length.

It appears that there are two groups of hydraulic conductivity results– one set between about 0.1 and 1.0 ft/d and another ranging up to 6 ft/d. If we accept the alluvial fan conceptual model for deposition, then we should infer that the higher numbers represent in-channel measurements, and the lower numbers out-of-channel measurements. A revised flow and transport model incorporating high permeability zones might better represent the site.

Table 8-4. Hydraulic conductivity data

Well ID	Company	Method	Perm (ft/day)	Perm (ft/min.)	Trans	Thickness	Adjusted K
MWC33	A	Jacob	0.22	1.53E-04	53	240	0.53
MWC33	B	Theis	0.23	1.60E-04	22.7	100	0.227
MWC33	B	Jacob	0.45	3.13E-04	45.1	100	0.451
MWC34	A	Jacob	0.28	1.94E-04	67	240	0.279167
MWC35	A	Jacob	0.78	5.42E-04	187	240	1.87
MWC35	B	Theis	0.12	8.33E-05	12	100	0.12
MWC36	A	Jacob	1.23	8.54E-04	341	240	6.82
MWC36	B	Theis	2.1	1.46E-03	105	50	2.1
MWC36	B	Jacob	3.3	2.29E-03	163	50	3.26
MWC37	B	Jacob	2	1.39E-03	40.8	20	2.04
MWC37	B	Theis	2.7	1.88E-03	53.5	20	2.675
MWC42	A	Jacob	0.6	4.17E-04	165	240	1.833333
MWC42	B	Theis	1	6.94E-04	90	90	1
MWC42	B	Jacob	3.34	2.32E-03	301	90	3.344444

8.9 Quality Assurance

Most sources of error in ground-water data can be controlled through a good quality assurance (QA) program. This is easy to say, but the hard part comes from the fact that a good QA program can only be designed and implemented if the physical principles and processes leading to some numerical result are well understood.

Error control in general can be approached using the principles of systems engineering. Each entity –feature or process – must be thought of as an assembly of components. Each component plays a role in meeting the requirements set forth for the whole system or process. Each is a link in a chain, and failure of any one leads to failure of the chain. Quality assurance requires a comprehensive plan that ensures data integrity through each step of the process. It is important to be aware of possible sources of error in every step. **A ground-water monitoring system, for example, has a number of subsystems:**

- Sampling
- Analysis
- Data storage
- Reporting

Drilling down, each subsystem has a number of components which introduce possible sources of error as well. Sampling, for example includes:

- Choice of monitoring point

- Access to monitoring point – usually a well
- Sampling method – pump, bailer…
- Sampling protocol – length of pumping, duplicates, transport of samples, documentation..
- Field measurements of pH, alkalinity, conductivity, temperature.

8.9.1 Quality Assurance Case Studies

Let us examine a case study to illustrate QA analysis for just one component in a system: the well. Figure 8-20 is a diagram of a typical well along with some notes on well construction. The well is the one component in this system that is usually trusted to reliably yield water samples whose chemistry is representative of the water-bearing zone being sampled. Yet well construction often includes several reactive parts:

- Bentonite, a clay with very high ion exchange capacity;
- Portland cement – essentially calcium hydroxide, a strong base, and
- (Usually) electrical wiring which may allow currents to flow between the ground surface and the zone being sampled.

Voltages between about plus 1 and minus 1 have been measured between galvanized or copper clad ground rods at the well head, and the grounding wire to the submerged pump at wells at the DOE-SRS. To the best of my knowledge, no systematic study has ever been made of electrochemical or electrophoretic effects of monitoring wells. (Electrical methods are used to reduce fouling of screens in production wells.)

The filter sand, bentonite seal, and the cement grout are poured from the surface through a 2” pipe called a tremie. The bentonite is a slurry of dried clay pellets which absorb water and swell to make a tight seal between the well casing and the earth. Either the tremie pipe or a separate tag line is used to verify that the various layers are at the correct depth – but it is almost impossible to assure that the casing to earth annulus is uniformly filled. Another issue is pouring cement weighing about half again as much as water through a 2” pipe without creating a jet that eats through or around the bentonite seal. The tremie can be very long, depending on the depth of the well. Once the cement is poured, it is not possible to view details of the “as built” configuration. Only care in the installation can assure proper construction. One approach is to pour a small amount of cement (perhaps mixed in a bucket) and wait for it to cure before pouring the rest.

Ideal Monitoring Well

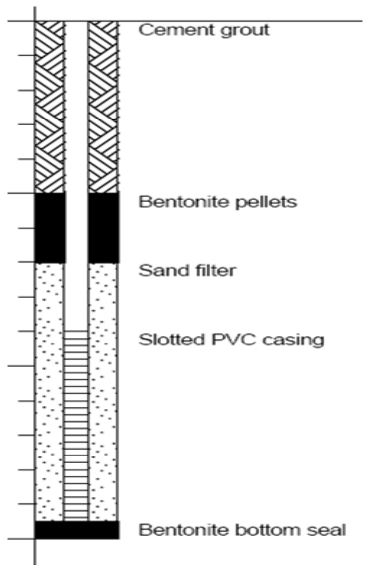

Drill Hole – walls are caked with mud

Insert casing with screen (slotted section)

Pour filter sand - get it right, like in the picture

Pour swelling clay seal pellets – wait until they swell – like in the picture

Pour cement in through a pipe. Do not jet a hole through the seal.

Develop well – pump until all drilling mud is removed from screen zone

Figure 8-20. Schematic of monitoring well with steps in installation.

The next few figures show pH measurements for several wells at the DOE SRS. In well ASB8B, field pH results are relatively stable, varying in the range of about 4 to 6 pH units (see Figure 8-21). The actual range in the aquifer may be a little less. Sample aeration and possible calibration errors for field pH meters may account for the observed range of measurements.

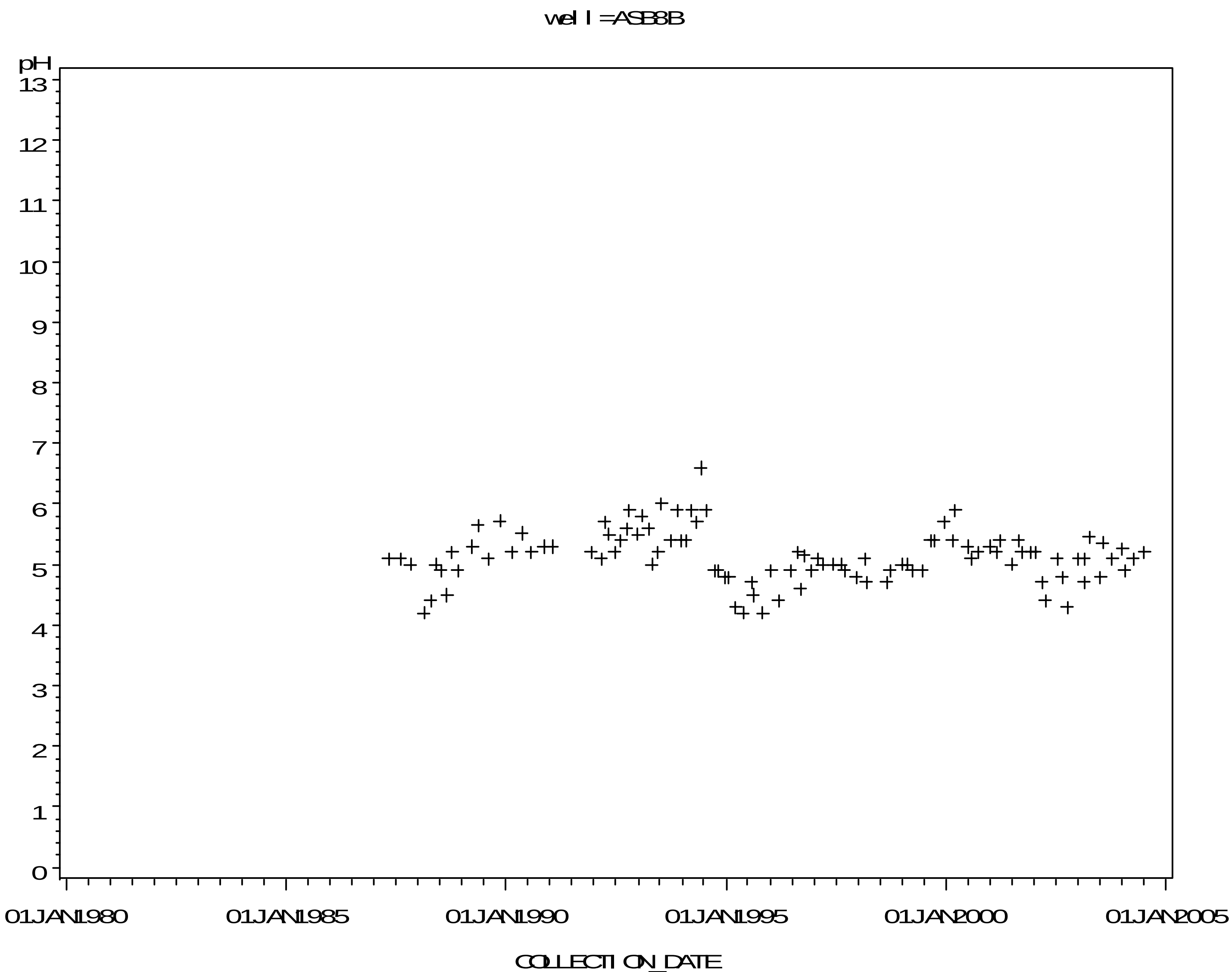

Figure 8-21. pH with time for well ASB8B

By contrast well ABP3 yields pHs between 12 and 3 (see Figure 8-22). Calcium hydroxide (cement) in water produces a pH of about 12.5. At this pH aluminum and zinc form soluble anions, and many transition metals are precipitated as hydroxides. Thus the disturbance in aquifer chemistry likely caused by poor well construction can render any effort to interpret metal chemistry useless.

As shown in Figure 8-22, with time, the pH lowers. The steepest decline is in about 1988, when sampling protocols were changed from pumping a fixed volume of water, to pumping until indicator parameters, including pH stabilized. The variation in pH is then about the same as observed in well ASB8 for a few years. Variance again increases at about the time that a change in sampling contractors went into effect.

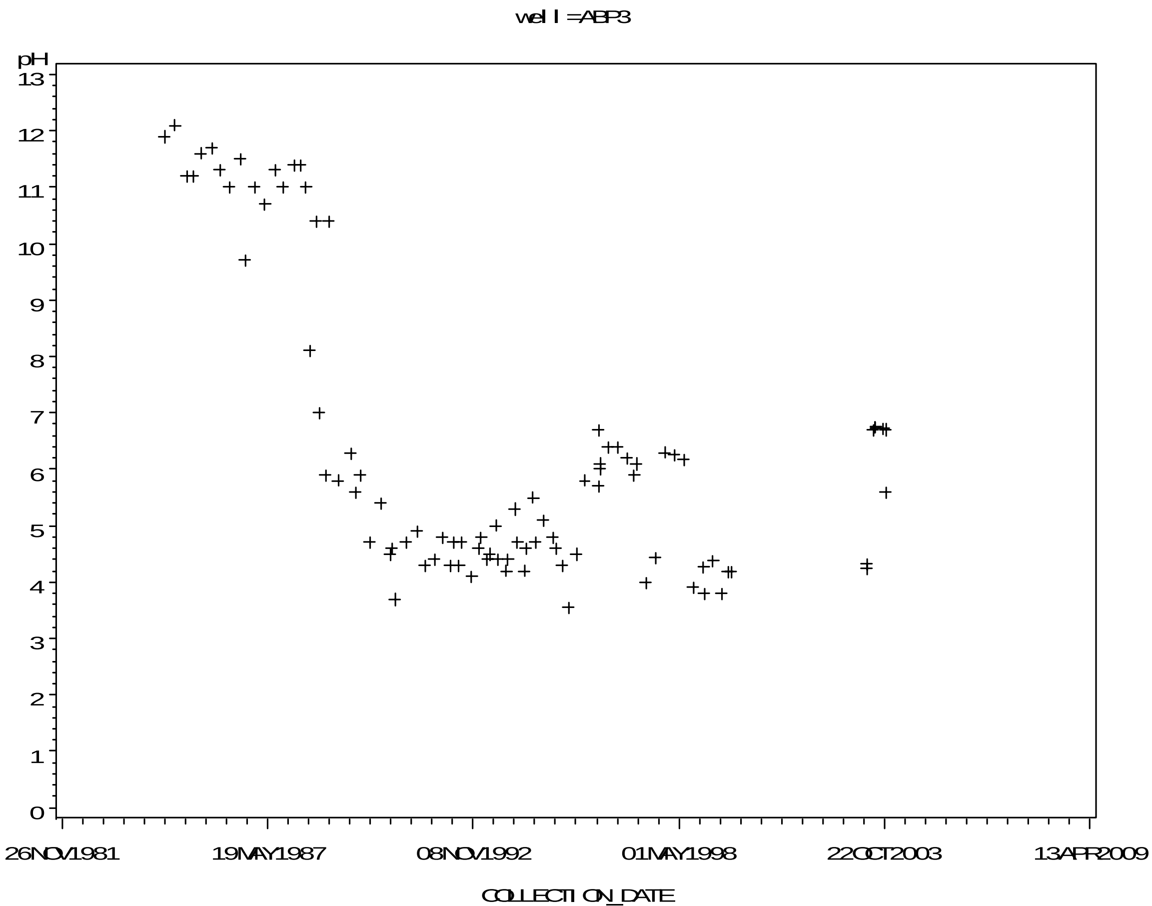

Figure 8-22. pH with time for well ABP3

Although wells are installed according to design specifications, it is almost impossible to inspect the as-built well. Acceptance criteria that include testing for well efficiency and for chemical parameters related to construction defects should be included in installation contracts. Training of samplers is important, but beyond this discussion.

This leads our discussion back to QA issues. Several sources of error can be found throughout the sample/data handling process. When analyzing data or assessing data anomalies, it is important to carefully consider factors that could be introduced throughout the sample process. This case illustrates how factors such as well construction, can significantly impact sample quality, and result in misconceptions about site conditions.

Obviously any geochemical understanding relying on accurate pH measurements from pumped wells could be clouded to the extent that the sampled values do not reflect aquifer conditions. Not only could pH be wrong, but concentrations of grout components, such as calcium, and concentrations of pH-sensitive chemicals – Zn, Al, to mention two - could be affected by highly alkaline conditions near the well.

Another issue with pH is the related to the chemicals that control ground-water pH. Commonly pH is controlled by calcium bicarbonate. When ground water is brought to the surface and exposed to the atmosphere, carbon dioxide can be gained or lost by exchange with the atmosphere. Figure 8-23 is taken from an unpublished report and shows results of pH and conductivity measured in the field and later in the laboratory. The samples are from an area underlain by limestone. Note that in every case pH decreases and conductivity increases between the field and the lab. There was no indication that the samples were acidified between collection and laboratory analysis, leading to the hypothesis that the observed changes are related to carbon dioxide exchange with the atmosphere.

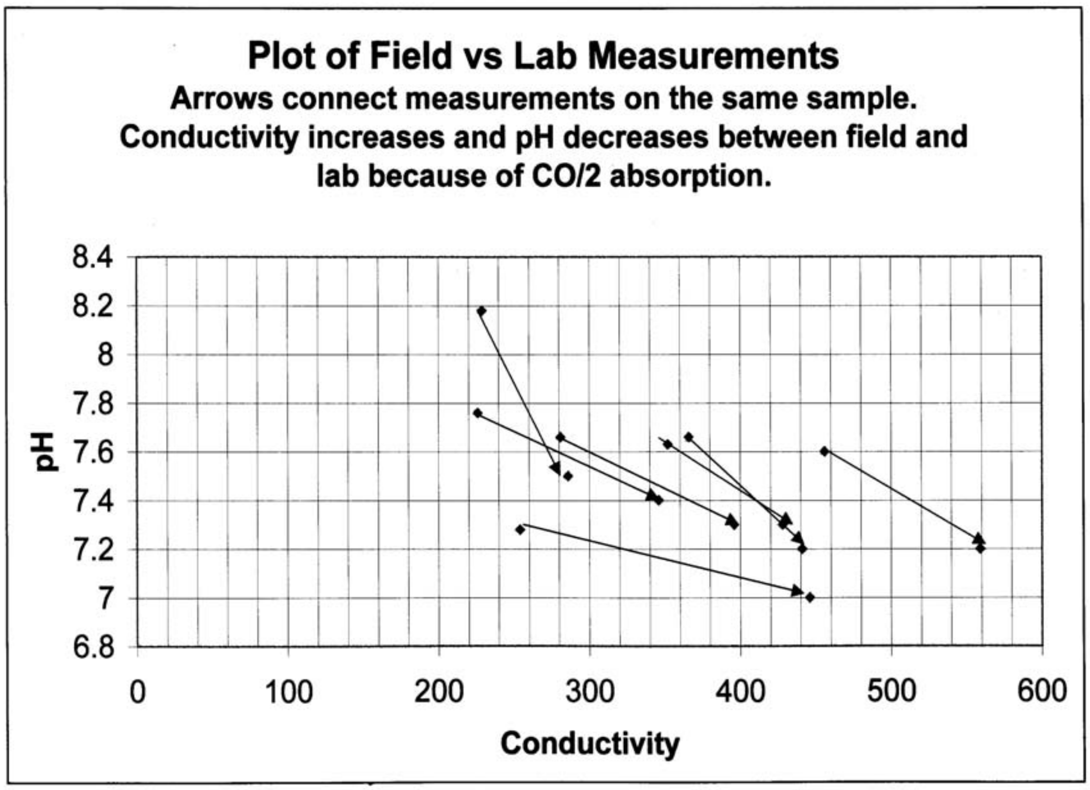

Figure 8-23 Field and laboratory measurements compared.

8.10 References

Anscombe, F.J. and J.W. Tukey. "Analysis of Residuals." *Technometrics*. pp.141. 1963.

Cumbest and others (Personal communication, 2004)

Dempster, A.P., N.M Laird, and D.B Rubin. "Maximum Likelihood from Incomplete Data via the EM Algorithm." *J. R. statist. Soc. B*. Vol. 39: 1–38.1977.

Environmental Protection Agency (EPA). "Guidance for Monitoring at Hazardous Waste Sites: Framework for Monitoring Plan Development and Implementation." OSWER

Directive No. 9355.4- 28, EPA. 2003. (access to this publication through www.clu-in.org)

Gilbert, R.O. *Statistical Methods for Environmental Pollution Monitoring*. New York:Van Nostrand Reinhold Company.1987.

Helsel, D. R. and R. M. Hirsch. “Statistical Methods in Water Resources.” Chapter A3, in Water-Resources Investigations Report of U. S. Geological Survey, Book 4, Hydrologic Analysis and Interpretation. U. S. Geological Survey. 2002.

Heslop, D., et al. “Analysis of Isothermal Remnant Magnetization Acquisition Curves Using the Expectation-Maximization Algorithm.” *Geophys. J. Int*. Vol.148: 58-64. 2002.

Jones, P.N. & G.J. McLachlan. “Algorithm AS 254: “Maximum Likelihood Estimation from Grouped and Truncated Data with Finite Normal Mixture Models.” *Applied. Statistics.* Vol. 39: 273–282. 1990.

Kendall. M.G. *Rank Correlation Methods*. 4th ed. London: Charles Griffin & Company. pp. 202. 1975.

Kruiver, P.P., M.J Dekkers,& D. Heslop. “Quantification of Magnetic Coercivity Components by the Analysis of Acquisition Curves of Isothermal Remnant Magnetization.” *Earth Planet. Sci. Lett.* VOl.189: 269–276. 2001.

Matheron, G. *Les Variables Regionalisees et Leur Estimation: Une Application de la Theorie des Fonctions Aleatoires Aux Sciences de la Nature*. Paris: Masson et Cie, Editeurs. pp. 305. 1965.

McLachlan, G. & D. Peel. *Finite Mixture Models*. New York: Wiley-Interscience. 2000.

National Institute of Standards and Technology (NIST)/SEMATECH e-Handbook of Statistical Methods, http://www.itl.nist.gov/div898/handbook/, date. Date created: 6/01/2003, Last updated: 7/18/2006

Peatman, John G. *Descriptive and Sampling Statistics*. New York: Harper & Brothers. 1936, ’41, ’47.

Siegel, S. *Nonparametric Statistics for the Behavioral Sciences.* New York: McGraw-Hill. 312 p.1956.

Sinclair, J. A. “Application of Probability Graphs in Mineral Exploration.” *The Association of Exploration Geochemists, Special*. Vol. 4: 95. 1981.

Snedecor, G.W. and W.G. Cochran. *Statistical Methods*. Ames, Iowa: The Iowa State University Press. Sixth Ed. 593pp.1976.

Soderberg K., R. Hennet and C. Muffels. “Uncertainty and Trend Analysis for Radium in Groundwater and Drinking Water.” Proceeding of 2005 NGWR Naturally Occurring Contaminants Conference: Arsenic, Radium, Radon, and Uranium, Charleston, South Carolina. p30-43. February 24-25. 2005.

Tukey, J. W. *Exploratory Data Analysis*. Massachusetts: Addison-Wesley, Reading. 688p. 1977.

Vanderbilt website control chart diagram (http://www.vanderbilt.edu/Engineering/CIS/Sloan/web/es130/quality/oldtool.htm#control)

Velleman, P.F. and L. Wilkinson. “Nominal, Ordinal, Interval, and Ratio Typologies are Misleading.” *The American Statistician*. Vol.47, No1: pp65-72. 1993.

Yarus, J.M. and R.L Chambers. “Stochastic Modeling and Geostatistics, Principles, Methods, and Case Studies.” *AAPG Computer Applications in Geology*. No. 3: 379p. 1994.

Appendix 8-A

Monitoring Well Analyses from Mill Tailings Site with Results of Cluster Analysis

Rads in pCi/l; non-rads and U in ppm. Galpha is gross alpha, which is a surrogate for radium plus uranium and other alpha-emitters. FL is West or Southwest flow direction – implied separate water bodies for wells. C is cluster number as assigned in SPSS

Obs#	Fl.	C	well	Date	ra226	ra228	ra	th230	u	pb210	G alpha	so4	tds	cl	as
1	SW	1	LA1	12/12/1996	7.2	6.0	13.2	0.050	0.029	0.60	49	851	1350	17.0	0.0005
2	SW	1	LA1	9/2/1997	4.7	5.3	10.0	0.005	0.013	0.05	30	893	1380	19.0	0.0020
3	SW	1	LA1	4/28/1998	4.1	4.6	8.7	0.010	0.006	0.20	36	875	1380	18.0	0.0005
4	SW	1	LA1	6/24/1998	2.1	1.6	3.7	0.090	0.002	0.40	28	862	1380	17.0	0.0060
5	SW	2	LA2	3/13/1996	11.0	11.0	22.0	20.000	0.074	1.80	51	770	1400	19.0	0.0005
6	SW	3	LA2	6/12/1996	13.0	9.9	22.9	0.050	0.042	0.05	67	768	1480	21.0	0.0015
7	SW	3	LA2	8/28/1996	14.0	7.0	21.0	0.200	0.059	0.40	55	760	1480	22.0	0.0010
8	SW	3	LA2	10/28/1996	11.0	11.0	22.0	0.050	0.051	1.70	57	710	1370	22.0	0.0005
9	SW	3	LA2	2/11/1997	10.0	9.6	19.6	0.100	0.051	0.80	62	704	1460	21.0	0.0030
10	SW	3	LA2	6/6/1997	11.0	6.0	17.0	0.005	0.110	1.90	98	788	1420	24.0	0.0020
11	SW	3	LA2	8/7/1997	21.0	9.2	30.2	0.150	0.008	0.50	81	812	1510	24.0	0.0030
12	SW	3	LA2	11/3/1997	13.0	10.0	23.0	0.050	0.096	0.60	72	780	1400	24.0	0.0020
13	SW	3	LA2	4/28/1998	13.7	9.7	23.4	0.100	0.078	0.10	84	818	1470	24.0	0.0015
14	SW	3	LA2	6/23/1998	15.1	9.1	24.2	0.400	0.150	0.90	155	786	1500	23.0	0.0050
15	SW	3	LA2	9/1/1998	14.9	9.7	24.6	0.020	0.075	0.30	84	792	1470	24.0	0.0040
16	SW	3	LA2	11/17/1998	16.0	9.4	25.4	0.020	0.063	0.60	67	814	1490	22.0	0.0020
17	SW	3	LA2	1/6/1999	12.7	9.6	22.3	0.050	0.073	0.40	48	834	1440	22.0	0.0060
18	SW	3	LA2	8/25/1999	16.8	9.8	26.6	0.030	0.066	0.80	54	763	1440	21.0	0.0015
19	SW	3	LA2	2/15/2000	14.0	8.8	22.8	0.500	0.063	0.67	74	780	1500	22.0	0.0015
20	SW	1	LA3	12/12/1996	5.1	5.4	10.5	0.050	0.017	1.80	42	790	1290	6.0	0.0010
21	SW	1	LA3	6/10/1997	3.8	6.8	10.6	0.100	0.420	0.40	356	831	1340	5.0	0.0020
22	SW	1	LA3	9/2/1997	5.3	6.8	12.1	0.100	0.012	0.50	30	877	1220	6.0	0.0020
23	SW	1	LA3	11/23/1997	5.0	5.8	10.8	0.050	0.020	0.30	29	890	1560	6.0	0.0005
24	SW	1	LA3	4/21/1998	6.2	6.6	12.8	0.100	0.016	0.10	41	914	1380	6.0	0.0020
25	SW	1	LA3	6/23/1998	7.8	7.6	15.4	0.200	0.032	0.20	46	836	1390	5.0	0.0050
26	SW	1	LA5	6/10/1997	6.0	2.4	8.4	0.100	0.130	0.10	123	632	1120	4.0	0.0005
27	SW	1	LA5	8/28/1997	14.0	3.5	17.5	0.100	0.040	0.10	58	677	1220	5.0	0.0030
28	SW	3	LA5	11/22/1997	33.0	7.2	40.2	0.400	0.066	2.50	126	937	1670	5.0	0.0050
29		3	LA5	4/21/1998	29.1	7.1	36.2	0.005	0.120	1.40	148	889	1610	5.0	0.0060

SW

30	SW	3	LA5	6/23/1998	24.3	6.9	31.2	0.100	0.091	0.90	122	905	1700	5.0	0.0120
31	SW	3	LA5	3/2/2000	26.0	7.8	33.8	0.240	0.073	1.40	150	890	1600	4.4	0.0040
32	SW	3	LA6	12/12/1996	17.0	8.7	25.7	0.050	0.470	2.10	551	990	1570	21.0	0.0160
33	SW	3	LA6	6/10/1997	15.0	7.7	22.7	0.100	0.053	0.90	74	962	1480	23.0	0.0160
34	SW	3	LA6	9/2/1997	12.0	7.8	19.8	0.005	0.044	1.00	97	968	1560	24.0	0.0170
35	SW	3	LA6	11/22/1997	18.0	8.4	26.4	0.500	1.200	1.70	906	1100	1830	20.0	0.0130
36	SW	3	LA6	4/21/1998	18.8	8.9	27.7	0.530	0.800	1.30	791	1130	1700	20.0	0.0150
37	SW	3	LA6	6/23/1998	18.3	9.8	28.1	0.800	0.830	0.80	865	1090	1760	20.0	0.0240
38	SW	1	LA7	6/10/1997	1.7	3.3	5.0	0.050	0.010	0.10	15	302	616	6.0	0.0010
39	SW	1	LA7	9/3/1997	2.0	3.1	5.1	0.005	0.005	0.20	10	497	910	11.0	0.0020
40	SW	1	LA7	12/1/1997	1.1	1.6	2.7	0.050	0.003	0.20	8.6	308	562	7.0	0.0040
41	SW	1	LA7	4/29/1998	2.7	2.3	5.0	0.050	0.006	0.10	14	323	604	7.0	0.0005
42	SW	1	LA7	6/25/1998	0.6	1.1	1.7	0.100	0.001	0.25	13	361	674	7.0	0.0040
43	SW	4	LA8	12/13/1996	12.0	7.3	19.3	0.400	4.400	6.40	2670	1480	2690	18.0	0.0150
44	SW	5	LA8	6/9/1997	9.5	4.6	14.1	0.200	2.000	0.20	1380	1400	2480	19.0	0.0040
45	SW	5	LA8	9/2/1997	6.1	3.8	9.9	6.900	4.100	1.10	2660	1180	2120	18.0	0.0030
46	SW	5	LA8	11/21/1997	16.0	6.5	22.5	1.800	4.900	1.10	2080	1500	2770	20.0	0.0080
47	SW	5	LA8	4/21/1998	11.6	4.4	16.0	1.180	3.300	1.20	2190	1580	2730	19.0	0.0060
48	SW	5	LA8	6/23/1998	11.2	4.8	16.0	2.300	3.500	0.70	2220	1500	2760	20.0	0.0150
49	SW	5	LA8	3/6/2000	10.0	6.4	16.4	8.200	3.600	3.30	1300	1400	2500	18.0	0.0015
50	SW	6	PW7	3/11/1996	15.0	6.8	21.8	0.200	0.660	1.60	553	830	1290	3.0	1.0800
51	SW	6	PW7	5/22/1996	19.0	5.0	24.0	0.800	0.730	0.90	757	850	1340	3.0	1.2600
52	SW	6	PW7	9/4/1996	17.0	5.7	22.7	1.500	0.660	1.40	558	819	1350	3.0	0.8890
53	SW	6	PW7	11/17/1996	14.0	5.4	19.4	2.700	0.700	2.30	509	860	1300	3.0	0.9460
54	SW	6	PW7	3/12/1997	15.0	5.0	20.0	0.005	0.710	1.90	762	860	1360	3.0	0.8500
55	SW	6	PW7	6/9/1997	12.0	5.1	17.1	0.200	0.640	1.80	621	814	1260	4.0	0.5130
56	SW	6	PW7	8/5/1997	16.0	0.0	15.6	0.200	0.700	0.50	579	840	1330	3.0	0.8620
57	SW	6	PW7	11/3/1997	15.0	5.4	20.4	0.300	0.600	0.80	638	859	1220	3.0	0.8120
58	SW	6	PW7	3/10/1998	17.0	5.6	22.6	0.005	0.510	2.00	597	787	1310	3.0	0.4400
59	SW	6	PW7	6/15/1998	15.0	6.5	21.5	0.300	0.560	1.70	480	692	1360	3.0	0.8100
60	SW	1	PW7	9/22/1998	12.6	4.3	16.9	0.070	0.500	0.60	433	484	796	21.0	0.3380
61	SW	6	PW7	12/8/1998	10.6	3.9	14.5	0.100	0.460	1.00	446	879	1200	3.0	0.3120
62	SW	6	PW7	3/2/1999	13.2	5.2	18.4	0.050	0.490	1.30	460	764	1300	3.0	0.4550
63	SW	6	PW7	2/15/2000	15.0	5.3	20.3	0.240	0.500	3.50	540	820	1400	2.5	0.4700

64	W	7	A8	7/8/1996	72.0	7.3	79.3	0.050	0.018	6.10	161	647	1160	8.0	0.0060
65	W	3	A8	9/19/1996	40.0	2.6	42.6	0.005	0.023	0.10	96	796	1210	11.0	0.0010
66	W	3	A8	9/8/1997	29.0	2.7	31.7	0.200	0.047	0.10	101	865	1370	13.0	0.0050
67	W	3	A8	10/14/1998	26.0	3.8	29.9	0.200	0.067	0.60	94	900	1420	14.0	0.0020
68	W	1	DOMW1	3/20/1995	0.5	0.5	1.5	0.100	0.006	1.30	0.5	133	441	4.6	0.0050
69	W	8	DOMW1	6/29/1995	1.0	2.2	3.2	0.500	0.620	0.50	1.6	388	8571	33.0	0.0050
70	W	1	DOMW1	8/23/1995	0.2	0.9	1.1	0.200	0.032	0.10	33	152	366	5.0	0.0010
71	W	1	DOMW1	12/14/1995	7.1	0.6	7.7	0.005	0.006	1.40	11	145	452	4.0	0.0020
72	W	1	DOMW1	3/22/1996	0.4	1.5	1.9	0.005	0.004	0.15	6.6	130	414	4.0	0.0010
73	W	1	DOMW1	7/1/1996	0.3	0.4	0.7	0.005	0.004	0.30	5.7	128	398	4.0	0.0005
74	W	1	DOMW1	11/11/1996	0.4	2.0	2.4	0.005	0.003	1.20	6.9	137	418	4.0	0.0005
75	W	1	MW27	3/13/1996	8.1	6.2	14.3	0.005	0.004	2.90	20	450	738	6.0	0.0070
76	W	1	MW27	6/11/1996	8.5	4.0	12.5	0.050	0.005	1.00	23	438	780	6.0	0.0050
77	W	1	MW27	8/22/1996	8.5	3.1	11.6	0.900	0.005	0.50	18	433	702	6.0	0.0080
78	W	1	MW27	10/11/1996	7.6	1.9	9.5	0.050	0.001	1.60	26	431	758	6.0	0.0080
79	W	1	MW27	5/7/1997	7.4	4.0	11.4	0.005	0.003	1.00	24	398	726	5.0	0.0100
80	W	1	MW27	7/28/1997	8.3	2.5	10.8	0.050	0.005	1.60	26	424	806	6.0	0.0120
81	W	1	MW27	10/13/1997	6.3	4.2	10.5	0.050	0.004	1.10	22	408	746	5.0	0.0080
82	W	1	MW27	2/4/1998	7.1	3.6	10.7	0.050	0.002	1.60	21	411	720	5.0	0.0060
83	W	1	MW27	5/6/1998	8.7	3.9	12.6	0.020	0.004	1.40	19	407	746	9.0	0.0080
84	W	1	MW27	7/29/1998	8.3	4.2	12.5	0.010	0.003	1.40	22	415	762	5.0	0.0110
85	W	1	MW27	10/21/1998	7.0	3.8	10.8	0.050	0.004	2.60	9.6	390	728	5.0	0.0090
86	W	1	MW27	1/6/1999	6.4	4.7	11.1	0.005	0.001	1.30	22	428	746	5.0	0.0120
87	W	1	MW27	8/9/1999	5.1	3.3	8.4	0.030	0.001	1.50	17	378	760	5.0	0.0080
88	W	1	MW27	1/20/2000	6.3	3.1	9.4	0.160	0.001	2.70	37	390	710	3.8	0.0065
89	W	1	MW28	3/29/1996	9.2	5.8	15.0	0.005	0.003	1.20	26	380	688	5.0	0.0100
90	W	1	MW28	6/5/1996	8.7	5.0	13.7	0.050	0.003	2.40	24	358	656	5.0	0.0080
91	W	1	MW28	8/14/1996	7.5	3.8	11.3	0.005	0.001	0.50	29	386	670	5.0	0.0070
92	W	1	MW28	10/28/1996	11.0	6.4	17.4	0.050	0.001	0.90	19	381	636	5.0	0.0060
93	W	1	MW28	2/3/1997	11.0	3.8	14.8	0.100	0.004	1.40	51	359	678	4.0	0.0090
94	W	1	MW28	4/30/1997	11.0	4.6	15.6	0.100	0.002	1.40	33	388	692	6.0	0.0090
95	W	1	MW28	7/25/1997	6.6	4.4	11.0	0.050	0.003	1.10	20	374	688	5.0	0.0060
96	W	1	MW28	10/8/1997	9.6	4.2	13.8	0.050	0.002	1.40	33	407	678	6.0	0.0090
97	W	1	MW28	1/28/1998	10.0	4.5	14.5	0.200	0.002	1.00	30	435	748	6.0	0.0070
98	W	1	MW28	4/28/1998	10.4	5.4	15.8	0.070	0.001	1.10	41	432	732	6.0	0.0040
99	W	1	MW28	7/29/1998	12.3	7.1	19.4	0.010	0.002	0.20	32	445	798	6.0	0.0090
100	W	1	MW28	10/20/1998	10.7	5.0	15.7	0.050	0.003	1.00	23	435	782	5.0	0.0100
101	W	1	MW28	1/19/1999	10.3	4.0	14.3	0.100	0.004	1.20	27	479	818	6.0	0.0080
102	W	1	MW28	1/20/2000	12.0	4.9	16.9	1.000	0.001	3.70	46	500	810	5.8	0.0078
103	W	1	MW30	3/20/1996	15.0	1.7	16.7	0.005	0.056	2.00	60	250	540	3.0	0.0005
104	W	1	MW30	6/17/1996	14.0	2.6	16.6	0.050	0.090	2.00	40	252	538	4.0	0.0050
105	W	1	MW30	8/26/1996	18.0	2.3	20.3	0.200	0.053	1.80	73	264	478	4.0	0.0040
106	W	1	MW30	10/29/1996	22.0	1.6	23.6	0.005	0.060	3.30	105	260	533	4.0	0.0040
107	W	1	MW30	2/13/1997	31.0	3.0	34.0	0.005	0.062	3.90	69	256	590	6.0	0.0020
108	W	1	MW30	5/7/1997	24.0	2.5	26.5	0.050	0.059	3.80	94	272	540	5.0	0.0060
109	W	1	MW30	7/29/1997	12.0	4.0	16.0	0.005	0.019	1.50	58	284	606	2.0	0.0090
110	W	1	MW30	10/22/1997	30.0	1.7	31.7	0.005	0.066	4.20	91	278	584	6.0	0.0050
111	W	1	MW30	2/3/1998	14.0	4.0	18.0	0.100	0.061	1.90	50	283	610	5.0	0.0040
112	W	1	MW30	6/16/1998	32.3	3.4	35.7	0.040	0.067	3.80	95	271	612	6.0	0.0070
113	W	1	MW30	8/13/1998	25.6	2.8	28.4	0.010	0.063	2.10	94	288	614	6.0	0.0050

114	W	1	MW30	11/11/1998	35.1	2.3	37.4	0.050	0.075	3.40	114	259	618	8.0	0.0090
115	W	1	MW30	1/7/1999	20.4	2.6	23.0	0.100	0.056	2.80	63	306	574	6.0	0.0080
116	W	9	MW30	8/17/1999	20.3	3.5	23.8	0.030	0.070	4.10	142	1840	602	39.0	0.0015
117	W	1	MW30	1/24/2000	28.0	3.5	31.5	1.000	0.065	4.60	180	310	620	6.5	0.0073
118	W	10	MW76	6/6/1997	42.0	12.0	54.0	0.100	0.240	2.20	276	1710	2480	7.0	0.0680
119	W	10	MW76	8/4/1997	35.0	9.8	44.8	0.005	0.200	2.20	380	1860	2570	8.0	0.0780
120	W	10	MW76	11/4/1997	42.0	11.0	53.0	0.100	0.250	3.10	161	1830	2510	16.0	0.0830
121	W	10	MW76	2/4/1998	36.0	11.0	47.0	0.100	0.260	3.00	355	1830	2610	7.0	0.0820
122	W	10	MW76	5/5/1998	36.0	12.0	48.0	0.080	0.250	2.00	255	1880	2360	8.0	0.0890
123	W	10	MW76	8/10/1998	42.8	9.8	52.6	0.100	0.230	1.70	220	1870	2710	7.0	0.0890
124	W	10	MW76	10/14/1998	54.2	11.0	65.2	0.100	0.220	2.00	209	1780	2640	7.0	0.0920
125	W	10	MW76	1/6/1999	39.0	11.0	50.0	0.100	0.220	2.30	249	1920	2600	6.0	0.0990
126	W	10	MW76	1/24/2000	35.0	8.9	43.9	0.800	0.240	3.80	210	1900	2600	6.1	0.0740
127	W	1	MW77	3/20/1997	4.2	5.4	9.6	0.050	0.003	0.90	16	444	730	0.5	0.0030
128	W	1	MW77	6/6/1997	5.5	5.0	10.5	0.005	0.018	0.40	21	437	740	4.0	0.0050
129	W	1	MW77	8/4/1997	5.7	4.9	10.6	0.005	0.001	0.80	24	442	714	4.0	0.0070
130	W	1	MW77	11/4/1997	5.3	4.8	10.1	0.100	0.004	0.80	22	507	780	4.0	0.0080
131	W	1	MW77	1/28/1998	6.3	5.4	11.7	0.005	0.001	0.60	11	511	798	4.0	0.0060
132	W	1	MW77	4/29/1998	5.6	5.7	11.3	0.050	0.001	1.00	28	558	812	4.0	0.0050
133	W	1	MW77	8/11/1998	6.8	5.6	12.4	0.020	0.005	0.30	26	573	876	4.0	0.0080
134	W	1	MW77	11/3/1998	6.3	5.7	12.0	0.050	0.001	0.05	41	531	866	4.0	0.0070
135	W	1	MW77	1/26/1999	5.2	6.4	11.6	0.040	0.001	0.70	30	560	878	4.0	0.0100
136	W	1	MW77	8/9/1999	7.5	5.6	13.1	0.050	0.001	0.80	17	520	868	4.0	0.0070
137	W	1	MW77	1/19/2000	6.7	5.4	12.1	6.200	0.001	1.20	43	590	900	3.2	0.0059

Appendix 8-B Fortran 90 code for well-well correlations and for the Mann-Kendall test

```
!   program trend.for
!   Developed on March 8, 2005 by Zhenxue Dai
! ******************************************************************
!   This code carries out the basic statistic analysis of the observed data
!   including the water heads and the concentrations, as well as the other types of data.
!   It uses the Mann-Kendall test to evaluate the trends of the time series observations.
!   This code also calculate the water head correlations between different wells
!   from the observation data to identify the connections of the groundwater at
!   different aquifers or geological structures.
!   The input data format is: first well name, then water heads in this well
!   W123456 120, 122, 123,....
!   W123457 120, 122, 123,....
!   nw== number of observation wells
!   nt== number of observation points in each well
!   Wnam== wall name; WHH== water heads; ave== mean; Var==Variance
!   Stan== standard deviation; Cv== Coefficients of variation; Cov==Covariance
!   Trend== Uptrend, Downtrend, or Flat
!   Pval== p-value, p<0.1 trend test significant, p>0.1, test result uncertain
```

```
!   Sman==Mann-Kendall statistic parameter in each well
!   Sz==modified Mann-Kendall statistic parameter in each well
!   Ssd==modified coefficient for each well.
!   Rela(k,i)== Correlation Coefficients between well k and well i.
!     alfa=1.68 for water head, and 1000 for concentrations
!   **************************************************************

      parameter (nw=150,nt=20)
      IMPLICIT DOUBLE PRECISION(A-H,O-Z),INTEGER(I-N)
      dimension WHH(nw,nt),Var(nw),ave(nw), Stan(nw),Cv(nw)
      dimension Rela(nw,nw),Cov(nw,nw),Hmin(nw),Hmax(nw),Pval(nw),
     +           Numt(nw),Sman(nw),Sz(nw),Ntie(nw),Ssd(nw)
      character*8 Wnam(nw),trend(nw)
      character*5 Waqu(nw)
      character*80 str1
      character*4 str2
      character*8 out
      alfa=1.0
         write(*,*) "ENTER INPUT FILENAME (NO HEADER): "
      read(*,'(a)')str1
         write(*,*) "ENTER 4 CHARACTERS FOR OUTPUT FILENAME "
      read(*,'(a)')str2
      open(99,file=str1,status='old')
      OUT=str2//'.out'

      open(91,file=out,status='unknown')

          write(*,*)  " "
          write(*,*)  "THINKING... "
          write(*,*)  " "
          num1 = 0
          tranN0=0

!   BRING IN FIRST LINE OF INPUT FROM DATA FILE
      read(99,*)Nww      !=137, number of observation wells
      read(99,*)Ntt      !=16, max number of data at one well


          do i=1,Nww
       read(99,*) Wnam(i),Waqu(i),(WHH(i,j), j=1,Ntt)
!        if(id(i).eq.0) go to 50 (commented out by ZDai)
       write(*,*) Wnam(i),Waqu(i)
     end do


 50    continue
```

```
          Iout=0
499      continue
      If(Iout.eq.0) Write(91,500)
500   format(/,'Statistic Analysis of the Original Observations'
    +  ,/,'WellNam AqNam ObNm MinVal MaxVal ',
    +    'MeanV  Varian Stand CoefV ',
    +    'Mann  ModM   Trend  p-val')
      If(Iout.eq.1) Write(91,801)
801   format(/,'Statistic Analysis of the Observations',
    +  ' After Rejecting the Outlier Points',
    +   /,'WellNam AqNam ObNm MinVal MaxVal ',
    +    'MeanV  Varian Stand CoefV ',
    +    'Mann  ModM   Trend  p-val')

!   calculate mean, variance of water head in each well(Var(nw),ave(nw), Stan(nw))
      do 60 i=1,Nww
          nwt=0
          hhh=0
          st=0
          Hm=0
          Hn=1.0e25
          Sm=0

        do j=1,Ntt
            Ntie(j)=0
                  if(WHH(i,j).eq.-100) go to 62
            nwt=nwt+1
          hhh=hhh+WHH(i,j)
            if(WHH(i,j).gt.Hm)Hm=WHH(i,j)    !Max value
            if(WHH(i,j).lt.Hn)Hn=WHH(i,j)    !Min Value

            do k=1,Ntt
              if(k.gt.j.and.WHH(i,k).ne.-100)then
                aa=WHH(i,k)-WHH(i,j)
                if(aa.gt.0.0) Ms=1
                if(aa.eq.0.0) then
                  Ms=0
                  Ntie(j)=Ntie(j)+1
                end if
                if(aa.lt.0.0) Ms=-1
                Sm=Sm+Ms
          end if
            end do

 62      continue
```

```
      end do

           Numt(i)=nwt
           Hmax(i)=Hm
           Hmin(i)=Hn
           Sman(i)=Sm
          if(nwt.ne.0)ave(i)=hhh/nwt
          Stie=0
          do k2=1,ntt
           Stie=Stie+Ntie(k2)*k2*(k2-1)*(2*k2+5)
          end do
          Ssd(i)=((Numt(i)*(Numt(i)-1)*(2*Numt(i)+5)-Stie)/18.0)
          If(Ssd(i).gt.0.0) Ssd(i)=Ssd(i)**0.5
          if(Sman(i).gt.0.0) then
          if(ssd(i).ne.0.0) Sz(i)=(Sman(i)-1.0)/Ssd(i)
                       trend(i)=' Uptrend'
            end if
          if(Sman(i).eq.0.0) then
               Sz(i)=0
                       trend(i)=' Flat'
            end if
          if(Sman(i).lt.0.0) then
            if(ssd(i).ne.0.0)Sz(i)=(Sman(i)+1.0)/Ssd(i)
                       trend(i)='Downtren'
            end if
           Szz=abs(Sz(i))
           if(Szz.gt.5) Pval(i)=0.00000
           if(Szz.gt.3.09.and.Szz.lt.5)
     +  Pval(i)=66.21327*exp(-szz/0.27834)-9.9998E-7
           if(Szz.gt.1.96.and.Szz.lt.3.09)
     +  Pval(i)=2.59485*exp(-szz/0.42511)-0.00081
           if(Szz.lt.1.96.and.Szz.gt.1.28)
     +  Pval(i)=0.8051*exp(-szz/0.66358)-0.01698
           if(Szz.lt.1.28) Pval(i)=0.71701*exp(-szz/1.56831)-0.21701
      do j=1,ntt
                     if(WHH(i,j).eq.-100) go to 63
        st=st+(WHH(i,j)-ave(i))**2.0
63      continue
      end do
           if(nwt.ne.0.0)then
           Var(i)=st/nwt
      Stan(i)=(st/nwt)**0.5
      end if
           if(ave(i).ne.0.0)Cv(i)= stan(i)/ave(i)
           if(nwt.eq.0)then
       Write(91,901)Wnam(i),Waqu(i),Numt(i)
```

```
901      format(A8,1x,A5,I3,1x,'This well is deleted!')
        go to 60
                     end if
!      Write(*,501) Wnam(i),Ave(i),Var(i),Stan(i),Cv(i)
       Write(91,501)Wnam(i),Waqu(i),Numt(i),Hmin(i),Hmax(i),Ave(i),
    +      Var(i),Stan(i),Cv(i),Sman(i),Sz(i),Trend(i),Pval(i)
 60    continue
501    format(A8,1x,A5,I3,1x,3f7.2,F7.2,f6.2,f6.3,1x,f4.0,f6.2,
    +        1x,A8,f6.3)
          If(Iout.eq.1) go to 808
!
!         Reject the extremal observation points
!
          aSd=0.0
          do i=1,nww
                     asd=asd+Stan(i)
          end do
                     asd=asd/nww
         do iw=1,nww
          Sp=0.025
       pp=(Numt(iw)-1)*Sp/Numt(iw)
         if(pp.le.0.00003) zz=4
         if(pp.gt.0.00003.and.pp.le.0.0062)
    +     zz=1.54688*exp(-pp/0.00117)+2.49239
         if(pp.le.0.0688.and.pp.gt.0.0062)
    +     zz=1.41193*exp(-pp/0.02866)+1.36272
         if(pp.gt.0.0688)
    +     zz=2.50842*exp(-pp/0.328)-0.54623
          if(zz.le.0.0) zz=0.0
!        write(*,*)pp, zz
         vk=1.4+0.85*zz
         vc=vk*(1.0-(vk**2.0-2.0)/(4.0*(Numt(iw)-1.0)))
    +        *((Numt(iw)-1.0)/Numt(iw))**0.5
          vCs=alfa*(vc*stan(iw))**2.0
!        write(*,*)Wnam(iw), vCs
         do j=1,ntt
         If(whh(iw,j).le.-100.0) go to 3721
         vd=(whh(iw,j)-ave(iw))**2.0
!        vd=abs(whh(iw,j)-ave(iw))*(1.0-2*Sp)
         if(vd.gt.vCs.or.vd.gt.100*alfa*asd)then
           orig=whh(iw,j)
       whh(iw,j)=-100
!        Numt(iw)=Numt(iw)-1
         write(*,*)Wnam(iw),orig,'vd=',vd,'st=',vCs

         end if
```

```
3721   continue
        end do
        end do
        Iout=1
        go to 499


!  LOOP calculate correlation coefficients between wells
!
808    continue
      do 80 k=1,Nww
      do 80 i=1,Nww
           nwt=0
           hhk=0
           hhi=0
           st=0
           vari=0
           vark=0
      do j=1,Ntt
                     if(WHH(k,j).eq.-100.or.WHH(i,j).eq.-100) go to 82
            nwt=nwt+1
        hhk=hhk+WHH(k,j)
        hhi=hhi+WHH(i,j)
 82     continue
       end do
          if(nwt.ge.1)then
        avek=hhk/nwt
        avei=hhi/nwt
           end if
       do j=1,ntt
                     if(WHH(k,j).eq.-100.or.WHH(i,j).eq.-100) go to 83
         st=st+(WHH(k,j)-avek)*(WHH(i,j)-avei)
         vari=vari+(WHH(i,j)-avei)**2.0
         vark=vark+(WHH(k,j)-avek)**2.0
 83     continue
        end do
          if(nwt.ge.1)then
            Cov(k,i)=st/nwt
            Varii=(vari/nwt)**0.5
            Varkk=(vark/nwt)**0.5
        Rela(k,i)=Cov(k,i)/(Varkk*Varii)
          end if
 80    continue

       Write(91,502)
502     format(/,'Following Wells are Highly Positively Correlated:',
```

```
     +        ' R > 0.95')

       do k=1,Nww
       do i=1,Nww
          If(i.le.k) go to 21
          If (Rela(k,i).ge.0.95) then
     Write(91,503) Wnam(k),Waqu(k),Wnam(i),Waqu(i),Rela(k,i)
503    format(A8,A5,'and  ',A8,A5,f5.2)
       end if
21     continue
      end do
      end do

      Write(91,602)
602    format(/,'Following Wells are Positively Correlated:',
     +        ' 0.9 < R < 0.95')

       do k=1,Nww
       do i=1,Nww
          If(i.le.k) go to 23
          If (Rela(k,i).ge.0.9.and.Rela(k,i).lt.0.95) then
     Write(91,603)Wnam(k),Waqu(k),Wnam(i),Waqu(i),Rela(k,i)
603    format(A8,A5,'and  ',A8,A5,f5.2)
       end if
23     continue
      end do
      end do


      Write(91,604)
604    format(/,'Following Wells are not Correlated:',
     +        ' -0.1 < R < 0.1')

       do k=1,Nww
       do i=1,Nww
          If(i.le.k) go to 84
          If (Rela(k,i).le.0.1.and.Rela(k,i).ge.-0.1) then
     Write(91,605)Wnam(k),Waqu(k),Wnam(i),Waqu(i),Rela(k,i)
605    format(A8,A5,'and  ',A8,A5,f5.2)
       end if
84     continue
      end do
      end do


      Write(91,504)
```

```
504   format(/,'Following Wells are Negatively Correlated:',
    +         ' R < -0.9')

       do k=1,Nww
       do i=1,Nww
           If(i.le.k) go to 88
           If (Rela(k,i).le.-0.9) then
      Write(91,505)Wnam(k),Waqu(k),Wnam(i),Waqu(i),Rela(k,i)
505     format(A8,A5,'and  ',A8,A5,f5.2)
       end if
88     continue
      end do
      end do


      Write(91,506) (Wnam(i), i=1,Nww)
506    format(/,'All Correlation Coeff of Water Head Between Wells',
    +     /,15x,137(A7))
      Write(91,406) (Waqu(i), i=1,Nww)
406    Format(15x,137(A5,2x))
       do k=1,Nww
      Write(91,508) Wnam(k), Waqu(k),(Rela(k,i),i=1,Nww)
508     format(A8,A5,137(f7.3))
      end do

      CALL BEEPQQ(200,400)
       CALL BEEPQQ(30,400)
      CALL BEEPQQ(200,400)
      CALL BEEPQQ(30,400)
      CALL BEEPQQ(400,1500)
            write(*,*) "  DONE! "
            stop
            End
```

GLOSSARY

Alluvium	A general term for clay, silt, sand, gravel, or similar unconsolidated detrital material, deposited during comparatively recent geologic time by a stream or other body of running water, as a sorted or semi sorted sediment in the bed of the stream or on its floodplain or delta, as a cone or fan at the base of a mountain slope.
Aquifer	A geological formation capable of storing and yielding significant quantities of water. It is usually composed of sand, gravel, or permeable rock which lies upon a layer of clay or other impermeable material.
Aquitard	Less permeable beds, also saturated with water, from which water can't be produced through wells, but where the flow is significant enough to feed adjacent aquifers through vertical leakage.
Becquerel (Bq)	The International System (SI) unit of activity equal to one nuclear transformation (disintegration) per second. 1 *Bq* = 2.7x10-11 *Curies (Ci)* = 27.03 picocuries (pCi).
Colluvium	A general term applied to any loose, mixed, and incoherent mass of soil material and/or rock fragments deposited by rainwash, sheetwash, or slow continuous downslope creep, usually collecting at the base of gentle slopes or hillsides.
Comprehensive Environmental Response, Compensation, and Liability Act (CERCLA)	Commonly referred to as "CERCLA" or "Superfund," this federal statute was enacted by Congress in 1980 and was amended several times thereafter. CERCLA was designed to respond to situations involving past disposal of hazardous substances. CERCLA provides EPA the authority to clean up hazardous substance sites under "response" or "remedial" provisions of the National Contingency Plan (NCP) and other implementing regulations. 42 U.S.C. §§ 9601 *et seq.*
Conceptual site model	A qualitative description of the processes, geometry, and boundary conditions associated with a disposal site or site sub-system component (i.e., ground-water system, flow-through covers, source term, etc.). Conceptual model development includes abstracting system, or sub-system, descriptions into more simplified forms that can be mathematically modeled.
Contaminant of Concern (COC)	A contaminant or a chemical that poses potential public health risks. Potential contaminants of concern (PCOCs) are all chemicals that have been detected at the site. Only those contaminants retained for the risk assessment are referred to as COCs.
Cuesta	A ridge with a gentle slope on one side and a steep slope on the other.
Curie (Ci)	The customary unit of radioactivity. One *curie* (Ci) is equal to 37 billion disintegrations per second (3.7 x 1010 dps = 3.7 x 1010 *Bq*), which is approximately equal to the decay rate of one gram of 226Ra.
Direct current electrical resistivity (DC-resistivity)	A geophysical technique used to measure the resistance of a rock formation to an electric current.

Effluent	Any substance, particularly a liquid, which enters the environment from a point source. Generally refers to wastewater from a sewage treatment or industrial plant.
Erratics	Boulders and other rock fragments transported by glacial ice from their place of origin to an area where the bedrock is different.
Ground-penetrating radar (gpr)	Geophysical exploration technique that utilizes pulses of electromagnetic radiation in the microwave band (UHF/VHF frequencies) of the radio spectrum, and reads the reflected signal to detect subsurface structures and objects without drilling, probing or otherwise breaking the ground surface.
Half-life (t1/2)	The time required for one-half of the radioactive isotopes in a sample to decay to radiogenic (daughter) isotopes or disintegrate.
Hazardous Waste	A category of waste regulated under RCRA. To be considered hazardous, a waste under RCRA must be a solid waste and must exhibit at least one of four characteristics described in 40 CFR 261.20 through 40 CFR 261.24 (i.e., ignitability, corrosivity, reactivity, or toxicity) or be specifically listed by EPA in 40 CFR 261.31 through 40 CFR 261.33. Hazardous waste does not include source, special nuclear, or by-product materials as defined by the AEA, nor material contained in point source discharges regulated under the Clean Water Act.
Infiltration	The net water intake into the native soils at the site or into a disposal unit(s) through the land or cover surface(s).
Kd	distribution coefficient.
Kriging	A geostatistical method of evaluating mine reserves based on a mathematical function known as a semivariogram.
Lacustrine	Of or applying to the sedimentary environment of a lake.
Low-Level Waste (LLW)	Radioactive waste that is not high level radioactive waste, spent nuclear fuel, transuranic waste, byproduct material (as defined in section 11e.(2) of the Atomic Energy Act of 1954, as amended), or naturally occurring radioactive material. [Adapted from *Nuclear Waste Policy Act* of 1982, as amended]
Maximum Contaminant Level (MCL)	Under the Safe Drinking Water Act, the maximum permissible level of a contaminant in water delivered to any user of a public water system.
Non-Aqueous Phase Liquid (NAPL)	Organic compounds or mixtures of such compounds that do not mix with water. A NAPL that is lighter than water is called light non-aqueous phase liquid (LNAPL) or a floater. A NAPL that is heavier than water is called dense non-aqueous phase liquid (DNAPL) or a sinker.
Neutron probe	A device used to measure the quantity of water present in soil.
Ohm-m	Unit of measure of electrical resistivity.
Operable Unit (OU)	A term given to large areas where remediation may be focused by grouping multiple units into a single management unit.
Performance Assessment (PA)	An analysis of a radioactive waste disposal facility conducted to demonstrate there is a reasonable expectation that performance objectives established for the long-term protection of the public and the environment will not be exceeded following closure of the facility. [DOE 435.1-1]

Petra	Software developed by the GeoPLUS Corporation. It’s primary use is to store and provide tools for interpreting geologic data.
Picocurie (pCi)	A "picocurie" is one-trillionth of a curie. The same mass (one gram) of other radioactive elements may have an activity higher or lower than one curie.
pCi/L	Represents the number of picocuries in a liter of water.
Plume	A body of contaminated groundwater flowing from a specific source.
Remediate	To cleanup or decontaminate ground water or soil.
Resource Conservation and Recovery Act (RCRA)	A federal law enacted in 1976 to address solid waste and the treatment, storage, and disposal of hazardous waste. 42 U.S.C. §§ 6901-6992k.
Semivariogram	A key function in geostatistics used to fit a model of the spatial/temporal correlation of an observed phenomenon.
Sorption coefficient (Kd)	The ratio of the mass of solute on the solid phase per unit mass of solid phase to the concentration of solute in solution. The validity of this ratio requires that the reactions that cause the partitioning are fast and reversible (e.g., chemical equilibrium is achieved) and the sorption isotherm is linear.
Stratigraphy	The sequence or order of rock or soil layers in a geologic formation.
Surface-based seismic surveys	A geophysical technique to determine the detailed structure of rocks underlying a particular area by passing acoustic shock waves from the surface into the underlying strata and detecting and measuring the reflected signals.
Surficial	Of, relating to, or occurring on or near the surface of the earth.
Thermocouple psychrometers (TCPs)	Probes for determining soil water potential in situ.
Till	A mix of fine silt, sand, gravel, and large boulders, usually in a glacial setting.
Tritium units	One tritium unit is equal to one molecule of tritium per 10^{18} molecules of hydrogen and has an activity of 0.118 Bq/kg (3.19 pCi/kg or pCi/L).
Vadose zone	The horizon between the earth’s surface and the water table, also know as the “unsaturated zone”. Vadose zone wells installed by the USGS at the ADRS are designated with the prefix “UZB-x”.

NRC FORM 335 (9-2004) NRCMD 3.7 U.S. NUCLEAR REGULATORY COMMISSION **BIBLIOGRAPHIC DATA SHEET** *(See instructions on the reverse)*	1. REPORT NUMBER (Assigned by NRC, Add Vol., Supp., Rev., and Addendum Numbers, if any.) NUREG/CR-6948, Vol 2	
2. TITLE AND SUBTITLE Integrated Ground-Water Monitoring Strategy for NRC-Licensed Facilities and Sites: Case Study Applications	3. DATE REPORT PUBLISHED MONTH: November	YEAR: 2007
	4. FIN OR GRANT NUMBER Y6020	
5. AUTHOR(S) Van Price, Tom Temples, Rex Hodges, Zhenxue Dai, David Watkins and Janice Imrich	6. TYPE OF REPORT Technical	
	7. PERIOD COVERED *(Inclusive Dates)* February 2003 - September 2007	

8. PERFORMING ORGANIZATION - NAME AND ADDRESS *(If NRC, provide Division, Office or Region, U.S. Nuclear Regulatory Commission, and mailing address; if contractor, provide name and mailing address.)*

Advanced Environmental Solutions, LLC
407 West Main Street
Lexington, SC 29072

9. SPONSORING ORGANIZATION - NAME AND ADDRESS *(If NRC, type "Same as above"; if contractor, provide NRC Division, Office or Region, U.S. Nuclear Regulatory Commission, and mailing address.)*

Division of Fuel, Engineering and Radiological Research
Office of Nuclear Regulatory Research
U.S. Nuclear Regulatory Commission
Washington, DC 20555-0001

10. SUPPLEMENTARY NOTES

T.J. Nicholson, NRC Project Manager

11. ABSTRACT *(200 words or less)*

This document discusses results of applying the Integrated Ground-Water Monitoring Strategy (the Strategy) to actual waste sites using existing field characterization and monitoring data. The Strategy is a systematic approach to dealing with complex sites. Application of such a systematic approach will reduce uncertainty associated with site analysis, and therefore uncertainty associated with management decisions about a site. The Strategy can be used to guide the development of a ground-water monitoring program or to review an existing one. The sites selected for study fall within a wide range of geologic and climatic settings, waste compositions, and site design characteristics and represent realistic cases that might be encountered by the NRC. No one case study illustrates a comprehensive application of the Strategy using all available site data. Rather, within each case study we focus on certain aspects of the Strategy, to illustrate concepts that can be applied generically to all sites. The test sites selected include:

- Charleston, South Carolina, Naval Weapons Station,
- Brookhaven National Laboratory on Long Island, New York,
- The USGS Amargosa Desert Research Site in Nevada,
- Rocky Flats in Colorado,
- C-Area at the Savannah River Site in South Carolina, and
- The Hanford 300 Area.

A Data Analysis section provides examples of detailed data analysis of monitoring data.

12. KEY WORDS/DESCRIPTORS *(List words or phrases that will assist researchers in locating the report.)*	13. AVAILABILITY STATEMENT
conceptual site model data management geology ground water monitoring outlier Performance Indicator tritium vadose wells	unlimited
	14. SECURITY CLASSIFICATION *(This Page)* unclassified *(This Report)* unclassified
	15. NUMBER OF PAGES
	16. PRICE